

This is to certify that the

dissertation entitled

Factors Influencing The C=N Stretching  
Frequency in Neutral and Protonated Schiff's  
Bases

presented by

Juan Lopez-Garriga

has been accepted towards fulfillment

of the requirements for

Ph.D. degree in Chemistry

Wald T. Babcock  
Major professor

Date October 30, 1986



RETURNING MATERIALS:

Place in book drop to  
remove this checkout from  
your record. FINES will  
be charged if book is  
returned after the date  
stamped below.

--	--	--

**FACTORS INFLUENCING THE C-N STRETCHING FREQUENCY IN NEUTRAL  
AND PROTONATED SCHIFF'S BASES.**

**by**

**JUAN LOPEZ-GARRIGA**

**A DISSERTATION**

**submitted to**

**Michigan State University**

**in partial fulfillment of the requirements**

**for the degree of**

**DOCTOR OF PHILOSOPHY**

**Department of Chemistry**

**1986**

422-2905

ABSTRACT

FACTORS INFLUENCING THE C=N STRETCHING FREQUENCY IN  
NEUTRAL AND PROTONATED SCHIFF'S BASES.

by

JUAN LOPEZ GARRIGA

The C=N stretching frequency has been studied in a series of aromatic Schiff's bases, their protonated derivatives and their reaction products with other Lewis acids. Protonation, deuteration or reaction with  $\text{BF}_3$  increases the C=N stretching frequency in a range from  $1 \text{ cm}^{-1}$  to  $80 \text{ cm}^{-1}$ . Linear polyene Schiff's bases show similar behavior: an increase in the C=N frequency of  $30 \text{ cm}^{-1}$  is observed upon complexation of trans-retinal Schiff's base with  $\text{BF}_3$ . The magnitude of the increase in the C=N vibrational mode is dependent on the extent of conjugation in the aromatic system, on the nature of the substituent, and on the strength of the Lewis acid. In the NMR spectra of the protonated and complexed species a downfield chemical shift of the protons nearby the C=N bond is observed which suggests that the nitrogen electronegativity increases in the reaction products relative to the free Schiff's base.

These observations, plus the similarities in the behavior of Schiff's bases and nitriles, suggest that rehybridization at the Schiff's base nitrogen occurs on the reaction of its lone pair with Lewis acids to increase the C=N bond order. Ab initio calculations on the Schiff's

base, methylimine, support this idea as the C=N bond length decreases and the C=N stretching force constant increases by 0.51 mdyn/Å upon protonation. Normal coordinate analysis of this species, of the model structure  $\text{CH}_3\text{HC}=\text{NCH}_3$ , and of their protonated and deuterated derivatives are reported here which show that an increase in the stretching force constant of this magnitude leads to an increase of  $\sim 30 \text{ cm}^{-1}$  in the frequency of the C=N stretching vibration. Analogous normal coordinate calculations were also carried out for the  $\text{BF}_3$  addition product which show that a similar increase in C=N stretching force constant upon complexation is likely. The results indicate that rehybridization effects, in particular, an increase in the s orbital contribution from the protonated nitrogen to the  $\text{sp}^2$  hybrid orbital in the Schiff's base linkage, are primary responsible for the increase in the C=N stretching frequency upon complexation of a Schiff's base by a Lewis acid.

**To: Carmen González, Marti López, Juan Francisco López,  
Teresa Garriga, Rebeca González, Miguel López,  
Francisca Roura and Marti Garriga.**

## ACKNOWLEDGMENTS

I am deeply grateful to Professors Gerald T. Babcock and James F. Harrison for their contributions to this research and to my graduate education.

I wish to thank to Professor George E. Leroy and Hak-Hyun Nam for their discussions and help with the set of the normal coordinate analysis programs.

I would also like to express my gratitude to all my companions in the chemistry building and in particular to those who have share their friendship, time and knowledge with me. So to Jerry, Jim, Aileen Alvarado, Asaad Salehi, Jose Centeno, Demetrios Ghanotakis, Dwight Lillie, Tony Oertling, Ivan Rodriguez, Robert Kean, Brigitte Barry, Harold Fonda, Nam, Pat Maroney, Pat Callahan, Brian Ward, and Margy Lynch. I like to thank to the personal of the chemistry shops for their assistance and patience in the development of the apparatus and equipment used during the course of this research. So to, Russ Geyer, Richard Menke, Carlton Watters, Keki Mistry, Manfred Langer, Scott Bankroff, Ron Hass, Thomas Clarke , Scott Sanderson and Marti Rabb. In particular I like to thank Ron Hass, Tony, Jose and Bob for their care and concern of our lasers system and to Dwight for his patience and help with the computer system.

I would also like to thank to my family and friends who in some instance of my walk, they have teach me with their thoughts, words and actions where my feet can go. Finally, I am in debt with my brothers

Franki, Wally, Paco Pepe, Luis, Roberto, L., Billy, Chiqui, Nieto and  
Albert who in different occasions save my life from the magnificent sea.

## TABLE OF CONTENTS

	PAGE
LIST OF TABLES .....	viii
LIST OF FIGURES.....	x
CHAPTER 1.	
INTRODUCTION.....	1
A. Importance of the Schiff's Base Bond (C=N) in Biological Systems. ....	1
B. Optical and Vibrational Properties of Chromophores Containing the C=N Bond.....	13
C. Previous Mechanism to Account for the Anomalous Increase in the C=N Stretching Frequency Upon Protonation of Schiff's Bases.....	16
D. Description of the Work to be Presented.....	18
CHAPTER 2.	
MATERIALS, INSTRUMENTATION AND METHODS.	
A. Materials.....	21
B. Synthesis of Imines.....	21
C. Synthesis of Ketimines.....	24
D. Schiff's Bases: Lewis Acid Derivatives.....	24
E. Instrumentation and Calculations.....	26
1. Ab initio.....	28
2. Normal Coordinate Analysis.....	31
CHAPTER 3.	
SPECTROSCOPIC STUDIES.	
A. Introduction.....	32
B. Spectroscopic Results.....	36

1. Imines.....	36
2. Ketimines.....	54
C. Discussion.....	60
1. C=N stretching frequency:Neutral Schiff's base.	60
2. C=N stretching frequency:Schiff's bases/Lewis acid complexes.....	67
3. Absorption maximum of trans-retinylidene-n- butylamine:Lewis acid complexes.....	72

**CHAPTER 4.**

**AB INITIO CALCULATION.**

A. Introduction.....	75
B. Theoretical Details.....	77
C. Results.....	78
D. Discussion.....	93

**CHAPTER 5.**

**NORMAL COORDINATE ANALYSES.**

A. Introduction.....	96
B. Numerical Calculations and Methylimine and Methylen- immonium ion force fields.....	98
C. Force Field of $\text{CH}_3\text{CH}=\text{NCH}_3$ and derivatives.....	102
D. Results of the vibrational Analyses.....	108
1. Methylimine and Methylenimmonium ion Vibrational Frequencies.....	108
2. $\text{CH}_3\text{CH}=\text{NCH}_3$ and Derivatives Vibrational Frequencies.....	108
E. Discussion.....	120

**CHAPTER 6.**

**SUMMARY AND FUTURE WORK.**

<b>A. Introduction.....</b>	<b>124</b>
<b>B. Summary.....</b>	<b>126</b>
<b>1. Spectroscopic Studies.....</b>	<b>126</b>
<b>2. Ab initio Studies.....</b>	<b>126</b>
<b>3. Normal Coordinate Analyses Studies.....</b>	<b>127</b>
<b>C. Conclusion.....</b>	<b>128</b>
<b>D. Future Work.....</b>	<b>129</b>
<b>LIST OF REFERENCES.....</b>	<b>135</b>

## LIST OF TABLES

TABLE	PAGE
1. Frequency assignments for N-benzylidene-n-butylamine (BnBI), and protonated (BnBIH <sup>+</sup> ) and deuterated (BnBID <sup>+</sup> ) derivatives.....	39
2. Frequency assignments for 2-naphtylidene-n-butylamine (NAPnBI), and protonated (NAPnBIH <sup>+</sup> ), and deuterated (NAPnBID <sup>+</sup> ) derivatives.....	47
3. Chemical shift for carbonyl and imine protons of aromatic Schiff's bases.....	51
4. Absorption maxima, C=C and C=N stretching frequencies of tran-retinylidene-n-butylamine and Lewis acid derivatives.....	57
5. Carbonyl and imine stretching frequency of polyene and aromatic compounds.....	63
6. Changes in the C=N stretching frequency upon complexation with Lewis acids.....	68
7. Methylimine potential curve. Total energy for the C=N stretching motion.....	81
8. Methylenimmonium ion potential curve. Total energy for the C=N stretching motion.....	82
9. Calculated force constants for the C=N and C=N stretching motion.....	85
10. Methylimine: Electron distribution.....	87
11. Methylenimmonium ion: Electron distribution.....	87
12. Electron distribution of the $\sigma$ bond system.....	90
13. F matrix elements for methylimine.....	100
14. F matrix elements for methylenimmonium ion.....	101

15. Symmetry coordinates for in-plane vibrations of methylen- immonium ion.....	103
16. Diagonal and off-diagonal force constants of some imines.....	105
17. F matrix elements for the model structures.....	106
18. Methylimine calculated frequencies of in-plane vibrations.....	109
19. Methylenimmonium ion calculated frequencies of in-plane vibrations.....	110
20. Calculated C=N stretching frequency of methylimine derivatives.....	111
21. Calculated C=N stretching frequency of model structures.....	112

## LIST OF FIGURES

FIGURE	PAGE
1.	Bleaching scheme of the visual pigment rhodopsin. The 11-cis retinal Schiff's base, in rhodopsin, absorbs a photon and is converted in picosecond to bathorhodopsin, which contains a distorted C <sub>11</sub> =C <sub>12</sub> trans chromophore..... 5
2.	Photochemical scheme of bacteriorhodopsin. The light-adapted bacteriorhodopsin (BR <sub>568</sub> ), contains an all-trans retinal chromophore attached to a lysine group, of the protein, through a protonated Schiff's ..... 7
3.	The condensation reaction illustrates other function of a Schiff's base, the activation of carbon via an enamine intermediate..... 12
4.	Model structures..... 23
5.	Schematic Raman spectrometer..... 27
6.	Schematic spinning cell..... 30
7.	Raman spectra of N-benzylidene-n-butylamine (BnBI) and protonated (BnBIH <sup>+</sup> ) and deuterated (BnBID <sup>+</sup> ) derivatives in CHCl <sub>3</sub> solution..... 38
8.	Raman spectra of N-benzylidene-n-butylamine (BnBI) and protonated (BnBIH <sup>+</sup> ) and BF <sub>3</sub> (BnBIBF <sub>3</sub> ) derivatives in DMSO solution..... 42
9.	Raman spectra of 2-naphthylidene-n-butylamine (NapBI) and protonated (NapBIH <sup>+</sup> ) and deuterated (NapBID <sup>+</sup> ) derivatives in CHCl <sub>3</sub> ..... 44

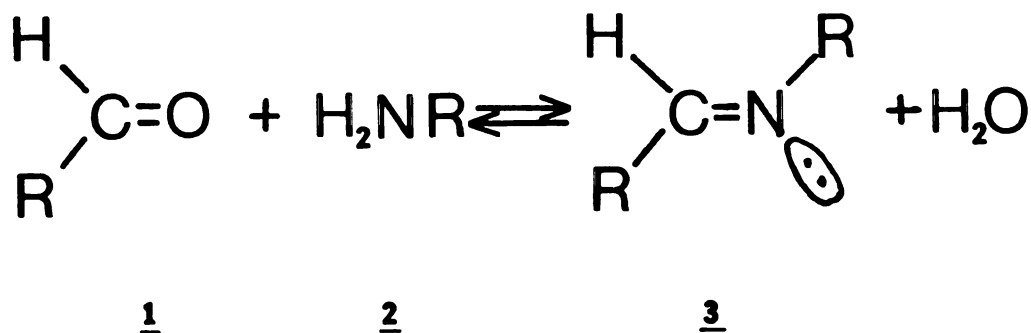
10.	Raman spectra of 2-naphthylidene-n-butylamine (a) and BCl <sub>3</sub> (b) and BF <sub>3</sub> (c) derivatives in DMSO solution.....	46
11.	250-NMR spectra of benzaldehyde (a), N-benzylidene-n-butyl- amine (b) and its protonated (c) and deuterated (d) derivatives in CDCl <sub>3</sub> .....	50
12.	Resonance Raman spectra of retinylidene-n-butylamine (RnB) and protonated (RnBH <sup>+</sup> ) and BF <sub>3</sub> (RnBBF <sub>3</sub> ) derivatives in DMSO solution.....	53
13.	Resonance Raman and absorption (inset) spectra of trans- retinal Schiff's base and Lewis acid derivatives in CH <sub>2</sub> Cl <sub>2</sub> . (a) Trans-retinylidene-n-butylamine. (b) BCl <sub>3</sub> complex. (c) BBr <sub>3</sub> complex. (d) BF <sub>3</sub> complex. (e) HClO <sub>4</sub> complex. (f) HCl complex.....	56
14.	Raman spectra of ω-phenylbenzylidene-n-butylamine (a) and protonated (b) and deuterated (c) derivatives in methanol solution.....	59
15.	Raman spectra of benzophenone (BBO), α-phenylbenzylidene- amine (BBI) and protonated (BBIH <sup>+</sup> ) and BF <sub>3</sub> (BBIBF <sub>3</sub> ) derivatives in DMSO.....	62
16.	Effect of increasing the aromatic ring conjugation on the characteristic group frequency of aldehydes (⊙), Schiff's bases (□) and protonated Schiff's bases (■).....	65
17.	Ab initio potential curves for the C=N stretching motion. (a) C=N <sub>SCF</sub> methylimine SCF. (b) C=N <sub>SCF</sub> methylenimmonium ion SCF. (c) C=N <sub>GVB</sub> methylimine GVB. (d) C=N <sub>GVB</sub> methylenimmonium ion GVB, calculations.....	80

18.	Geometry of methylimine (a) and methylenimmonium ion (b)....	83
19.	$\sigma$ system, $\pi$ system and total charge distribution for methylimine.....	88
20.	$\sigma$ system, $\pi$ system and total charge distribution for methylenimmonium ion.....	89
21.	s-p and p electron distribution of the $\sigma$ and $\pi$ systems in the C=N bond of methylimine and methylenimmonium ion....	92
22.	Geometry and internal coordinates employed for the normal coordinate analyses of methylimine and methylimmonium ion...	99
23.	Geometry and internal coordinates employed for the normal coordinate analyses of the model $\text{CH}_3\text{CH}=\text{NCH}_3$ and its protonated and $\text{BF}_3$ derivatives.....	104
24.	Difference between the C=N stretching frequency in the protonated and neutral Schiff's base $\text{CH}_3\text{CH}=\text{NCH}_3$ , as a function of the force constant of the principal modes which contributed to the potential energy distribution.....	115
25.	Difference between the C=N stretching frequency in the $\text{BF}_3$ and neutral Schiff's base $\text{CH}_3\text{CH}=\text{NCH}_3$ , as a function of the force constant of the principal modes which contributed to the potential energy distribution.....	119

CHAPTER 1  
INTRODUCTION

A. Importance of the Schiff's Base Bond, C=N, in Biological Systems.

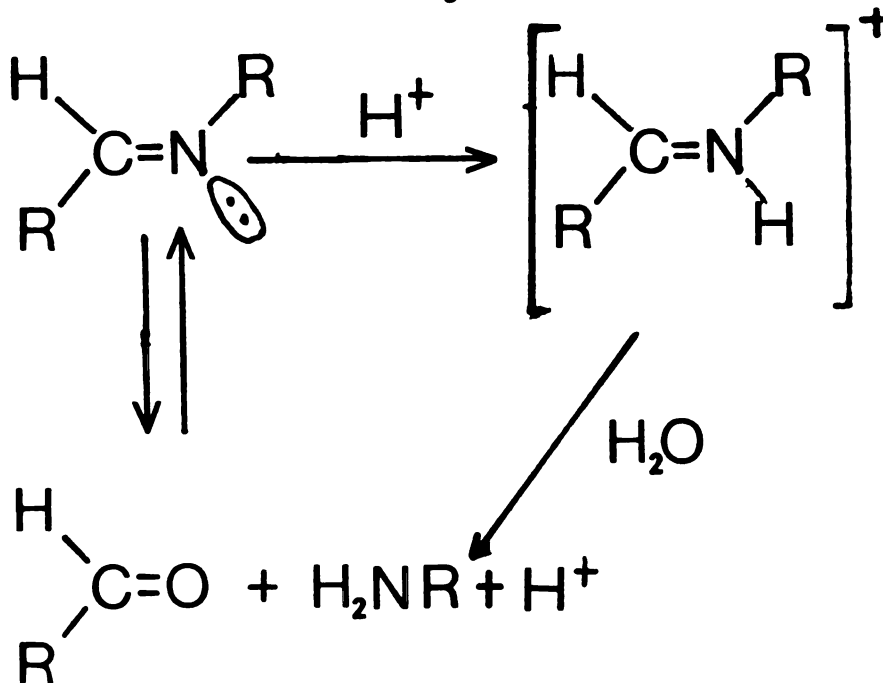
Nitrogen and carbon are able to change their hybridization readily to form different kinds of bonds. It is not surprising, therefore, that their interrelationship plays a number of important roles in biological systems. The reaction between a carbonyl group of an aldehyde (1) with the amino group of a primary amine (2) leads to the formation of one of these peculiar nitrogen-carbon-bonds, the Schiff's base (3) linkage:



The Schiff's base (C=N) bond, has attracted interest because of its occurrence in rhodopsin, bacteriorhodopsin and its photocycle derivatives<sup>1-17</sup> and in pyridoxal enzyme systems.<sup>18-22</sup> Metalloporphyrin and metallochlorin Schiff's bases have been synthesized recently and the possibility that these occur in vivo has been raised.<sup>23-27</sup>

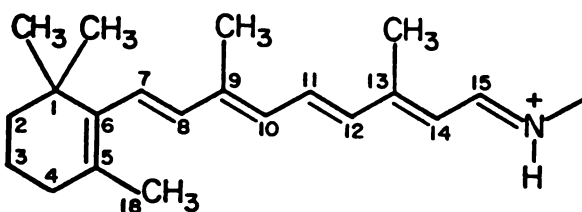
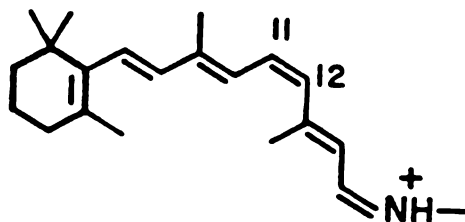
The fact that Schiff's base linkages are versatile in their physical

and chemical properties no doubt accounts for their importance in biological catalysis. The C=N bond, for example, is fairly labile and can be hydrolyzed and reformed readily (4). Protonation of the C=N nitrogen in a Schiff's base containing



4

chromophore generally leads to a marked red-shift in the chromophore absorption spectrum. This reaction is of importance in controlling the optical properties of the retinal Schiff's base (5a) in the visual pigment, rhodopsin.<sup>1-10</sup>

5a5b

All-trans-retinylidene-n-butylamine.

11-cis-retinylidene-n-butylamine.

The primary amino acid sequence of bovine rhodopsin has been determined<sup>28-30</sup> and it has been established that a lysine group of the protein is bound to the retinal moiety via a Schiff's base linkage.<sup>31</sup>

After the absorption of light, the 11-cis retinal protonated Schiff's base (5b) chromophore in rhodopsin<sup>32,33</sup> photoisomerizes to a red shifted intermediate, bathorhodopsin, with a distorted all-trans retinal configuration.<sup>34,35</sup> Following the formation of this primary photoproduct, a series of thermal events occur (see Figure 1) which initiate a change in the photoreceptor cell membrane that leads to a transmitted signal to the brain through the corresponding synaptic processes.<sup>1-10,35</sup>

Bacteriorhodopsin (BR) is another retinal-protein and it functions as a photochemical proton-pump in the purple membrane of Halobacteria.<sup>11-17,36-38</sup> Under normal illumination conditions, bacteriorhodopsin is in its light-adapted form, a protonated retinal Schiff's base with an absorption maximum at 560 nm.<sup>1,2,35</sup> Absorption of light by the bacteriorhodopsin retinal prosthetic group converts this light-adapted BR<sub>568</sub> form to a red-shifted intermediate K<sub>610</sub> which absorbs maximally at 610 nm. This species decays thermally to BR<sub>568</sub>, through a series of intermediates, one of them a deprotonated Schiff's base, i.e. M<sub>412</sub>, (see Figure 2). This light-driven protonation/deprotonation sequence of the Schiff's base nitrogen is the key step in the mechanism of the proton pump action of bacteriorhodopsin.<sup>11-17,34-38</sup>

Many naturally occurring porphyrinoid compounds contain a ketone or a formyl as functional groups as in the case of chlorophyll a (6) in the

Figure 1. Bleaching scheme of the visual pigment rhodopsin (from ref. 35). The 11-cis retinal Schiff's base, in rhodopsin, absorbs a photon and is converted in picosecond to bathorhodopsin, which contains a distorted C<sub>11</sub>=C<sub>12</sub> trans chromophore. At physiological temperatures bathorhodopsin decays through a series of intermediates to all-trans retinal and the apoprotein, opsin.

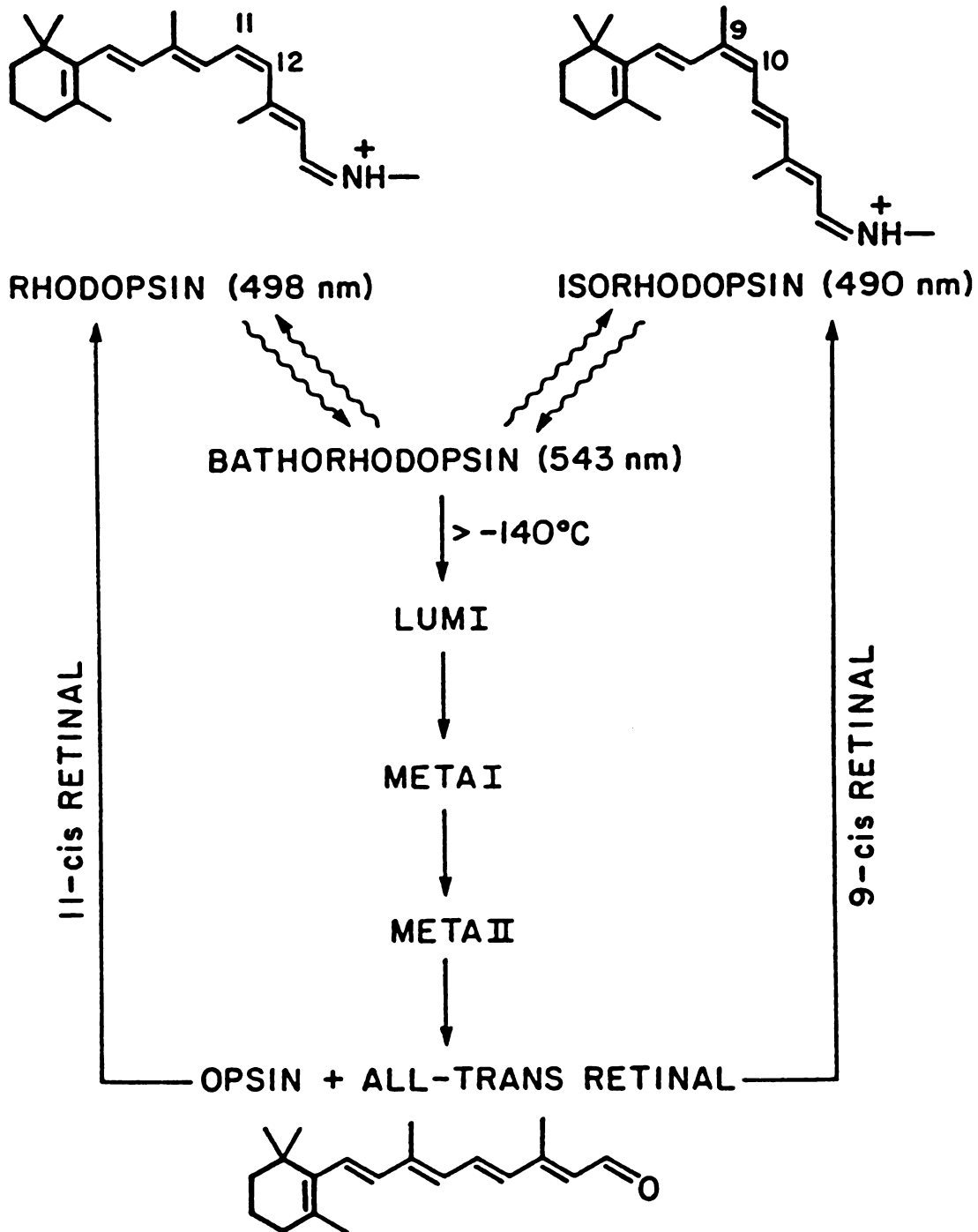


Figure 1

Figure 2. Photochemical scheme of bacteriorhodopsin. The light-adapted bacteriorhodopsin (BR<sub>568</sub>), contains an all-trans retinal chromophore attached to a lysine group, of the protein, through a protonated Schiff's base. Photoisomerization about the C<sub>13</sub>=C<sub>14</sub> bond forms the K<sub>610</sub> intermediate, which cycles in ~ 10 msec back to BR<sub>568</sub> through L<sub>550</sub>, M<sub>412</sub> and O<sub>640</sub>. From reference 35.

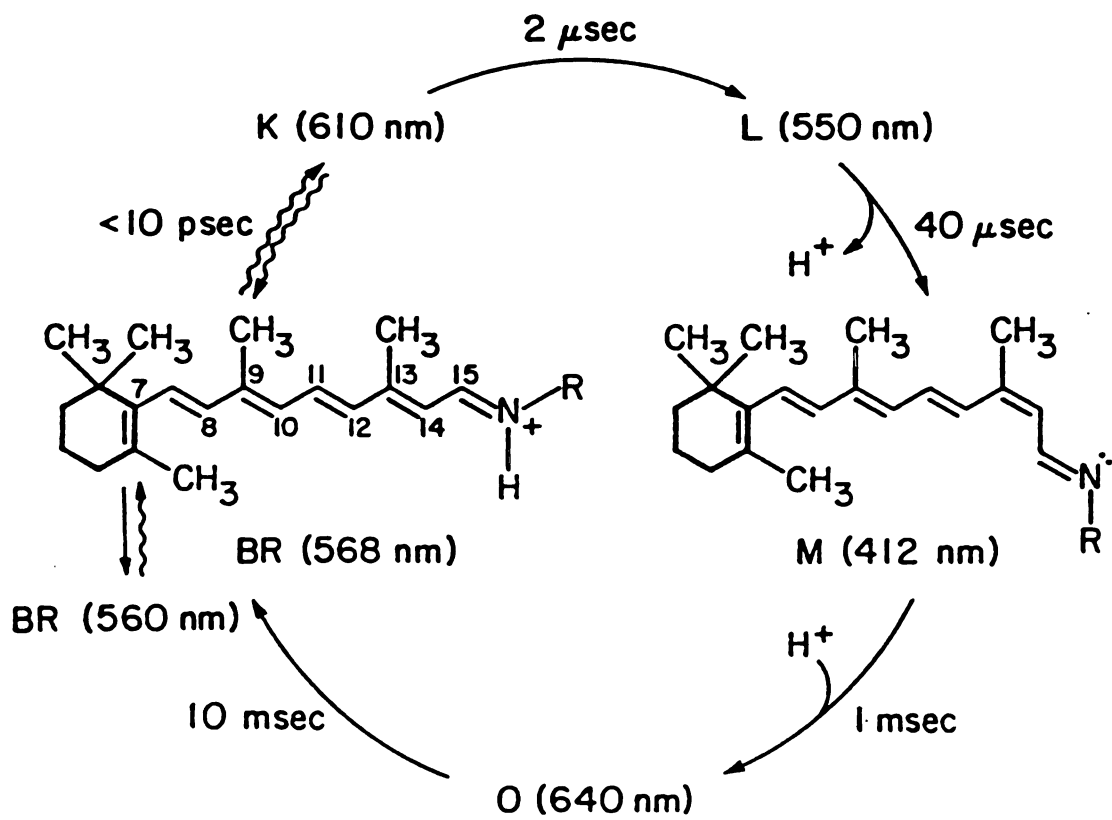
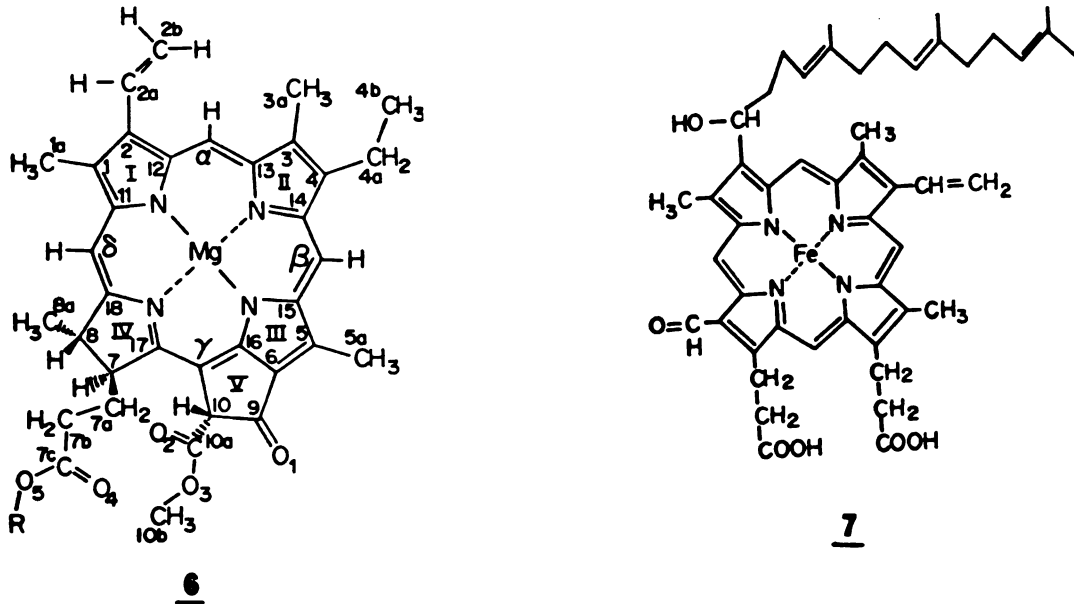


Figure 2

photosynthetic systems or of heme a (7) in cytochrome oxidase. It is generally observed that the spectral properties of the *in vivo* chromophores are, as in the case of rhodopsin and bacteriorhodopsin, red shifted relative to the *in vitro* chromophore.<sup>23-27</sup>



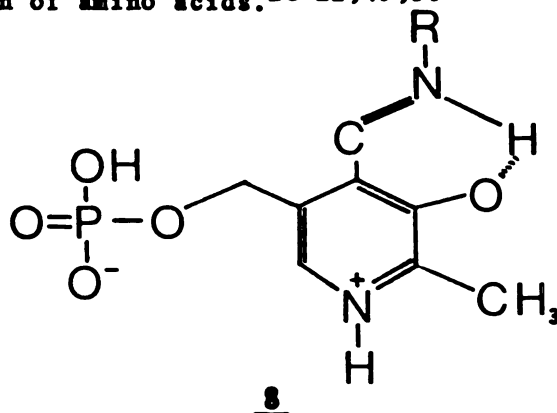
For example, cytochrome oxidase catalyses the oxidation of ferrocyanide c and the four electron reduction of dioxygen to water through the centers cytochrome a and cytochrome a<sub>3</sub>. Each cytochrome center contains a heme group and a protein-bound copper ion, and because of their different chemical environments they are denoted heme a and copper a and heme a<sub>3</sub> and copper a<sub>3</sub> respectively.<sup>41,42</sup> In addition to its redox chemistry, cytochrome oxidase is involved in proton translocation from the inside to the outside of the membrane.<sup>39-42</sup> Such proton pumping action has been postulated to be associated with the cytochrome a center<sup>42</sup> and in particular with the heme a chromophore.<sup>39,40,43</sup> Heme a is the main absorbing chromophore of the redox active center, cytochrome a, in the mitochondrial enzyme, cytochrome oxidase, and is low-spin in both its  $Fe^{2+}$  and  $Fe^{3+}$  states in the protein. Compared to low spin heme a

model compounds, red-shifted visible absorption spectra of 10 nm and 17 nm for the oxidized (i.e. 598 nm and 588 nm) and reduced (604 nm and 588 nm) species, respectively are observed.<sup>39,40</sup> From an historical point of view, it was originally thought that the red-shifted absorption maximum of the heme a chromophore was produced by a protonated Schiff's base formed between the carboxyl group of heme a (7) and an amino group from the protein. In analogy to bacteriorhodopsin, a protonation/deprotonation step of the nitrogen Schiff's base following the redox chemistry of that center was postulated to be involved in the proton pump activity of the enzyme.<sup>44,45</sup> However, spectroscopic studies have shown that a protonated Schiff's base is unlikely to be present in heme a<sup>4a</sup> and that the proton pumping activity of the enzyme may be attributed to redox-linked activity at a hydrogen bond involving the carbonyl group of heme a and a nearby amino acid side chain.<sup>39,40,43</sup>

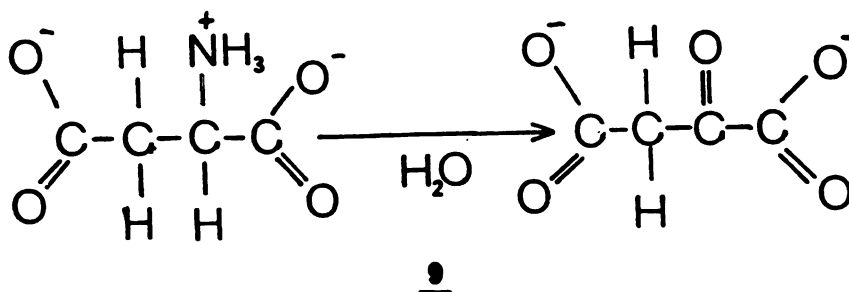
Nevertheless, the former observation has led to the suggestion that the red-shift observed for chlorophyll *in vivo* may originate, at least in part, from similar phenomena, i.e., from formation and protonation of Schiff's base linkages in the protein environment.<sup>23-25</sup> The chlorophylls in the reaction centers of the photosynthetic apparatus in alga and green plants, with absorption maximum at 700 nm (P<sub>700</sub>) and 680 nm (P<sub>680</sub>) and located in photosystem I and in the photosystem II, respectively, show red-shifted absorption spectra relative to monomeric chlorophyll a. This spectral shift has been attributed to dimers or to higher order aggregates of chlorophyll a.<sup>46-48</sup> However, partly because in the photopigment rhodopsin a protonated Schiff's base is directly involved in the regulation of the optical absorption wavelength maximum, the dimer

hypothesis has been challenged and a protonated Schiff's base has been proposed as source of the P<sub>700</sub> and P<sub>680</sub> red shifted absorption maximum.<sup>23-25</sup>

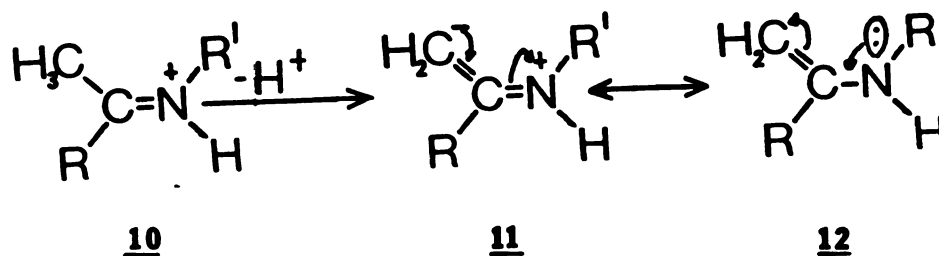
In addition to the above proteins, there is a set of enzymatic systems in which the prosthetic group and the catalytic function depend explicitly on a protonated Schiff's base. For instance, the coenzyme, pyridoxal phosphate (8), plays an important role in the metabolic interconversion of amino acids.<sup>18-22,49,50</sup>



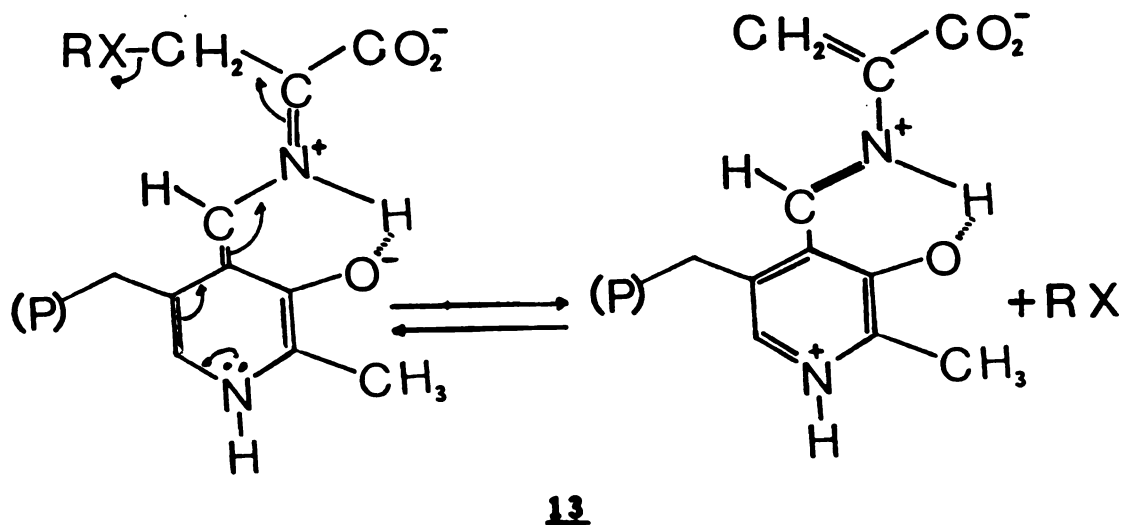
The protonation reaction of the Schiff's base group (C=N) of the coenzyme produces the key intermediate which can lead to transamination (9), or the interchange reaction, of an amino group of the protein amino acid by a carboxylic group. The reaction mechanism of the enzyme, aspartate amino transferase<sup>49</sup>, a classical example of transamination, together with other transaminases involving Schiff's bases, has been extensively discussed in a recent book by Christen and Metzler.<sup>50</sup>



Another group of protonated Schiff's base-related enzymes involves a ketimine (10), instead of an imine (3), Schiff's base. This condensation reaction leads to the formation of an enamine intermediate (11,12) during the catalytic cycle of a particular process. Such an intermediate, for instance, is involved in the decarboxylation reaction of acetoacetate by the enzyme acetoacetate decarboxylase<sup>52,53</sup>, and in the aldol condensation and reverse cleavage reaction of the RCHO group by the enzymes, aldolase and transaldolase, respectively.<sup>54-57</sup> The condensation reaction is shown in Figure 3.



A similar mechanism is present when the pyridoxal cofactor Schiff's base is involved in the decarboxylation reaction of aspartate and in the interconversion (13) and/or degradation of aminoacids such as serine, threonine, cysteine, tryptophan, and cystathionine.<sup>50,51</sup>



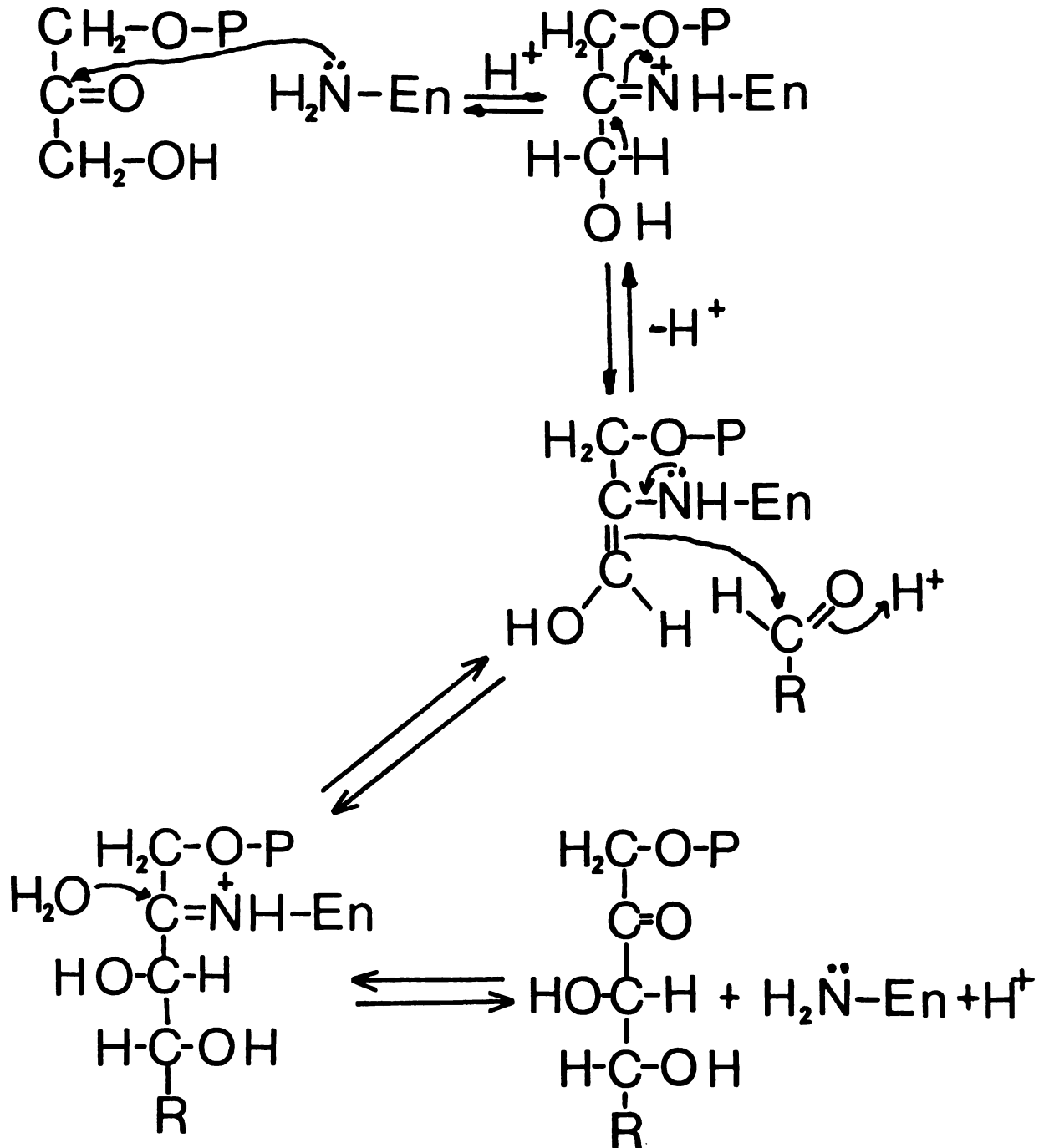


**Figure 3.** The condensation reaction illustrates other function of a Schiff's base, the activation of carbon via an enamine intermediate. P and En represent the phosphate group and aldolase enzyme respectively.

The above survey of biological systems has indicated the importance of the protonated Schiff's bases in the biological kingdom. In the next section, the optical and vibrational spectroscopic properties of chromophores involving the C=N group will be discussed.

#### B. Optical and Vibrational Properties of Chromophores Containing the C=N Group.

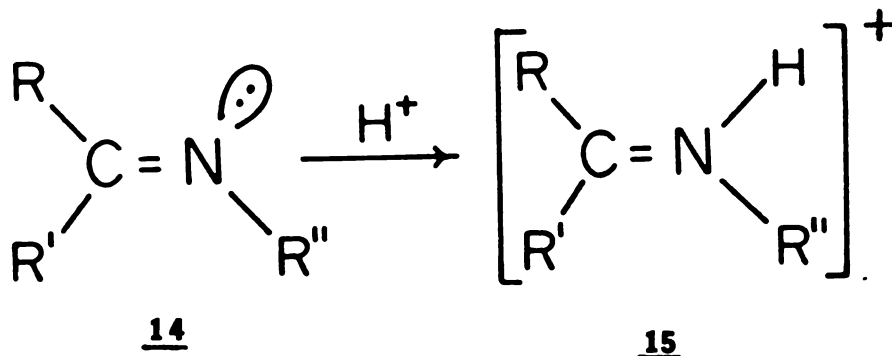
Visual excitation is initiated by photon absorption in the rhodopsin pigment. This chromophore-protein complex consists of a protonated retinal Schiff's base bound to an apoprotein, opsin. The 11-cis-retinal protonated Schiff's base, formed from n-butylamine and 11-cis-retinal, has its absorption maximum at 440 nm in methanol<sup>61</sup>, whereas the bovine rhodopsin pigment (see Figure 1) absorbs at 500 nm. Honig, Nakanishi and co-workers<sup>61,66</sup> proposed to call this in vivo red-shift from the in vitro absorption maximum, the "opsin shift" (in  $\text{cm}^{-1}$ ). For instance, the opsin shift for cattle opsin would be  $2700 \text{ cm}^{-1}$  [ $22700 \text{ cm}^{-1}$  (i.e. 440 nm) -  $20000 \text{ cm}^{-1}$  (i.e. 500 nm)]. Similarly, the opsin shift in bacteriorhodopsin is  $\sim 5100 \text{ cm}^{-1}$  since the absorption maximum of the protein is at 560 nm.<sup>74</sup> The development of this opsin shift, or wavelength regulation, is caused by the protein environment and constitutes one of the central problems in the visual research.

Numerous models have been proposed to account for the opsin shifts in rhodopsin, bacteriorhodopsin and their various photocycle intermediates.<sup>61,66,74,95-101</sup> Blatz et al.<sup>60,95,102</sup> in their early studies of retinal Schiff's base models, concluded that upon protonation

of the retinal imine the partially positive charge on the nitrogen depends on the separation between the center of charge of the cation and anion (counter ion effect). In this way, the fractional charge on the Schiff's base nitrogen not engaged in the ionic bond polarizes the  $\pi$  system to produce a resulting excitation energy lower than the unprotonated Schiff's base species.

To explain the opsin shift in rhodopsin and bacteriorhodopsin, Nakanishi et al.<sup>61,66</sup> proposed that, in addition to the counter ion effect<sup>102</sup>, a negative charge in the vicinity of carbons 11 and 12 (see Figure 1) can account for the  $\sim 2700$   $\text{cm}^{-1}$  opsin shift of rhodopsin. They also proposed<sup>61,66</sup> that for bacteriorhodopsin a negative charge near carbon 5 can account for the  $5000$   $\text{cm}^{-1}$  opsin shift. However, recent data from Mathies and his group<sup>74</sup>, and others in the field<sup>103</sup> suggested that the bacteriorhodopsin shift can be partitioned into a  $1200$   $\text{cm}^{-1}$  shift due to ground state configurational changes and a  $3900$   $\text{cm}^{-1}$  shift due to a weak hydrogen bond between the Schiff's base proton and an electronegative group in the protein.<sup>74</sup> These observations on the bacteriorhodopsin shift suggest that the environment at the protonated retinal Schiff's base moiety plays an important role in regulating the absorption maxima of the photopigments.

Schiff's base (14) and protonated Schiff's base (15) C=N vibrational modes have been studied for at least the past three decades.<sup>58,59</sup>



Part of the interest in these species derives from the observation of functionally significant Schiff's base linkages in biological systems, for example, in pyridoxal enzymes<sup>18-22</sup> and, more recently, in bacteriorhodopsin, rhodopsin and related visual cycle intermediates and models.<sup>1-17</sup> In rhodopsin, the retinal chromophore is bound to the opsin protein moiety through a Schiff's base linkage and resonance Raman spectroscopy has been used extensively to monitor changes in the C=N stretching frequency during the rhodopsin photocycle. For example the C=N stretching mode in the neutral species occurs at  $1620 \text{ cm}^{-1}$ . This increases to  $1655 \text{ cm}^{-1}$  upon protonation and to  $1630 \text{ cm}^{-1}$  upon deuteration.<sup>1,10</sup> In bacteriorhodopsin, smaller frequency changes, presumably originating in the protonated Schiff's base, occur at stages in the photocycle and suggest different degrees of protein-chromophore interaction for the various intermediates.<sup>35</sup> Thus, the decrease in the C=N stretching frequency from the protonated  $L_{550}$  intermediate ( $\nu_{\text{C=N}}=1644 \text{ cm}^{-1}$ ) to the  $M_{412}$  intermediate ( $\nu_{\text{C=N}}=1632 \text{ cm}^{-1}$ ) has been used as an indicator of the proton pump cycle of bacteriorhodopsin.<sup>2,11-17,35</sup>

Analogously, pyridoxal Schiff's bases show the same trend in the

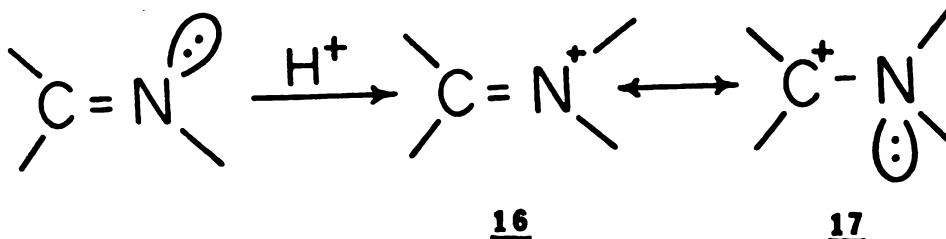
absorption spectra and C=N stretching frequency. For instance, at pH=13 the pyridoxal-valine Schiff's base complex shows an absorption maximum at 385 nm and a C=N stretching frequency at  $1630\text{ cm}^{-1}$ . Upon protonation at pH=9, the absorption maximum red shifts to 415 nm and the C=N stretching frequency increase to  $1643\text{ cm}^{-1}$ . Deuteration at the nitrogen shifts this vibrational frequency to  $1635\text{ cm}^{-1}$ . Similarly, the pyridoxal enzyme, aspartate aminotransferase, show a C=N stretching frequency of  $1649\text{ cm}^{-1}$  at pH=5 and this mode decreases to  $1617\text{ cm}^{-1}$  upon deuteration.<sup>21,22</sup>

Work from this laboratory<sup>23</sup> on the Schiff's bases formed between formylated metalloporphyrins or metallochlorins and primary amines shows that upon protonation of these aromatic Schiff's base there is an increase in the C=N stretching frequency as well. For example, for the Schiff's base of Ni(II) porphyrin a the C=N stretching vibration occurs at  $1639\text{ cm}^{-1}$ ,  $1650\text{ cm}^{-1}$  and  $1640\text{ cm}^{-1}$ , respectively, for neutral, protonated and deuterated species. Accompanying the protonation reaction, there is a marked optical red-shift in the visible region<sup>23-25</sup> as also occurs in the polyene case.<sup>1-17,60-66</sup>

### C. Previous Mechanisms for the Anomalous Increases in the C=N Stretching Frequency Upon Protonation of Schiff's Bases.

While the origin of the optical red-shift has been explored theoretically in both aromatic heterocycle<sup>26,27</sup> and polyene cases<sup>60-66</sup> the mechanism underlying the increase in the characteristic Schiff's base frequency upon protonation remains obscure. Both the resonance structures (16,17) and the increase in the reduced mass of the nitrogen

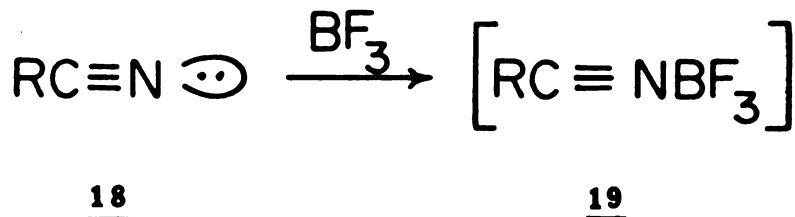
suggest that the C=N vibrational frequency should decrease.



In the visual pigments and their model compounds the frequency increase associated with the C=N stretching mode upon protonation has been attributed to the interaction between the C=N stretching mode and the C=N-H bending mode.<sup>4,5,8,11,13</sup> The presence of this new internal coordinate, (i.e. the C=N-H bending), is reflected in the C=N vibrational frequency by the C=N-H (bending) and C=N/C=N-H (stretch-bend) interaction force constants. As pointed out by Marcus et al.<sup>13</sup>, however, the stretch-bend interaction model can not account for the increase in the C=N vibrational mode which occurs when retinal Schiff's base derivatives are methylated instead of protonated.

Increases in the unsaturated carbon-nitrogen stretching vibrational frequency upon reaction with a Lewis acid have been reported for other systems. For example, I.R studies on ketimines ( $R^1R^2C=NR$ ) indicate that the increase in the frequency of the C=N stretching mode when the nitrogen lone pair is shared with a Lewis acid substituent (e.g.  $H^+$ ,  $BF_3$  or  $BCl_3$ ) results from an increase in the C=N bond order.<sup>67</sup>

Similarly, when nitriles (18) react with Lewis acids such as  $\text{BF}_3$  (19) and  $\text{BCl}_3$ ,



the  $\text{C}\equiv\text{N}$  stretching mode increases in frequency. This behavior has also been attributed to an increase in the  $\text{C}\equiv\text{N}$  stretching force constant and to a decrease in the  $\text{C}\equiv\text{N}$  bond distance.<sup>68-72</sup> Because of the structural analogies between these species and the Schiff's base system, these results suggest that a similar mechanism may occur for the Schiff's base  $\text{C}=\text{N}$  group.

#### D. Description of the Work to be Presented.

In the work described here, absorption, nuclear magnetic resonance and Raman spectroscopic studies have been carried out on aromatic and retinal Schiff's bases and protonated, deuterated,  $\text{BBr}_3$ ,  $\text{BCl}_3$  and  $\text{BF}_3$  complexed derivatives. The aromatic Schiff's bases serve as simple models for the aromatic metalloporphyrin systems and protonation of the above systems also allows us to compare the behavior of the  $\text{C}=\text{N}$  group in aromatic vs linear polyene Schiff's bases. The  $\text{BF}_3$ ,  $\text{BCl}_3$  and  $\text{BBr}_3$  adducts are very useful complexes for studying the behavior of the  $\text{C}=\text{N}$  stretching frequency when the nitrogen lone pair is encumbered by a Lewis acid other than the proton. Complexation of trans-retinal Schiff's base

(5a) with a general Lewis acid, such as  $\text{BF}_3$ , should remove the C=N-H bending interaction effects (i.e. the C=N-H bending is substituted by the C=N-B motion) on the C=N stretching frequency while maintaining delocalization of the  $\pi$  system and thus provide a means by which to test the C=N stretch-C=N-H bend interaction or mechanical coupling hypothesis.

Absorption spectroscopy was useful in the characterization of the Schiff's bases and their Lewis acid derivatives. The magnetic technique (NMR) was employed to observe the effect of the protonation on the atoms near the C=N group. Raman and resonance Raman spectroscopy were used to determine the frequencies of the vibrational modes associated with the Schiff's base models and, in particular, to note the behavior of the C=N stretching frequency upon changes in the conjugation, protonation, and Lewis acid adduct formation.

The spectroscopic results show<sup>73-76</sup> that upon protonation of the Schiff's bases, there is a marked red shift in the absorption maximum, the near by protons of the imine group shift downfield and the C=N stretching frequency increases. Similar trends in the absorption maxima and changes in the C=N stretching frequency are observed upon the reaction of the free Schiff's base with  $\text{BF}_3$ ,  $\text{BCl}_3$  and  $\text{BBr}_3$ .

With this work in mind, ab initio electronic structure calculation for methylimine and its protonated derivative at the Generalized Valence Bond<sup>77</sup> (GVB) and Self Consistent Fields<sup>78</sup> (SCF) levels were carried out. The GVB calculations show [73] that upon protonation of methylimine there

is a reorganization of the electronic character of the nitrogen lone pair in such a way that the C=N bond order increases (we call this effect the rehybridization model) and surprisingly, the nitrogen appears to be partially negatively charged.

Finally, numerical calculations within the normal coordinate analysis framework, were conducted for the models  $\text{CH}_2=\text{NH}$  and  $\text{CH}_3\text{HC}=\text{NCH}_3$  and their protonated, deuterated and  $\text{BF}_3$  derivatives to explore the predictions of the stretch/bend interaction model in light of a restricted set of force constants and to determine the effect of the increase in the C=N bond order (rehybridization model) on the C=N stretching frequency. The results of these analyses indicate that the electron density redistribution (i.e. rehybridization of the C=N bond) which increases the C=N stretching force constant upon protonation of Schiff's bases plays a major role in determining the increase in the C=N stretching frequency.

## CHAPTER 2

### MATERIALS, INSTRUMENTATION AND METHODS

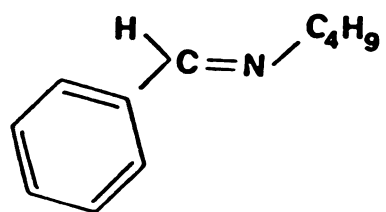
#### A. Materials

Benzaldehyde, trans-retinal, methylamine, n-butylamine, tert-butylamine, benzophenone, bromo-bencene, benzonitrile and the Lewis acids,  $\text{BCl}_3$ ,  $\text{BBr}_3$  and  $\text{BF}_3$ , were obtained from Aldrich Chemical Co. 2-naphthaldehyde and 9-anthraldehyde were obtained from Alfa Products. The solvents used,  $\text{CH}_2\text{Cl}_2$ ,  $\text{HCCl}_3$  and DMSO (dimethyl sulfoxide), were freshly distilled and kept in a dry nitrogen atmosphere over  $5\text{\AA}$  molecular sieves. Benzaldehyde was purified by distillation in vacuum, 2-naphthaldehyde and 9-anthraldehyde were re-crystallized from a methanol-water mixture. All the other starting materials were used with no further purification.

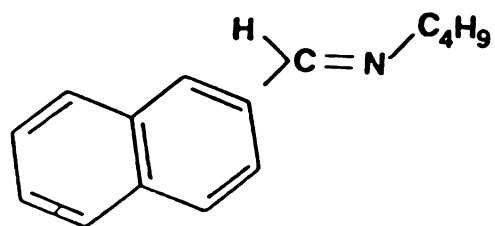
#### B. Synthesis of Imines

N-benzylidene-n-butylamine (Figure 4a), 2-naphthylidene-n-butylamine (Figure 4b), and 9-anthrylidene-n-butylamine (Figure 4c) were prepared by reaction of the appropriate aldehyde in 4h reflux with dry benzene containing an excess of n-butylamine. Following completion, excess n-butylamine and benzene were removed by vacuum evaporation. N-benzylidene-n-butylamine was purified by distillation in a vacuum, while 2-naphthalidene Schiff's base was purified by a sublimation technique. Retinylidene-n-butylamine (Figure 4d) was prepared by two different routes. One employed the same procedures as for the aromatic

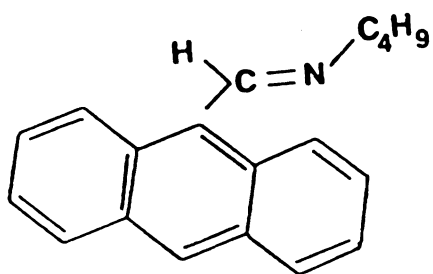
- Figure 4. a. N-benzylidene-n-butylamine.**
- b. 2-naphthylidene-n-butylamine.**
- c. 9-anthrylidene-n-butylamine.**
- d. All-trans-retinylidene-n-butylamine.**
- e.  $\alpha'$ -phenylbenzylidene-n-butylamine.**
- f.  $\alpha'$ -phenylbenzylideneamine.**



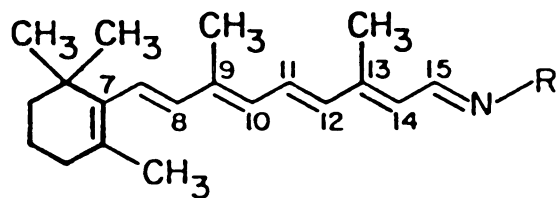
A



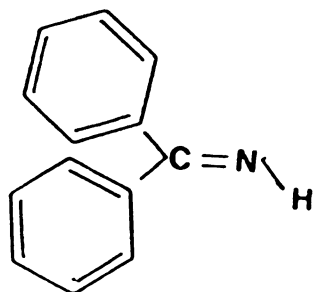
B



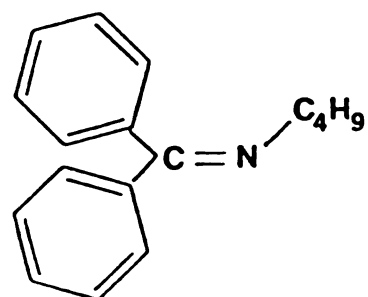
G



D



E



F

Figure 4

imines. The other involved combining the corresponding retinal isomer with an excess of n-butylamine in ethanol. This solution was mixed at 0 °C for 2hr under a stream of nitrogen and freeze-dried.<sup>14</sup> The two preparative techniques gave product which produced the same spectroscopic results.

### C. Synthesis of Ketimines

$\alpha$ -phenylbenzylidene-n-butylamine<sup>80</sup> (Figure 4e) was obtained as the reaction product between benzophenone and the amine with aluminum chloride as catalytic agent.  $\alpha$ -phenylbenzylideneamine (Figure 4f) was prepared by means of a reaction between a bromo-benzene-magnesium complex (Grignard reagent) and benzonitrile.<sup>81</sup> The Grignard-nitrile complex was prepared by the dropwise addition of 0.45 mole of the nitrile to a stirred Grignard reagent prepared from 0.50 mole of the corresponding halide and 0.51g of magnesium in 300 ml of anhydrous ether, followed by a 24 hr. reflux. After cooling to room temperature, the complex was decomposed by the dropwise addition of 100 ml of anhydrous methanol (40 min). This last reaction was very vigorous. Completion of the decomposition gave a slurry solid. The slurry was filtered, and the filtrate was vacuum distilled. The ketimine was collected between 125-130 °C.

### D. Schiff's bases: Lewis acid Derivatives

Protonated and deuterated derivatives were obtained by adding equivalent amounts of dry HCl(g) or DCl(g) to the corresponding imine

solutions, by bubbling the acid through a solution of the Schiff's base in ether until precipitation was completed, or by bubbling the acid in the solvent and then adding equivalent amounts of the acidified solvent to the Schiff's base solution. The products obtained following the three methods gave identical spectroscopic results.

The aromatic and polyene Schiff's bases Lewis acids derivatives ( $\text{BF}_3$ ,  $\text{BCl}_3$ ) were prepared by reacting a stoichiometric amount of the Lewis acid with the particular imine (i.e. benzaldehyde, 2-naphthaldehyde and retinal Schiff's base) in dimethyl sulfoxide (DMSO). The trans-retinal Schiff's base: Lewis acid complexes in  $\text{CH}_2\text{Cl}_2$ , were prepared by adding to the retinal Schiff's base solution in  $\text{CH}_2\text{Cl}_2$  an equivalent amount of 0.001M solution of the corresponding Lewis acid ( $\text{BCl}_3$ ,  $\text{BBr}_3$ ,  $\text{BF}_3$ ) in  $\text{CH}_2\text{Cl}_2$ . All reactions were carried out after degassing solvents and imine solutions in a nitrogen environment. The transfer of the Lewis acid to the solvents or to the Schiff's base solutions was carried out in a dry nitrogen environment in dry, preheated glassware.<sup>82</sup> The solids were washed with ether and dried and stored in a dry nitrogen atmosphere. The formation of the Schiff's bases from its parent aldehydes was, in general, indicated by a blue shift of the absorption spectra while the formation of the Schiff's base complex was indicated, relative to the free base, by a red shift of the spectrum.<sup>23-25,60-66</sup>

### E. Instrumentation and Calculations

Optical spectra were recorded with a Perkin Elmer Lambda 5, UV/Vis spectrophotometer. Concentration of the neutral, protonated and Lewis acid ( $\text{BF}_3$ ,  $\text{BBr}_3$ ,  $\text{BCl}_3$ ) Schiff's base complexes were typically  $1.0\text{--}5.0 \times 10^{-4}\text{M}$  in methylene chloride, chloroform or dimethyl sulfoxide for the optical measurements. For the 250-MHz NMR spectra, benzaldehyde and its corresponding imine were prepared in deuterated chloroform; protonated and deuterated derivatives were obtained by adding equivalent amounts of dry HCl or DCl gas.

In the Raman experiments, the incident laser frequency was directed through the bottom of a clear cuvette or spinning cell that contained the sample. The scattered light was collected at  $90^\circ$  to the incident beam (see Figure 5), focused and passed through a polarization scrambler. Following dispersion by the double monochromator (Spex 1401), the various light frequencies were selectively focused upon a cooled photomultiplier (RCA C31034). Photon counting electronics were used and the scattered intensity versus frequency was displayed on a chart recorder. Static and spinning cell arrangements were used for the experiment.

Raman spectra of the aromatic Schiff's bases and their derivatives ( $\sim 0.1\text{--}0.25\text{ M}$  in the different solvents) were obtained by using two different laser excitation frequencies:  $\lambda_{\text{ex}}=647.1\text{ nm}$  (from a krypton ion spectra Physics model 164-11) for 2-naphthalidene and 9-anthralidene derivative and  $\lambda_{\text{ex}}=514.5\text{ nm}$  (from an argon ion Spectra Physics model 164) for the other samples. Resonance Raman spectra of the retinal

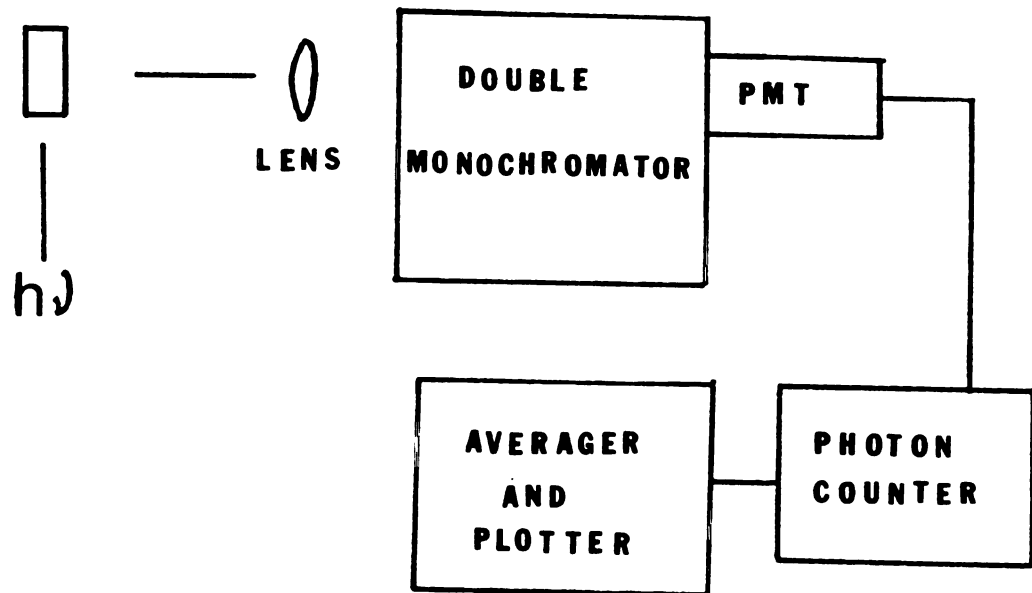


Figure 5. Schematic Raman Spectrometer

Schiff's base derivatives were recorded by using 441.6 nm excitation from a helium-cadmium laser.

A scan speed of 50  $\text{cm}^{-1}/\text{min}$ , a time constant of 2.5 sec and 5  $\text{cm}^{-1}$  spectral resolution were used in recording the Raman spectra on a Spex 1401 double monochromator. For recording the Raman spectra of the light sensitive retinal Schiff's bases and derivative, a spinning cell system, consisting of a quartz cylindrical cell, spinning on a precision ball bearing (Model 00-450-082885 from Detroit Ball Bearing Co.) and connected by a O-ring ( 568-026 from Detroit Ball Bearings Co.) to a motor ( 5.25 v and 4500 rpm model 1950 from C and H Sales Co.) (see Figure 6), was developed and constructed at Michigan State University.

1. Ab Initio Calculations. The ab initio C=N bond distance and C=N stretching force constant were determined for methylimine and methylenimmonium ion under the SCF (Self Consistent Field)<sup>78</sup> and GVB (Generalize Valence Bond)<sup>77</sup> formalisms. All calculations were carried out by using the Argonne National Laboratory collection of Electronic Structure Codes (QUEST-164). In particular, the integrals were done by using the program ARGOS written by Pitzer<sup>83</sup> and the GVB calculations were done by using the program GVB 164 written by R. Bair.<sup>84</sup> The calculations were done on an FPS 164 attached array processor. The details of the calculations and results will be discussed in Chapter 4.

**Figure 6. Schematic Spinning Cell**

**a. Plataform supporting system.**

**b. 5.25 v motor.**

**c. Quartz spinning cell.**

**d. Ball bearing.**

**e. O-ring.**

**f. Distance in mm.**

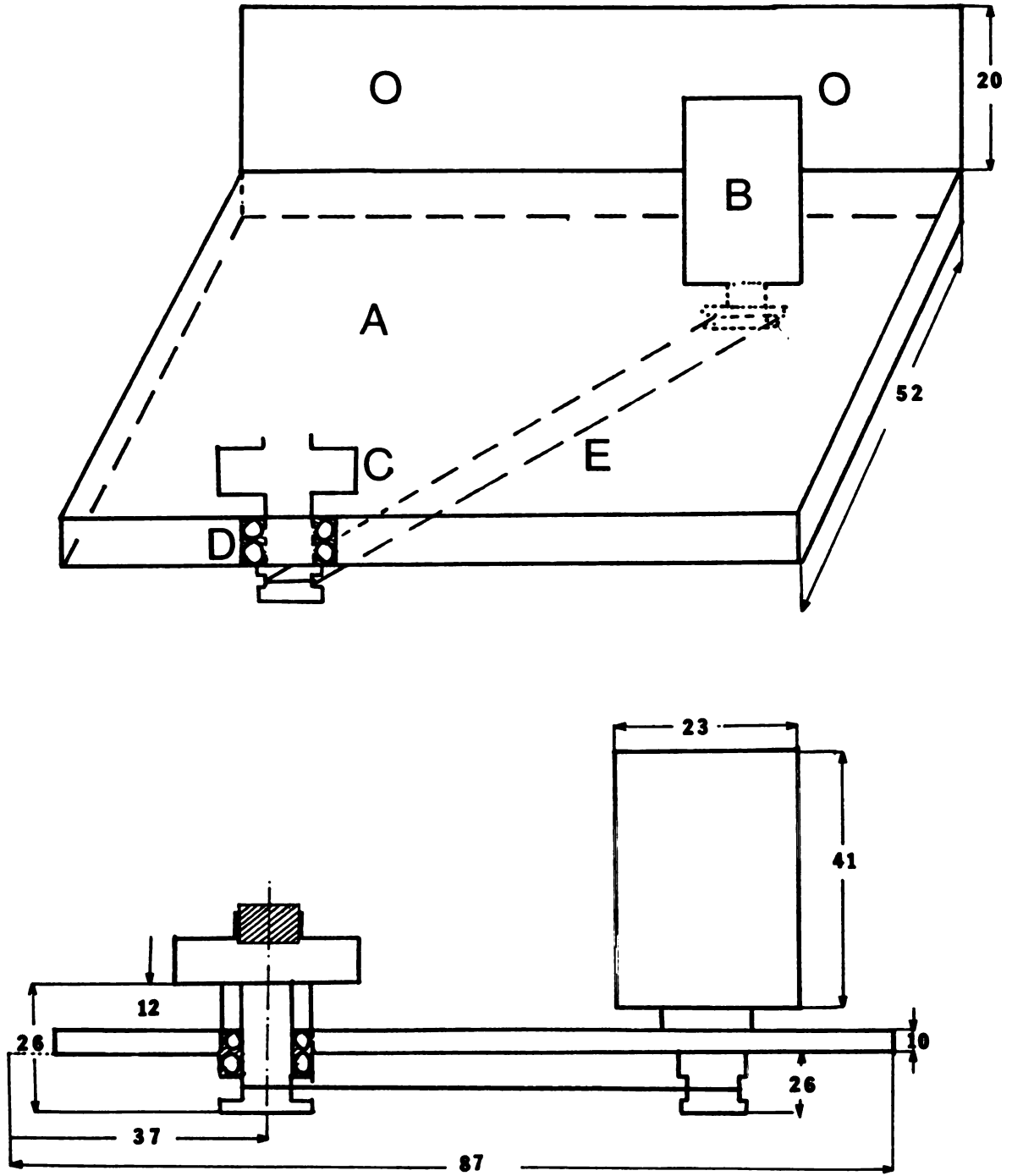


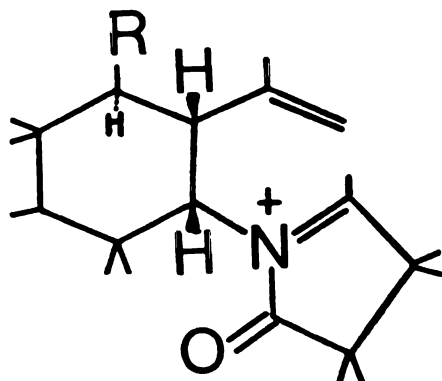
Figure 6

2. Normal Coordinate Analysis. In-plane vibrational frequencies and the corresponding potential energy distribution for methylimine, for a hypothetical methylenimmonium ion and for the model structure  $\text{CH}_3\text{CH}=\text{NCH}_3$  and the corresponding isotopically substituted derivatives were calculated by using the Shimanouchi normal coordinate analysis programs.<sup>85,86</sup> For the specific details of the calculations and results see Chapter 5.

CHAPTER 3  
SPECTROSCOPIC STUDIES

A. Introduction.

Vibrational spectroscopic studies provide a powerful means of elucidating donor-acceptor interactions through a comparison of the vibrational frequencies of the complex with those of free acid and base. The present study is centered on the specific effects that these interactions can have on the optical absorption and vibrational properties of the Schiff's bases upon complexation of the nitrogen lone pair electrons of the C=N linkage with Lewis acids such as  $H^+$ ,  $BF_3$ ,  $BCl_3$ , and  $BBr_3$ . The interest in the optical and vibrational properties of the Schiff's bases and their complexed derivatives derives from the important role that the C=N linkage plays in biological systems (see Chapter 1), in organic syntheses via the cyclization of *n*-acyliminium ions (20) of naturally occurring alkaloids<sup>87</sup>, and in the nature of intramolecular electron transfer in olefin-N-heteroaromatic salt systems.<sup>88</sup>



20

Most of our present knowledge on the spectroscopic properties of the

chromophores containing the C=N bond comes from the pyridoxal<sup>18-22</sup> and retinal Schiff's bases model systems and from the biologically occurring pyridoxal enzymes and photopigments, rhodopsin and bacteriorhodopsin.<sup>1-17</sup> Also, scattered studies on porphyrin Schiff's bases and aromatic ketimines are present in the literature.<sup>23-25,47</sup> However, a systematic investigation of saturated, unsaturated and aromatic Schiff's bases and their Lewis acid complexes (i.e.  $H^+$ ,  $BF_3$ ,  $BCl_3$  and  $BBr_3$ ) has not appeared. Rather, most reports deal with compounds specific to the problem at hand. Thus, the C=N stretching frequency for saturated aldimines was assigned by Fabian et al.<sup>58,59</sup> to the 1665-1674  $cm^{-1}$  range. This work was extended by Steele<sup>89</sup> compounds with frequencies in the to 1665-1680  $cm^{-1}$ . Aromatic aldimines of the type  $C_6H_5-CH=N-R$  present the C=N stretch in the 1658-1629  $cm^{-1}$  region and in the 1637-1626  $cm^{-1}$  range when the R group is substituted by a phenyl group<sup>89</sup>. Witkop et al.<sup>18</sup> in a study of possible pyridoxal models indicates a 1639-1626  $cm^{-1}$  range for aromatic Schiff's base models. A further reduction in the vibrational frequency of this mode is obtained when the number of substituent phenyl rings increases.<sup>89</sup>

In general, these reports show that the region over which the C=N stretching frequency occurs in uncomplexed Schiff's bases is relatively extensive and that the physical and chemical environment of the C=N group, including factors such as the presence of electron donating or electron withdrawing substituents, conjugation effects, resonance effects and hydrogen bonding, contribute to the C=N stretching frequency variations.

More extensive insight into the spectral changes of a system containing the C=N chromophore comes from resonance Raman vibrational studies of the retinal Schiff's bases and their derivatives. These studies have helped to develop an understanding of the relationship between the vibrational properties of these species and the different conformations that the polyene can assume in rhodopsin, bacteriorhodopsin and their respective photocycle intermediates. Heyde et al<sup>12</sup>, Mathies et al<sup>2,35</sup> and other workers<sup>4,15,90</sup> recognized that the vibrational spectrum of retinal Schiff's base isomers provides a characteristic vibrational fingerprint region (i.e. 1100 - 1400 cm<sup>-1</sup>) unique to its molecular structure. For example, conversion of all-trans retinal to its Schiff's base causes a 50 cm<sup>-1</sup> increase ( see 5a, Chapter 1) of the C<sub>14</sub>-C<sub>15</sub> stretching frequency (i.e. from 1111 cm<sup>-1</sup> to 1161 cm<sup>-1</sup>). In addition to the shift of the C<sub>14</sub>-C<sub>15</sub> normal mode, other C-C frequencies in retinal Schiff's base and protonated species have been found to be altered.<sup>35</sup> In this regard, the use of <sup>2</sup>H and <sup>13</sup>C isotopic derivative has been key to assessing the C-C, C=C and C-H vibrational modes. More detailed discussion of the trans-retinal Schiff's base and protonated derivatives vibrations can be found in the extensive work by Mathies et al<sup>2,11,36</sup> The identification of the all-trans-retinal vibrational frequencies has been used as the reference point to distinguish the presence of other isomers, i.e. 9-cis, 11-cis and 13-cis retinal protonated Schiff's bases in the photopigments intermediates.

It appears, as discussed in Chapter 1, that co-ordination of Schiff's bases (i.e.C=N) with Lewis acid acceptor like H<sup>+</sup> or BF<sub>3</sub> increases the C=N stretching frequency. For example, reaction of alkene ketimines with the

above Lewis acids increases the C=N stretching frequency from  $1610\text{ cm}^{-1}$  to  $1672\text{ cm}^{-1}$ . Similarly, aromatic ketimines show increases of the order of  $7\text{-}64\text{ cm}^{-1}$  upon protonation<sup>67</sup> and protonation of retinal Schiff's bases produces a  $35\text{ cm}^{-1}$  increases in the same vibrational mode i.e. from  $1620\text{ cm}^{-1}$  to  $1655\text{ cm}^{-1}$ .<sup>1-17</sup> This increase in the C=N vibrational frequency is surprising because it might be expected that co-ordination would cause, in analogy to carbonyl compounds<sup>91-93</sup> of the general type  $\text{RHCOX}$ , a lowering of the C=N bond order and hence lengthening of the C=N bond, with a consequent decrease in the Schiff's base (C=N) stretching frequency. From this point of view, as indicated in Chapter 1, the C=N frequency increases associated with the visual pigments, and Schiff's bases in general, have been attributed to the interaction between the C=N stretching mode and the C=N-H bending vibration.<sup>4,5,8,11,13</sup>

However, the fact that increases in the C=N stretching frequency are observed for a large variety of substituted Schiff's bases (e.g. aromatic, alkene, polyene and porphyrin) Lewis acid complexes and that the corresponding C=N-H or C=N-B bending motion are expected to be at very different vibrational frequencies leads us to the idea of testing the stretch-bend interaction model. In order to achieve this task, we have studied the vibrational properties of the C=N stretching motion in a set of aromatic imines and ketimines as a function of increasing the ring size substituents and in terms of the interaction between the Schiff's base bond and the Lewis acids  $\text{H}^+$ ,  $\text{BF}_3$ ,  $\text{BCl}_3$  and  $\text{BBr}_3$ . Similarly, we have studied the effects of Lewis acid complexation of the nitrogen lone pair electrons (in retinal Schiff's bases) on the absorption maximum and C=N stretching frequency of the model chromophore. In principle,

complexation of the retinal Schiff's bases with Lewis acids, other than the proton, can help to determine whether the optical absorption red shift in the protonated species is a unique property of the protonated complexes (due, for example, to the presence of a counter ion or to mechanical coupling) or is a general property that follows the encounter of the nitrogen lone pair with any Lewis acid. The results of this study and the effects on the C=N stretching frequency in the complexed aromatic and polyene Schiff's bases are below.

#### B. Spectroscopic Results.

1 Imines. Figure 7 shows Raman spectra of N-benzylidene-n-butylamine Schiff's base and its protonated and deuterated derivatives in chloroform. The work on benzaldehyde<sup>104</sup> provides assignments for the ring and related vibrational motions (see Table 1). Thus, the band at  $1696\text{ cm}^{-1}$ , assigned to C=O stretching frequency in benzaldehyde, is shifted upon Schiff's base formation to  $1646\text{ cm}^{-1}$  and is assigned to the C=N stretching frequency.<sup>105,106</sup> Upon protonation, the frequency of this mode increases to  $1680\text{ cm}^{-1}$  and a new band appears at  $1425\text{ cm}^{-1}$  in Raman and at  $1418\text{ cm}^{-1}$  in IR; this band is absent in the unprotonated and deuterated Schiff's base derivatives and is assigned to the C=N-H bending motion. Deuteration of the Schiff's base increases the C=N frequency mode to  $1660\text{ cm}^{-1}$ . The highest frequency shoulder in the protonated and deuterated species is due to decomposition products. Complexation of benzylidene-n-butylamine with  $\text{BF}_3$ , in dimethyl sulfoxide (DMSO) solution, increases the frequency of the C=N normal mode to  $1690\text{ cm}^{-1}$ . Spectra of the parent aldehyde and the

**Figure 7. Raman spectra of N-benzylidene-n-butylamine (BnBI) and protonated (BnBIH<sup>+</sup>) and deuterated (BnBID<sup>+</sup>) derivatives in CHCl<sub>3</sub> solution. The highest frequency shoulder in the protonated and deuterated species is due to decomposition products.**

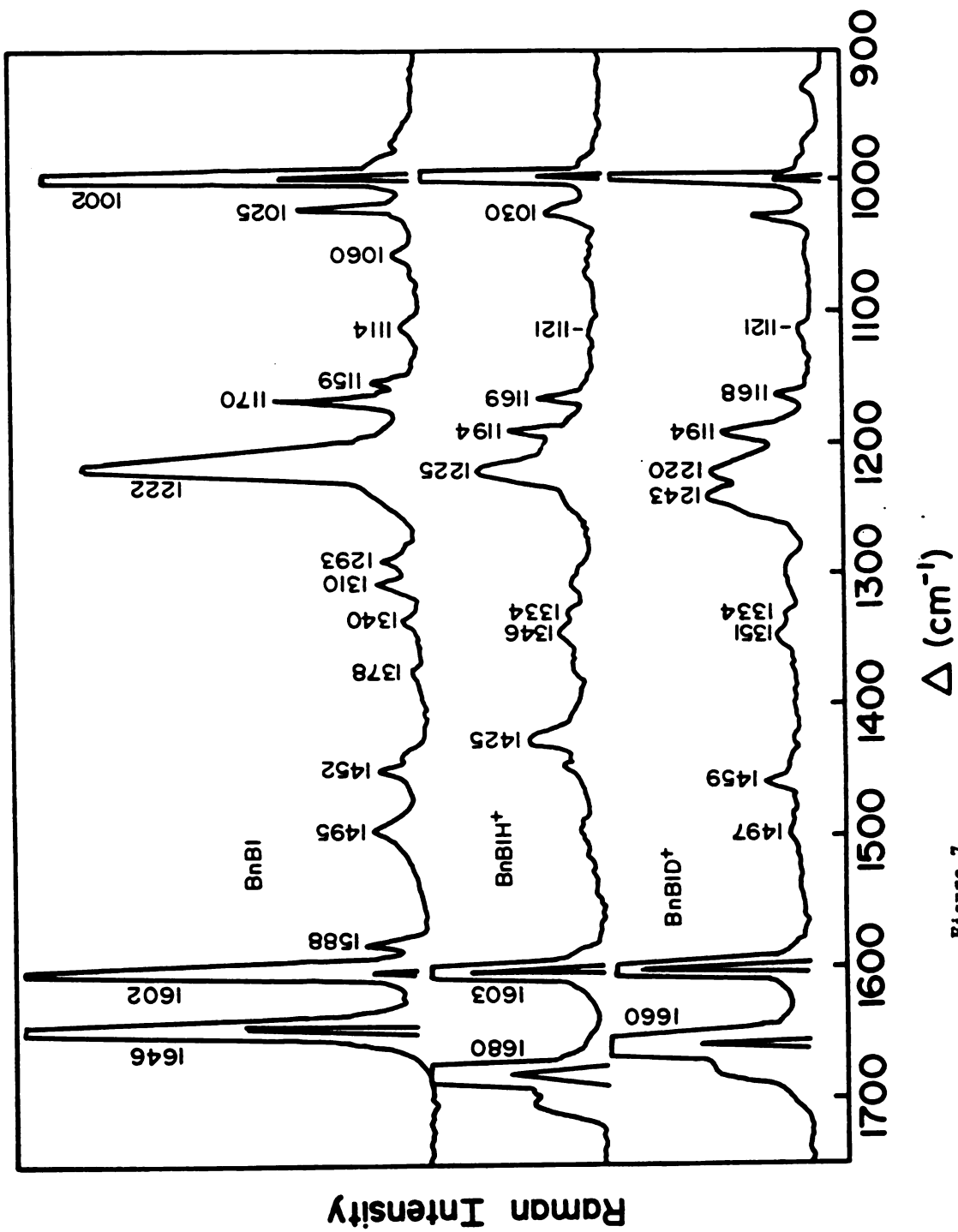


Figure 7

**Table 1** Frequency ( $\text{cm}^{-1}$ ) Assignments for N-benzylidene-n-butylamine (BnBI), and Protonated (BnBIH) and Deuterated (DnBID) Derivatives.

<u>BnBI</u>	<u>BnBIH</u>	<u>BnBID</u>	<u>Assignments</u>
1002s	1002s	1002s	$\nu_{12}$
1025m	1030m	1030m	$\nu_{19a}$
1060w	1060w	1060w	chain
1114w			
	1121w	1121w	
1159w			solvent
1170m	1169m	1168m	$\nu_{9a}$
	1194m	1194m	
1222vs	1225s	1220s	solvent
1221	1228	1224	$\phi\text{-C=N-R}^{**}$
		1243m	
1293w	1294w	1294w	$\text{CH}_2$ wag chain
	1306w	1306w	
1310w	1312w	1311w	$\nu_3$
	1334w	1334w	
1340w			
	1346w	1351w	
1378			CH aldehyde
	1425m		C=N-H bending
1452w	1451w	1459w	$\nu_{18b}$
1495m	1497w	1497w	$\nu_{18?}$
1588w			$\nu_{8a}$
1602vs	1603vs	1602vs	$\nu_{8a}$
1646s	1680s	1660s	$\nu_{\text{C=N}}$

neutral and protonated Schiff's base species in this solvent are also shown in Figure 8.

The C=N stretching frequency is sensitive to the nature of the amine used in forming the Schiff's base. For the benzaldehyde system, substitution of the n-butyl group by a methyl group shifts the C=N stretching frequency to  $1650\text{ cm}^{-1}$ . The small  $4\text{ cm}^{-1}$  increase in the C=N vibrational frequency of this species may be due to the small mass of the methyl group relative to the n-butyl derivative. Upon protonation, this mode increases to  $1684\text{ cm}^{-1}$ . The corresponding frequencies for tert-butyl substitution are  $1640\text{ cm}^{-1}$  and  $1666\text{ cm}^{-1}$ , respectively (spectra not shown).

The Raman spectra of 2-naphthalidene-n-butylamine and its protonated and deuterated Schiff's bases are shown in Figure 9. The C=N stretch increases from  $1643\text{ cm}^{-1}$  (in the neutral species) to  $1675\text{ cm}^{-1}$  upon protonation and to  $1655\text{ cm}^{-1}$  in the deuterated derivative. Similar to the protonated benzaldehyde Schiff's base derivative, the protonated 2-naphthylidene-n-butyl amine derivative shows a band at  $1420\text{ cm}^{-1}$  in the Raman spectrum which is absent in the spectra of the unprotonated and deuterated species. The Lewis acid ( $\text{BF}_3$ ,  $\text{BCl}_3$ ) complexes of the above species also show an increased C=N vibrational frequency (to  $1683$  or  $1681\text{ cm}^{-1}$ , see Figure 10). Table 2 shows the assignments for the observed vibrational frequencies; the work on naphthalene<sup>107</sup> and naphthaldehydes<sup>108</sup> have been used for the main assignments. We have also recorded vibrational spectra for Schiff's base species in a series of anthracene derivatives (spectra not show). Protonation of

**Figure 8. Raman spectra of N-benzylidene-n-butylamine (BnBI) and protonated (BnBIH<sup>+</sup>) and BF<sub>3</sub> (BnBIBF<sub>3</sub>) derivatives in DMSO solution. The solvent peaks are denoted by \*.**

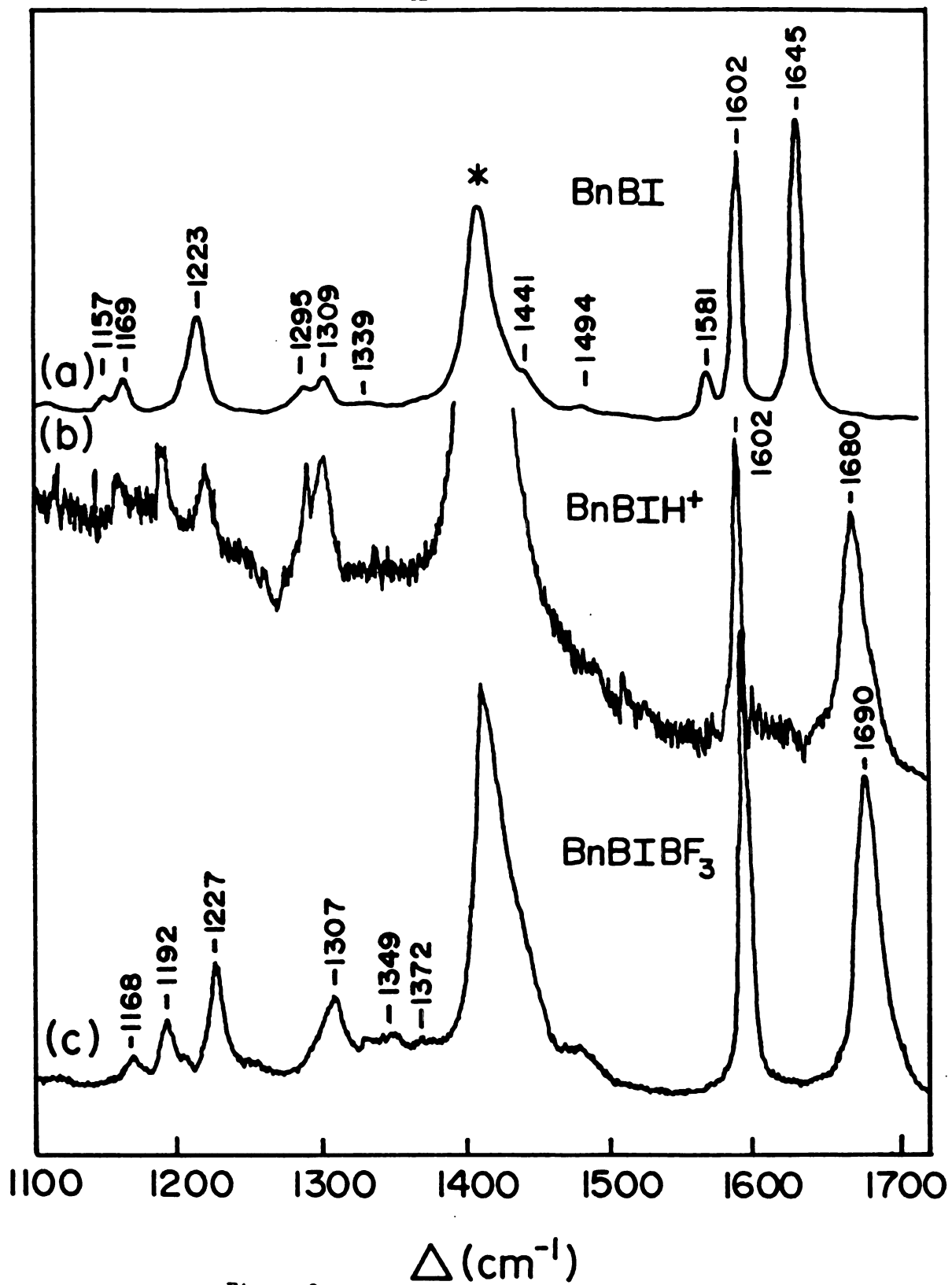


Figure 8

**Figure 9. Raman spectra of 2-naphthylidene-n-butylamine (NapBI)  
and protonated (NapBIH<sup>+</sup>) and deuterated (NapBID<sup>+</sup>)  
derivatives in CHCl<sub>3</sub> solution.**

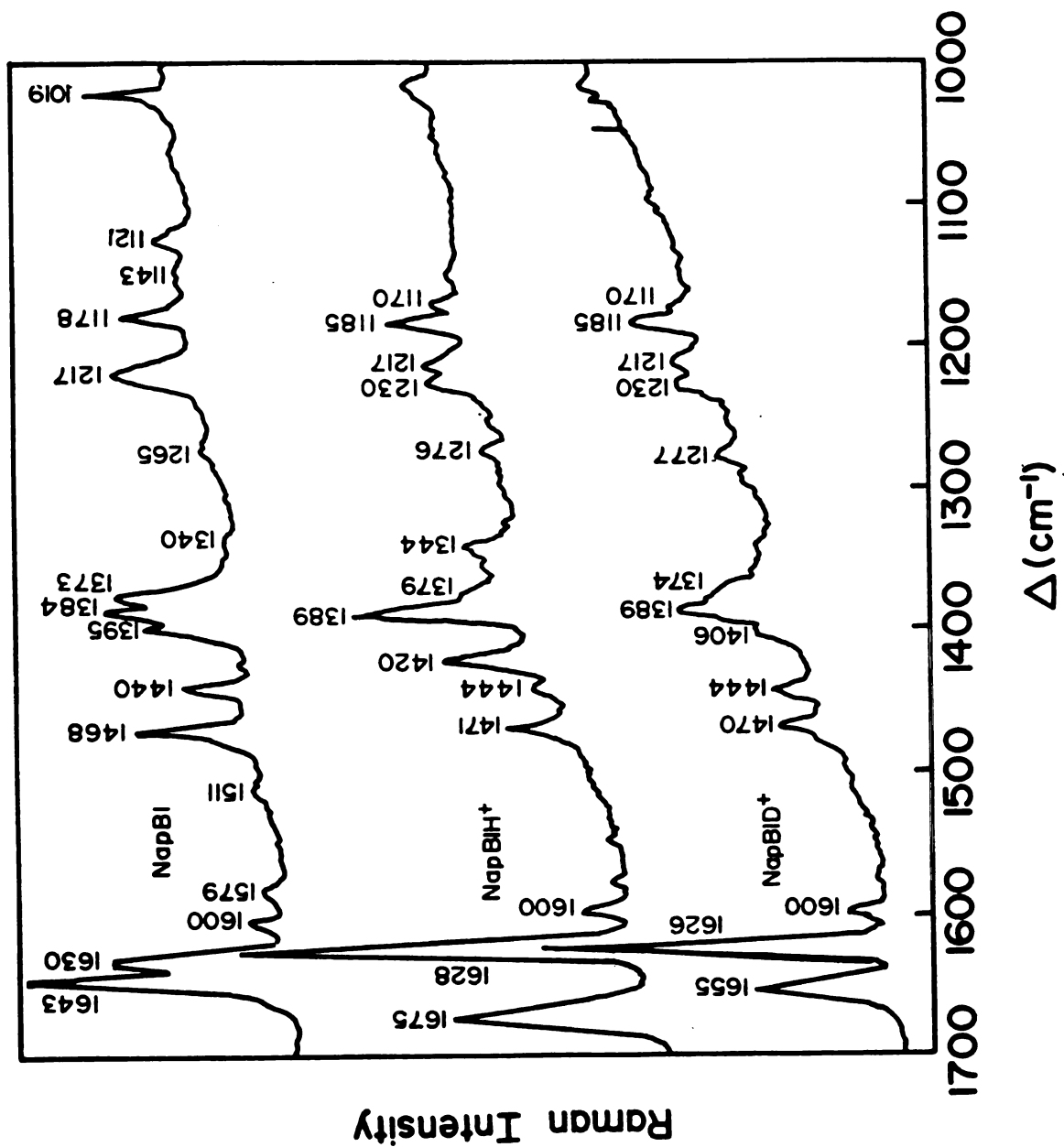


Figure 9

**Figure 10. Raman spectra of 2-naphthylidene-n-butylamine (a) and  
BCl<sub>3</sub> (b) and BF<sub>3</sub> (c) derivatives in DMSO solution.  
The solvent peaks are denoted by \*.**

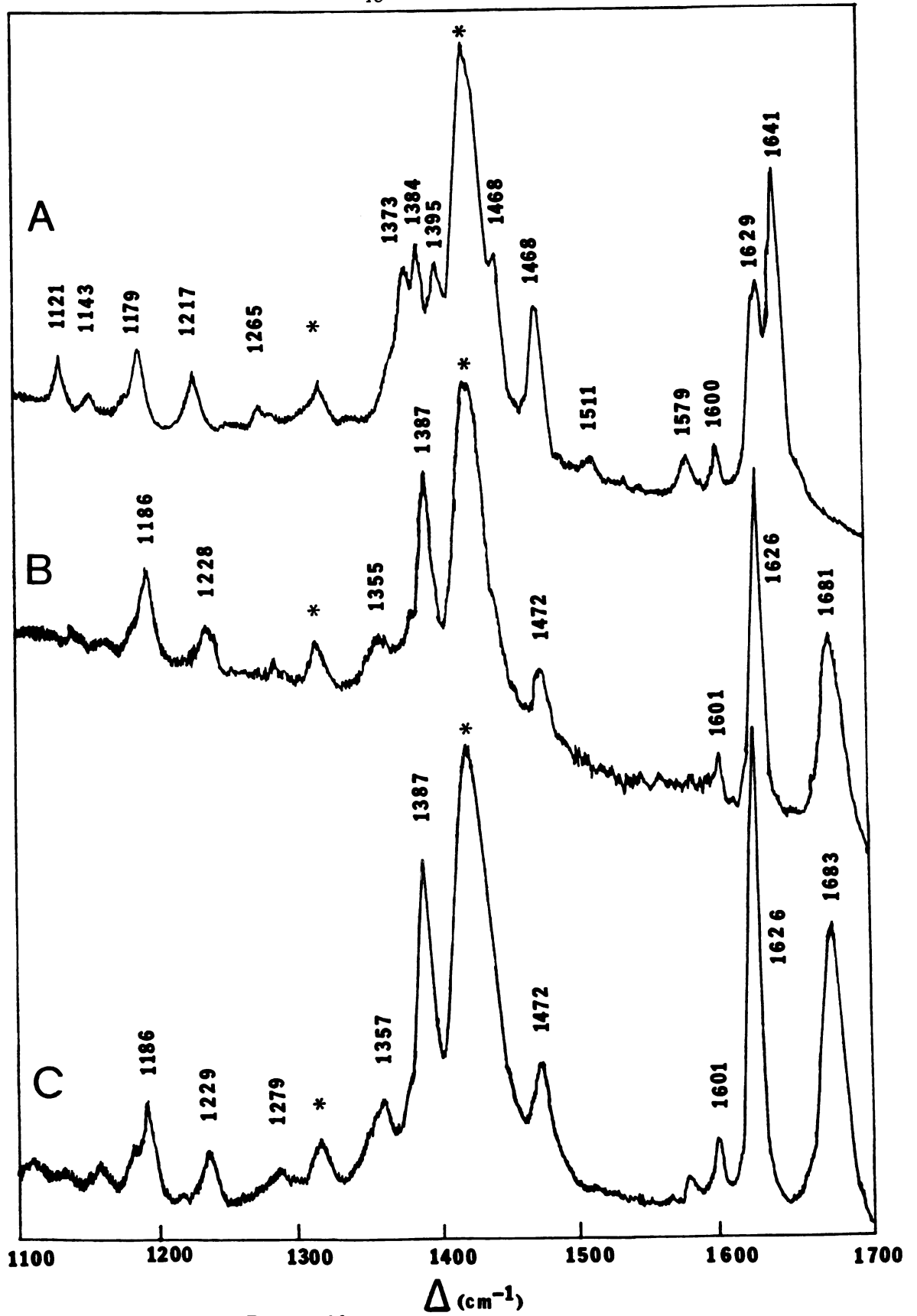


Figure 10

**Table 2** Frequency ( $\text{cm}^{-1}$ ) Assignments for 2-Naphtylidene-n-butylamine (NAPnBI), and Protonated (NAPnBIH) and Deuterated (NAPnBID) Derivatives.

<u>NAPn BI</u>	<u>NAPnBIH</u>	<u>NAPnBID</u>	<u>Assignments</u>
1019m	1019w	1019w	a <sup>1</sup>
1121w			
1143w	1143w	1143w	a <sup>11</sup>
	1170w	1170w	
1178m			a <sup>1</sup>
	1185m	1185m	
1217m	1217m	1217m	solvent (CHCl <sub>3</sub> )
	1230m	1230m	a <sup>1</sup>
1265w			skeletal
	1276w	1277w	a <sup>1</sup>
1340w	1344m		a <sup>1</sup>
1373m	1379m	1374m	a <sup>1</sup>
1384s	1389s	1389s	a <sup>1</sup>
1395s			a <sup>1</sup>
	1420s		C=N-H bending
1440m	1444m	1444m	a <sup>1</sup>
1468m	1471m	1470m	a <sup>1</sup>
1511w	1511w	1510w	a <sup>1</sup>
1579w	1579w	1579w	a <sup>1</sup>
1600w	1600w	1600w	a <sup>1</sup>
1630s	1628s	1626s	a <sup>1</sup>
1643s	1675s	1655s	C=N stretching

9-anthrylidene-n-butylamine increases the C=N stretching frequency from  $1644 \text{ cm}^{-1}$  to  $1663 \text{ cm}^{-1}$ .

The NMR spectra recorded for benzaldehyde Schiff's bases and their protonated and deuterated forms are presented in Figure 11. Table 3 collects the NMR chemical shift data for the H(a) and  $\alpha\text{-CH}_2$  protons of N-benzylidene-n-butylamine, 2-naphthylidene-n-butylamine and 9-anthrylidene-n-butylamine and their protonated and deuterated forms. The data indicate, in agreement with similar studies<sup>13,109</sup>, that a downfield shift of the H(a) and  $\alpha\text{-CH}_2$  protons occurs upon protonation or deuteration of the aromatic Schiff's bases. The splitting of the H(a) proton into a doublet and of the  $\alpha\text{-CH}_2$  into a quartet is due to the H(b) proton present on the imine nitrogen. As expected, these features are absent in the unprotonated and deuterated Schiff's bases where the (Ha) proton gives a singlet and the  $\alpha\text{-CH}_2$  protons appear as a triplet.

Linear polyene Schiff's bases are well-known to exhibit behavior analogous to that observed for the aromatic Schiff's bases: upon protonation the C=N stretching frequency increases.<sup>1-17</sup> The Raman data in Figure 12 show that the analogy extends to the retinal Schiff's base:BF<sub>3</sub> complex as well. Figure 12a shows the spectrum of the neutral Schiff's base in DMSO; the C=N stretch occurs at  $1623 \text{ cm}^{-1}$ . Protonation (Figure 12b) increases this mode to  $1654 \text{ cm}^{-1}$ . In the BF<sub>3</sub> complexed retinal Schiff's base derivative (Figure 12c) the C=N stretching mode occurs at  $1656 \text{ cm}^{-1}$ . In addition, a series of trans-retinal Schiff's base: Lewis acid complexes (BF<sub>3</sub>, BCl<sub>3</sub>, BBr<sub>3</sub>) were prepared and characterized in a less polar solvent, i.e. CH<sub>2</sub>Cl<sub>2</sub>. As expected, strong optical absorption

**Figure 11. 250-NMR spectra of benzaldehyde (a), N-benzylidene-n-butylamine (b) and its protonated (c) and deuterated (d) derivatives in  $\text{CDCl}_3$ .**

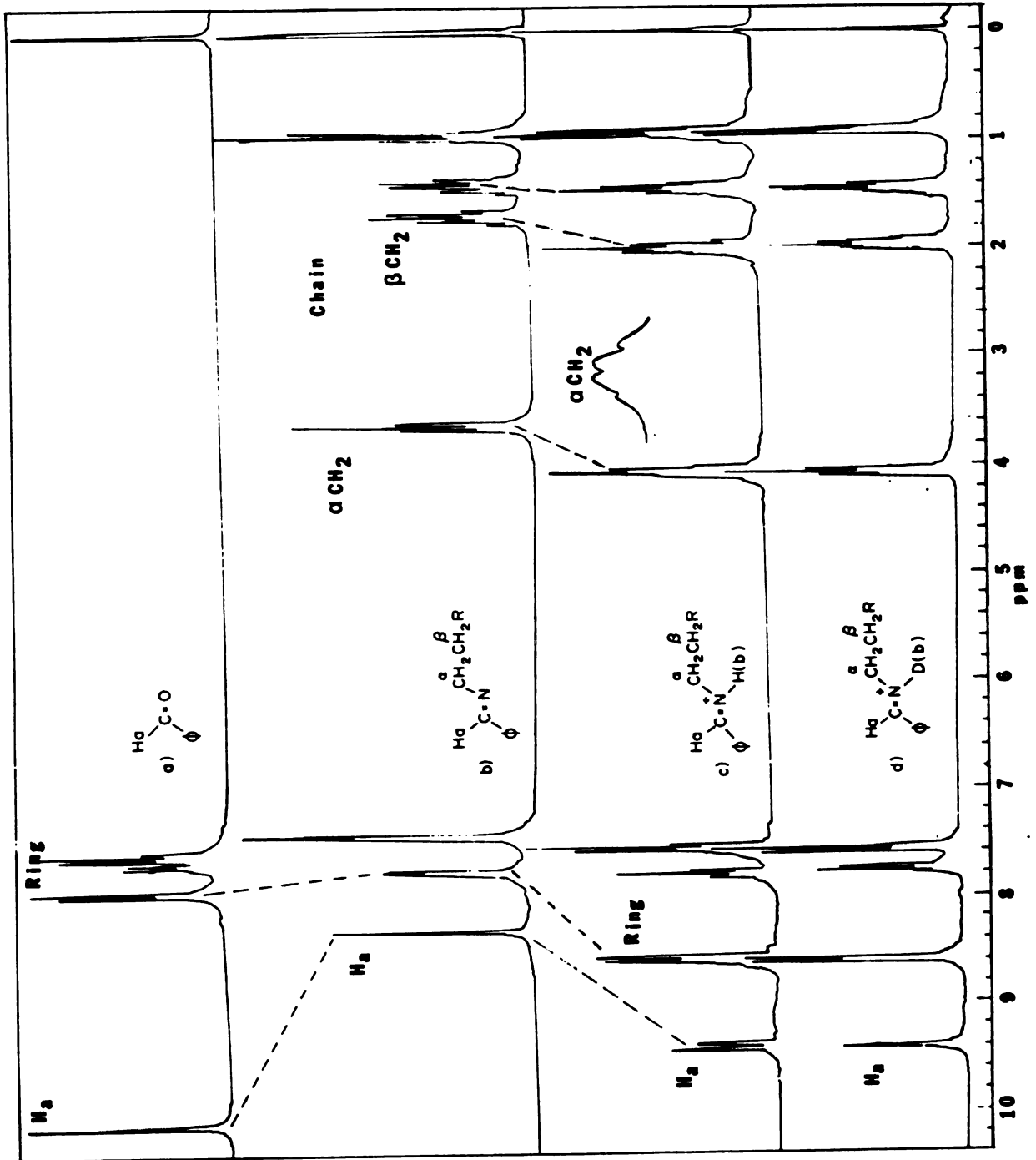
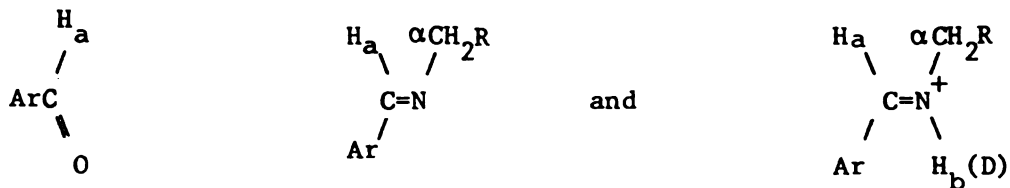


Figure 11

**Table 3 Chemical Shift for Carbonyl and Imine Protons of the Kind:**

<u>Ar</u>	<u>Substituent</u>	<u>H<sub>a</sub></u>	<u>α-CH<sub>2</sub></u>
C <sub>5</sub> H <sub>5</sub> <sup>a</sup>	Carbonyl	10.08	
	Imine	8.30 (s)	3.65(t)
	Prot. Imine	9.38 (d)	4.10(q)
	Deut. Imine	9.38 (s)	4.10(t)
C <sub>10</sub> H <sub>8</sub> <sup>b</sup>	Carbonyl	10.04 (s)	
	Imine	8.30 (s)	3.60 (t)
	Prot. Imine	8.8 (s)	3.95 (b)
	Deut. Imine	8.7 (s)	3.95 (t)
C <sub>14</sub> H <sub>10</sub> <sup>b</sup>	Carbonyl	11.32 (s)	
	Imine	9.28 (s)	3.86 (t)
	Prot. Imine	9.75 (b)	4.29 (b)

r = Propyl group; s = singlet; d = doublet; t = triplet; q = quartet;  
 b = broad. a. 250-MHz, b. 60-MHz NMR.

**Figure 12. Resonance Raman spectra of reinylidene-n-butylamine (RnB) and protonated (RnBH<sup>+</sup>) and BF<sub>3</sub> (RnBBF<sub>3</sub>) derivatives in DMSO solution. The solvent peaks are denoted by \*.**

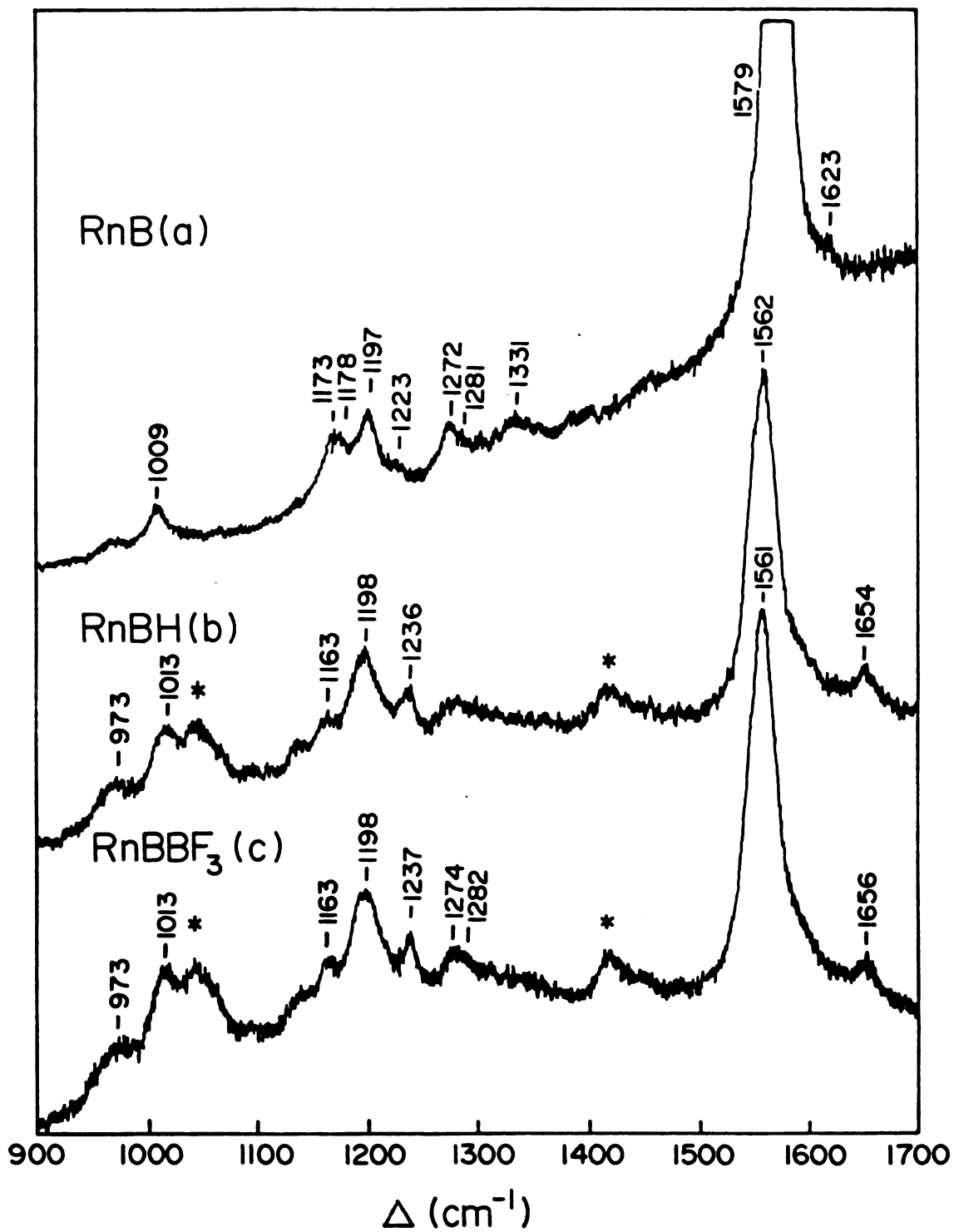
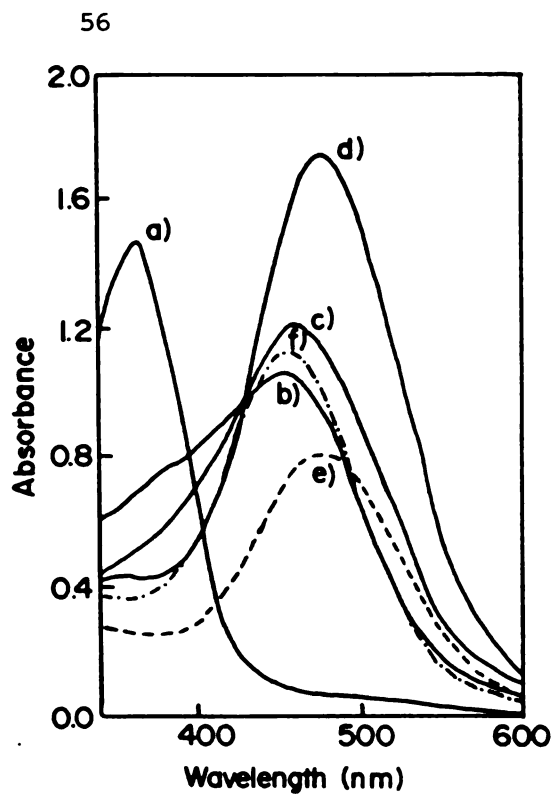
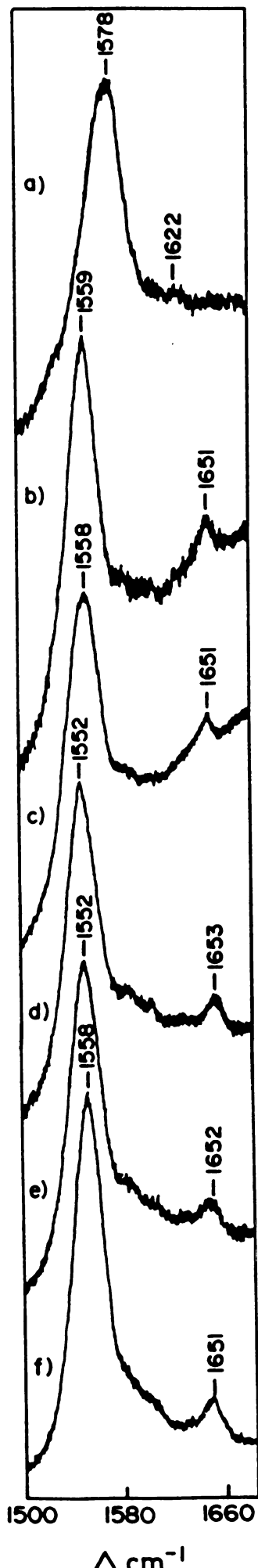


Figure 12

red-shifts are observed for these species (Figure 13). The absorption maximum for protonated Schiff's base complexes is solvent dependent, as has been pointed out by Blatz and co-workers.<sup>60,95,102</sup> Similar solvent dependencies are observed for the Schiff's base: general Lewis acid complexes (compare for example, the extent of the red-shift in the  $\text{BF}_3$  and  $\text{HCl}$  adducts in  $\text{CH}_2\text{Cl}_2$  and in  $\text{DMSO}$  in Table 4). This supports the idea that the physical phenomena underlying the behavior of protonated and general Lewis acid complexed Schiff's bases are similar. The corresponding resonance Raman data indicate, however, that the C=N stretching frequency in the Schiff's base increases by an amount similar to that observed upon protonation. For example,  $\text{BF}_3$  (Figure 13d) increases the C=N stretching frequency by  $31 \text{ cm}^{-1}$ , while in the  $\text{HClO}_4$  complex (Figure 13e) an increase of  $30 \text{ cm}^{-1}$  is seen. The other Lewis acid complexes ( $\text{BCl}_3$ ,  $\text{BBr}_3$  and  $\text{HCl}$ ) show comparable increase in the C=N stretching frequency (Figure 13). The small increase in (C=N) for the Schiff's base- $\text{BCl}_3$  complex, is similar to the observed trend<sup>68</sup> for aromatic nitriles upon complexation with  $\text{BF}_3$  and  $\text{BCl}_3$ . At this point it is useful to mention that the possibility that a retinal Schiff's base:  $\text{HF}$  complex was formed instead of the retinal Schiff's base:  $\text{BF}_3$  complex can be ruled out since the  $\text{HF}$  complexes in  $\text{CCl}_4$  and  $\text{CHCl}_3$  solutions have absorption maximum at 447 nm and 468 nm, respectively.<sup>102</sup> In these solvents, the absorption maximum for the  $\text{BF}_3$  complexes appears at 456 nm and 480 nm (Table 4), respectively.

2. Ketiminies. Figure 14 shows high frequency Raman spectra for the  $\alpha$ -phenylbenzylidene-n-butylamine system,  $(\text{C}_6\text{H}_5)_2\text{C}=\text{N}(\text{CH}_2)_3\text{CH}_3$ . For the neutral species (Figure 14a), the C=N stretching frequency appears at

**Figure 13. Resonance Raman and absorption (inset) spectra of trans-retinal Schiff's base and Lewis acid derivatives in  $\text{CH}_2\text{Cl}_2$ . (a) Trans-retinylidene-n-butylamine. (b)  $\text{BCl}_3$  complex. (c)  $\text{BBr}_3$  complex. (d)  $\text{BF}_3$  complex. (e)  $\text{HClO}_4$  complex. (f)  $\text{HCl}$  complex.**



- a. SB
- b. SB:BCl<sub>3</sub>
- c. SB:BBr<sub>3</sub>
- d. SB:BF<sub>3</sub>
- e. SB:HClO<sub>4</sub>
- f. SB:HCl

Figure 13

**Table 4 Absorption Maxima, C=C and C=N stretching Frequencies<sup>a</sup> of trans-retinylidene-n-butylamine and Lewis Acid Derivatives.**

<u>Retinal Schiff's Base</u> <u>Lewis Acid</u>	<u><math>\lambda(\text{max})</math></u>	<u>C=C</u>	<u>C=N</u>	<u>Solvent</u>
Schiff's Base <sup>(c)</sup>	364	1578	1622	CH <sub>2</sub> Cl <sub>2</sub>
BCl <sub>3</sub> <sup>(c)</sup>	452	1559	1651	CH <sub>2</sub> Cl <sub>2</sub>
BBr <sub>3</sub> <sup>(c)</sup>	458	1558	1651	CH <sub>2</sub> Cl <sub>2</sub>
BF <sub>3</sub> <sup>(c)</sup>	477	1552	1653	CH <sub>2</sub> Cl <sub>2</sub>
HClO <sub>4</sub> <sup>(c)</sup>	476	1552	1652	CH <sub>2</sub> Cl <sub>2</sub>
HCl <sup>(c)</sup>	456	1558	1651	CH <sub>2</sub> Cl <sub>2</sub>
BF <sub>3</sub> <sup>(d)</sup>	441	1561	1656	(CH <sub>3</sub> ) <sub>2</sub> SO
HCl <sup>(d)</sup>	440	1562	1654	(CH <sub>3</sub> ) <sub>2</sub> SO
BF <sub>3</sub> <sup>(e)</sup>	456	--	--	CCl <sub>4</sub>
BF <sub>3</sub> <sup>(e)</sup>	480	--	--	CHCl <sub>3</sub>

- a. Absorption maximum in nm.  
 b. Stretching frequencies in cm<sup>-1</sup>.  
 c. From Reference 97.  
 d. This work (spectra not shown).

**Figure 14. Raman spectra of  $\alpha$ -phenylbenzylidene-n-butylamine (a) and protonated (b) and deuterated (c) derivatives in methanol solution.**

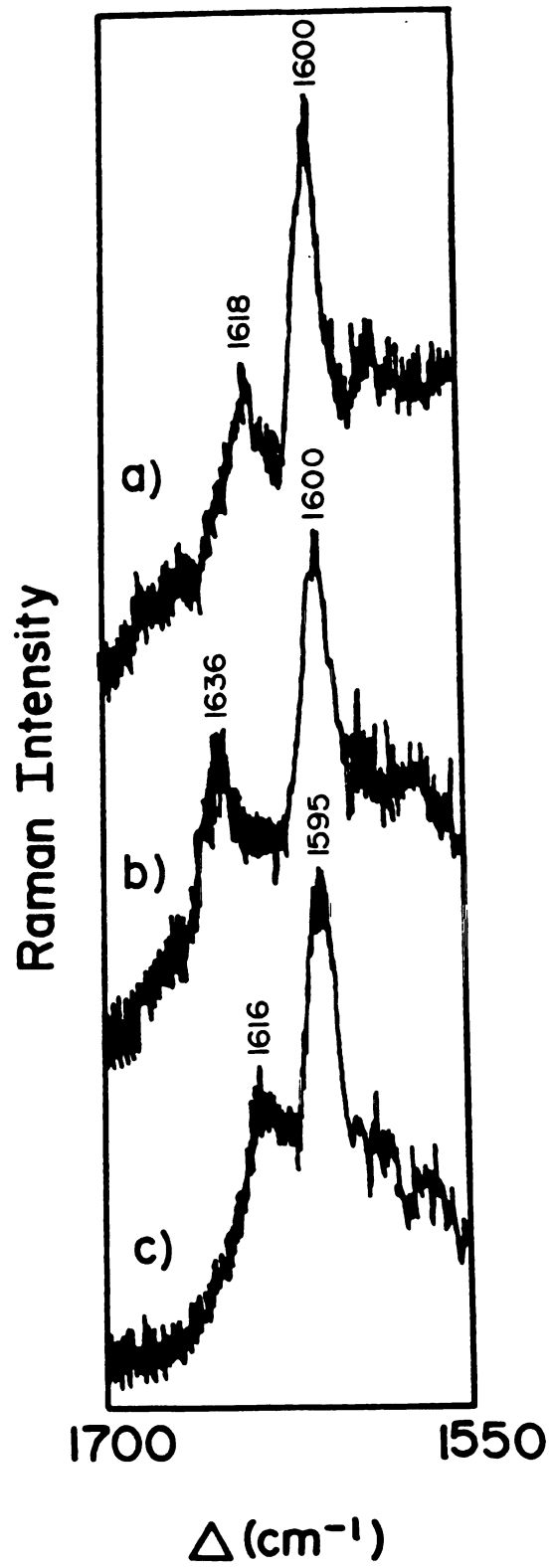


Figure 14

1618  $\text{cm}^{-1}$ ; upon protonation (Figure 14b) or deuteration (Figure 14c), this mode is shifted to 1636  $\text{cm}^{-1}$  or to 1616  $\text{cm}^{-1}$ , respectively. Figure 15 shows Raman spectra for a second ketimine system,  $\alpha$ -phenylbenzylidene amine,  $(\text{C}_6\text{H}_5)_2\text{C}=\text{NH}$ . The spectrum of the parent ketone, benzophenone, is shown in Figure 15a. The C=N stretching occurs at 1600  $\text{cm}^{-1}$  and the C=N-H bending mode appears at 1364  $\text{cm}^{-1}$  in the neutral Schiff's base (Figure 15b). These assignments are based on the isotope studies carried out by Datin et al.<sup>110</sup> Protonation (Figure 15c) increases the C=N stretching mode to 1661  $\text{cm}^{-1}$  and in the  $\text{BF}_3$  complex (Figure 15d) this mode is shifted to 1679  $\text{cm}^{-1}$ .

### C. Discussion.

1. C=N Stretching Frequency: Neutral Schiff's Bases. Table 5 summarizes aldehyde and neutral Schiff's base functional group stretching frequencies for a number of linear polyenes and aromatic species. For both classes of compounds, conjugation effects are apparent as increasing the number of double bonds leads to a decrease in the C=O and C=N stretching frequency. This trend is summarized in Figure 16, where the C=O frequency in aromatic aldehydes and the C=N frequency in the corresponding neutral Schiff's base formed by reaction with n-butylamine are plotted as functions of the number of double bonds in the aromatic system. The slopes of the two plots show that conjugation effects are more pronounced for the aldehyde group than for the neutral Schiff's base, most likely the result of the stronger electron withdrawing character of the carbonyl. For example, increasing the resonance system from benzaldehyde to a formylated metalloporphyrin brings about a change

**Figure 15. Raman spectra of benzophenone (BBO),  $\alpha$ -phenylbenzylidene-amine (EBI) and protonated (BBIH<sup>+</sup>) and BF<sub>3</sub> (BBIBF<sub>3</sub>) derivatives in DMSO. The solvent peaks are denoted by \*.**

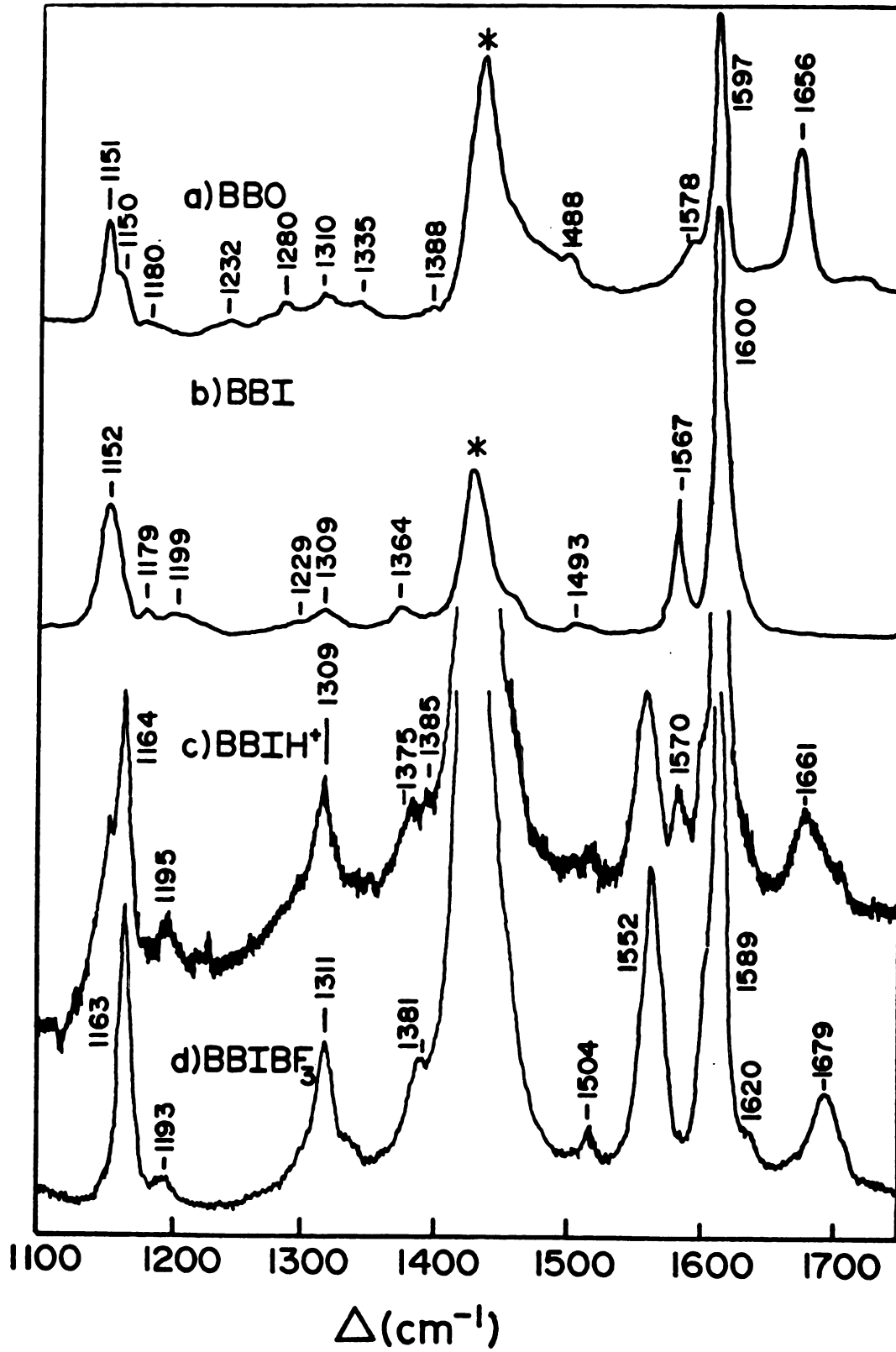


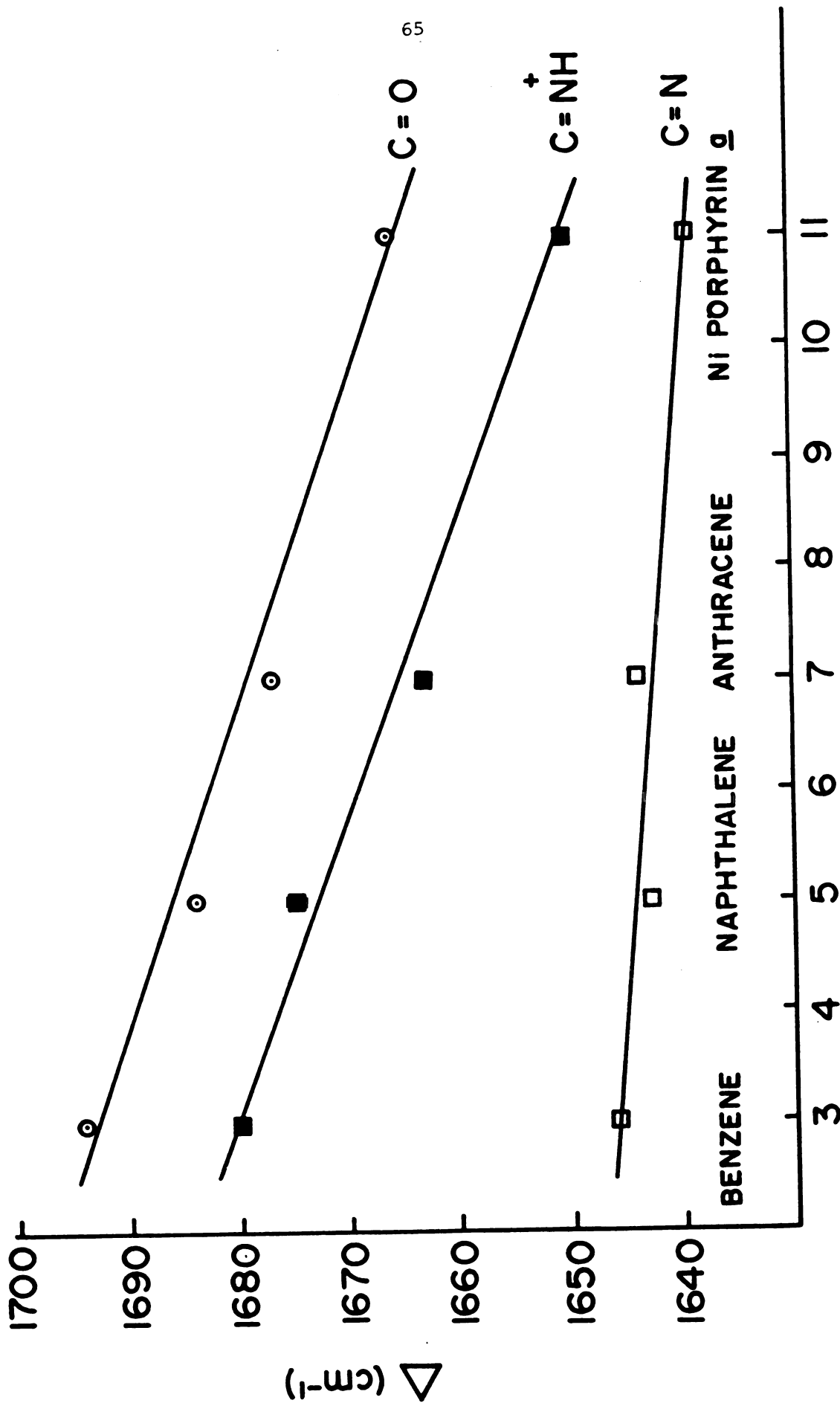
Figure 15

**Table 5 Carbonyl and Imine Stretching Frequency of Polyene and Aromatic Compounds**

Compound	C=O (cm <sup>-1</sup> )	Compound	C=N (cm <sup>-1</sup> )
CH <sub>3</sub> CHO <sup>a</sup>	1715	(CH <sub>3</sub> ) <sub>2</sub> CHCH=NCH(CH <sub>3</sub> ) <sub>2</sub> <sup>h</sup>	1667
CH <sub>3</sub> CH=CHCHO <sup>a</sup>	1690	CH <sub>3</sub> (CH=CH)CH=NCH(CH <sub>3</sub> ) <sub>2</sub> <sup>h</sup>	1658
CH <sub>3</sub> (CH=CH) <sub>2</sub> CHO <sup>a</sup>	1680	CH <sub>3</sub> CH <sub>2</sub> (CH=CH) <sub>2</sub> CH=NCH(CH <sub>3</sub> ) <sub>2</sub> <sup>h</sup>	1643
CH <sub>3</sub> (CH=CH) <sub>3</sub> CHO <sup>a</sup>	1678	Trans-retinal + hexylamine <sup>b</sup>	1625
Trans-retinal <sup>b</sup>	1673	M <sub>412</sub> chromophore <sup>i</sup>	1620
Benzaldehyde <sup>c, d</sup>	1694	N-Benzylidene-n-butylamine <sup>c</sup>	1646
Naphthaldehyde <sup>c, e</sup>	1684	2-Naphthylidene-n-butylamine <sup>c</sup>	1643
Anthraldehyde <sup>c</sup>	1677	9-Anthrylidene-n-butylamine <sup>c</sup> (C <sub>6</sub> H <sub>5</sub> )HC=N(C <sub>6</sub> H <sub>5</sub> ) <sup>k</sup>	1644 1634
Cu <sup>+2</sup> porphyrin <sup>a, f</sup>	1666	Ni porphyrin <sup>a, j</sup>	1639
(C <sub>6</sub> H <sub>5</sub> ) <sub>2</sub> C=O <sup>c, g</sup>	1665	(C <sub>6</sub> H <sub>5</sub> ) <sub>2</sub> C=N(CH <sub>2</sub> ) <sub>3</sub> CH <sub>3</sub> <sup>c</sup>	1618
		(C <sub>6</sub> H <sub>5</sub> ) <sub>2</sub> C=N(C <sub>6</sub> H <sub>5</sub> ) <sup>k</sup>	1616

a. Reference 111; b. Reference 12; c. This work; d. Reference 104;  
 e. Reference 108; f. Reference 50; g. Reference 110; h. Reference 112;  
 i. Reference 1; j. Reference 23; k. Reference 67.

**Figure 16. Effect of increasing the aromatic ring conjugation on the characteristic group frequency of aldehydes (⊙), Schiff's bases (◻) and protonated Schiff's bases (■).**



DOUBLE BONDS

Figure 16

in the C=O stretching frequency of  $28\text{ cm}^{-1}$  whereas the corresponding shift in the Schiff's base analogs is only  $7\text{ cm}^{-1}$ . Similar effects are apparent in the optical spectroscopy of these two classes of compounds<sup>23-25</sup>, that is, the optical spectra of aromatic aldehydes are more strongly red-shifted than those of the corresponding neutral Schiff's bases.

When the alkyl amine is replaced by an aromatic amine in the Schiff's base linkage, there is a decrease in the C=N frequency although this effect is still fairly small; for the benzaldehyde system, for example there is a  $12\text{ cm}^{-1}$  difference in the C=N mode for the Schiff's bases formed from n-butylamine and aminobenzene. A further reduction in the frequency of the C=N stretch (to  $1616\text{ cm}^{-1}$ ) is observed as the number of substituent phenyl rings is increased to three. These trends indicate that conjugation effects play a role in determining the C=N stretching frequency but that the dependence is fairly weak.

In comparison with the aromatic compounds, it is apparent from Table 5 that the linear polyene Schiff's bases show a much stronger relationship between C=N frequency and number of double bonds. Similar behavior has been reported for the neutral nitrile system where the C≡N frequency shows a more pronounced dependence on extent of conjugation in linear unsaturated systems than in analogous aromatic species.<sup>113</sup> For the nitrile system, these conjugation effects were suggested to be the determining factor in accounting for the frequency differences between these two classes of compounds, i.e., the interaction of the C=N  $\pi$  orbital with the  $\pi$  system of the aromatic ring is smaller than its interaction

with that of the linear, unsaturated systems. The same phenomenon appears to be in effect in the Schiff's base systems and thus we expect the extent of conjugation to be higher for the C=N group in the linear polyene Schiff's bases than in the aromatic imine Schiff's bases, with the consequent decrease in the C=N stretching frequency of the former.

## 2. C=N<sup>+</sup> Stretching Frequency: Schiff's Base/Lewis Acid Complexes.

Table 6 collects data on various Schiff's base: Lewis acid adducts which were studied in the present work or described by other workers. The dependence of the C=N<sup>+</sup> stretching frequency on the size of the conjugated system in protonated aromatic Schiff's bases is shown in Figure 16. The same type of dependence as noted above for aromatic aldehydes and neutral Schiff's bases is observed: as the number of double bonds increases the C=N<sup>+</sup> stretching frequency decreases. Moreover, the slope is steeper than in the neutral Schiff's base compounds, probably reflecting the effect of the increased electronegativity of the protonated substituent on the conjugated system.

The data in Table 6 show that the increase in C=N frequency upon complexation with BF<sub>3</sub> is comparable to that observed upon protonation. Moreover, for both of these Lewis acids (H<sup>+</sup>, BF<sub>3</sub>) the largest shifts arise for compounds in which the Schiff's base nitrogen is substituted only by protons whereas the smallest shift occurs for the fully phenyl substituted species. These observations indicate that a common mechanism is likely to be responsible for the increase in the C=N stretching frequency in both cases.

Table 6 Changes in the C-N Stretching Frequency Upon Complexation With Lewis Acids.

Complex	$\nu_{\text{CN}}$ (a)	$\nu_{\text{CNH}}^+$	$\nu_{\text{CND}}^+$	$\nu_{\text{CNA}}$	$\Delta\nu_{\text{H}^+}$ (b)	$\Delta\nu_{\text{D}^+}$	$\Delta\nu_{\text{A}}$	$\delta_{\text{CNH}}$ (c)
PhHCNC <sub>4</sub> H <sub>9</sub> (d)	1646	1680	1660	1690	34	20	43	1425
Ph <sub>2</sub> CNC <sub>4</sub> H <sub>9</sub> (d)	1618	1636	1616		18	-2		
Ph <sub>2</sub> CNH (d)	1600	1661		1679	61		79	1364
NaphCNC <sub>4</sub> H <sub>9</sub> (d)	1643	1675	1655		32	12		1420
AntCNC <sub>4</sub> H <sub>9</sub> (d)	1644	1663			19			
PhHCNMe (e)	1658	1695		1712	37		54	
PhHCNPh (e)	1634	1672		1673	38		39	
Ph <sub>2</sub> CNMe (e)	1634	1669		1661	35		27	
Ph <sub>2</sub> CNPh (e)	1616	1623		1621	7		5	
Bu <sub>2</sub> CNH (e)	1610	1670		1672	60		62	
Ni-porphyrin <u>a</u> (f)	1639	1650	1640		11	1		
M <sub>412</sub> (g)	1620							
Rhodopsin (g)*		1655	1630		35	10		
BR <sub>570</sub> (h)		1642	1625		22	5		1350
BR <sub>603</sub> (h)		1641	1623		21	3		1346
HR <sub>578</sub> (i)		1633	1621		13	1		1349
Retinylidene-n-butylamine (j)	1622	1655	1630		33	8		
Retinylidene-n-butylamine (d)	1623	1654		1656	31		33	

a.  $\nu_{\text{C}=\text{N}}$  stretching frequency, protonated ( $\nu_{\text{CNH}}^+$ ), deuterated ( $\nu_{\text{CND}}^+$ ) and  $\text{BF}_3$  complex ( $\nu_{\text{CNA}}$ ). Frequency in  $\text{cm}^{-1}$ .

b.  $\Delta\nu_{\text{H}^+} = \nu_{\text{CNH}}^+ - \nu_{\text{CN}}$ ;  $\nu_{\text{D}^+} = \nu_{\text{CND}}^+ - \nu_{\text{CN}}$ ;  $\Delta\nu = \nu_{\text{CNA}} - \nu_{\text{CN}}$

c. C = N - H bending mode ( $\delta_{\text{CNH}}$ )

d. This work; e. Reference 67; f. Reference 23; g. Reference 1; h. Reference 9;

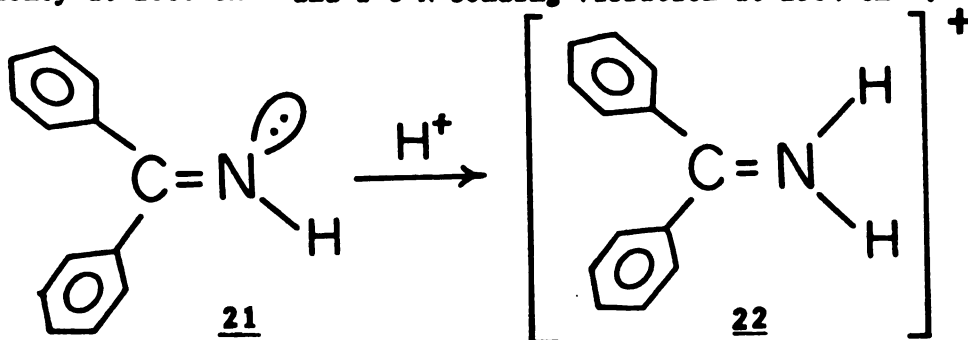
As noted in the introduction to this Chapter and also in Chapter 1, the increase in frequency upon protonation is counterintuitive. For linear polyene Schiff's bases a C=N stretch: C=N-H bend model has been invoked to explain this phenomenon. This model has difficulty, however, in accounting for the increase in C=N stretching frequency observed upon methylation, as pointed out by Marcus et al.<sup>13</sup> It is also unable to explain the similarity in behavior for protonated Schiff's bases and Schiff's base:BF<sub>3</sub> addition complexes reported here. The experiments in Figures 12 and 13 show that this similarity, which we have studied most extensively in the aromatic systems, is also observed in linear polyene systems: protonated retinal and the retinal: BF<sub>3</sub> complex in DMSO show increases in C=N stretching frequencies, relative to the neutral Schiff's base (1623 cm<sup>-1</sup>) of 31 cm<sup>-1</sup> and 33 cm<sup>-1</sup>, respectively.

Table 4 summarizes the absorption maximum, and the C=N and C=C stretching frequency data for the retinal Schiff's bases, its protonated and Lewis acid-complexed species in various solvents. The similarities in these properties for the aromatic and retinal Schiff's bases, as well as their solvent dependencies (see also ref. 60,95,102), demonstrate that the absorption red-shift, the increase in C=N vibrational frequency, and the decrease in C=C stretching frequency are general properties of Lewis acid Schiff's base reactions. In agreement with previous results<sup>8,13</sup>, the ethylenic (C=C) frequency of the retinal Schiff's base: Lewis acid complexes shows a stronger correlation with the magnitude of the absorption red shift than the C=N stretching frequency. For example, the difference between the absorption maximum values for the BF<sub>3</sub> and BBr<sub>3</sub> complexes is 19 nm. The corresponding differences in their C=C and C=N

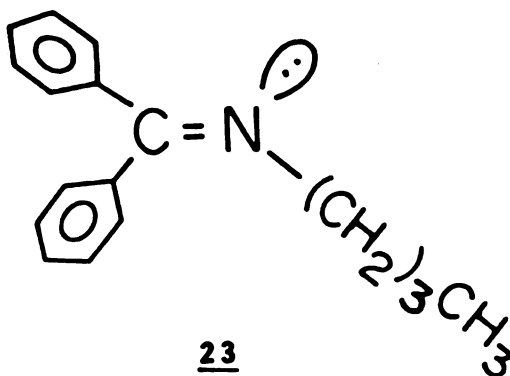
stretching frequencies are  $6\text{ cm}^{-1}$  and  $2\text{ cm}^{-1}$ , respectively, which indicates that the C=C stretching force constant is more sensitive to changes in the  $\pi$  system than is the C=N stretching frequency. This suggests, in turn, that the changes associated with the C=C and C=N stretching frequencies upon reaction with Lewis acids are regulated by more than a single mechanism.

Complexation of trans-retinal Schiff's base with general Lewis acids, such as  $\text{BF}_3$ , should remove the C-N-H bending interaction effects on the C=N stretching frequency while maintaining delocalization of the system and thus provide a means by which to test the mechanical coupling (stretch-bend interaction) hypothesis. Our results for such complexes show (see Figure 12-13 and Table 4) that there is little influence of stretch-bend coupling in determining the C=N stretching frequency; rather electronic effects which strengthen the C=N force constant upon complexation appear to be responsible for the observed frequency increase.<sup>73</sup>

The ketimine data provide another example of the difficulties of the stretch-bend interaction model. The Raman data in Figure 15 show that  $\alpha$ -phenylbenzylideneamine<sup>110</sup> (21) in its neutral form has a C=N stretching frequency at  $1600\text{ cm}^{-1}$  and a C=N bending vibration at  $1364\text{ cm}^{-1}$ .



One might expect in the stretch-bend model that these modes would interact in the neutral species to drive the C=N stretch to higher frequencies. However, the C=N stretch at  $1600\text{ cm}^{-1}$  is lower than the C=N mode in  $\alpha$ -phenylbenzylidene-n-butylamine (23) by  $18\text{ cm}^{-1}$ .



Moreover, protonation of (21) to form (22) results in a  $61\text{ cm}^{-1}$  increase in the C=N stretching mode to  $1661\text{ cm}^{-1}$ , and  $\text{BF}_3$  substitution increases the frequency of this mode by  $79\text{ cm}^{-1}$ .

These observations suggest that the change in the electronic environment of the nitrogen upon protonation or reaction with a Lewis acid, rather than mechanical coupling, is likely to be critical in determining the increase in the C=N stretching frequency. An analogy may be drawn to nitrile systems where the increase in the C≡N stretching frequency which usually accompanies reaction with a Lewis acid (e.g.  $\text{H}^+$ ,  $\text{BF}_3$ ,  $\text{BCl}_3$ ) has been explained<sup>68</sup> by suggesting that the C≡N stretching force constant increases upon complexation.

The results of the analysis above indicate that the behavior of the nitrogen lone pair is involved in determining the properties of the C=N

vibrational mode; changes in the electronic environment of this lone pair upon protonation or reaction with a Lewis acid affect the electron density distribution in the C=N linkage. The later statement is supported by the NMR data shown in Figure 11 and Table 3 which suggest, in agreement with previous results<sup>23,109</sup> that an increase in the electronegativity of the nitrogen occurs upon protonation of Schiff's bases. The protonation of a Schiff's base seems to be analogous to the situation which occurs when a proton is brought up to NH to give  $\text{NH}_2^+$ . The lone pair electrons forming the new N-H bond will not stay unaltered in their  $\text{sp}^2$  hybrid orbital, neither will they be equally shared between N and H.<sup>115</sup>

We have explored the possibility that a similar phenomenon occurs for Schiff's bases upon protonation by carrying out ab initio calculations at the GVB level for methylimine and protonated methylimine. The calculations are given in the following Chapter and show that a decrease in C=N bond length occurs upon protonation. Accompanying this, there is an increase of  $0.51 \text{ mdyn/\AA}$  in the C=N stretching force constant.

3. Absorption Maximum of trans-retinylidene-n-butylamine: Lewis acid complexes.

A general introduction to the problem and importance, of the absorption maximum red shift of the protonated retinal Schiff's base model was given in Chapter 1, (see also references 60,95,102). It was indicated that the bathochromic shift of the protonated species, relative to the unprotonated derivative, was regulated by the separation between

the center of charge in the cation (i.e.  $C=N^+$ ) and anion ( $X^-$ ). This was called the anion effect since the interatomic distance between the positive and negative centers controls the excitation energy<sup>102</sup> (or energy gap between the ground and excited states) of the cation and thus, the polyene  $\pi$  system delocalization. Blatz et al,<sup>60,95,102</sup> noted that solvent plays a major role in the determination of the absorption maximum shift of the cation. For instance, N-retinylidene-n-butylammonium chloride has an absorption maximum at 442 nm in  $CH_3OH$ , but the same salt shows its absorption maximum at 469 nm in  $CHCl_3$ . A solvent like methanol is said to be a leveling solvent, since it leveled the action of the anion (i.e. different anions show very similar absorption maxima). It has been proposed<sup>60,95,102</sup> that in methanol the N-retinylidene salts, are fully dissociated and the cation might be expected to absorb at a lower energy (long wavelength). However, because of the strong interaction between the electron-rich oxygen and the polarizable nitrogen, a significant charge is still localized in the nitrogen with the consequent increase of the retinyl cation excitation energy relative to a less polar solvent like  $HCCl_3$ .

The same trends in absorption maximum as a function of the solvent are reported in Table 4. For example, the protonated retinal Schiff's base chloride species has an absorption maximum at 456 nm in  $CH_2Cl_2$  but only 440 in DMSO. Analogously, the  $BF_3$  complex shows absorption maxima at 477 nm and 441 nm in these two solvents, respectively. In other solvents like  $CCl_4$  or  $CHCl_3$  the retinal Schiff's base: $BF_3$  complexes also behaves as the protonated analog. For example, the absorption maximum for the  $BF_3$  complex ion  $CHCl_3$  is red shifted relative to its absorption

maximum in  $\text{CCl}_4$ . The constancy and similarity between the red shifted absorption maximum of the retinal Schiff's bases: Lewis acid complexes (i.e.  $\text{BF}_3$ ,  $\text{BCl}_3$ ,  $\text{BBr}_3$ ) and protonated retinal Schiff's bases indicates that the presence of salt (i.e. cation-anion pair) is not unique in inducing a significant red shift in the absorption maxima of the complexed chromophore.

This in turn indicates that the solvent dependency in both cases is likely to be governed by a similar mechanism in which the counter ion may play only a limited role. However, at this point more work is needed in this area in order that this hypothesis can be further developed.

CHAPTER 4  
AB INITIO CALCULATIONS

A. Introduction.

An interesting aspect of the Schiff's base protonation reaction (and reactions with Lewis' bases in general) is the observation that the C=N stretching frequency increases.<sup>73-36</sup> The molecular mechanism underlying this increase is not well understood. In Chapters 1 and 3, we point out an analogy between the vibrational properties of Schiff's bases and nitriles. In nitriles, the observed decrease of the C≡N bond length and the accompanying increase in the C≡N vibrational frequency upon reaction with a Lewis acid has been interpreted in terms of an increase in the bond order of the C≡N linkage.<sup>68-72</sup> This interpretation suggests that a similar effect could be responsible for the increase in the C=N stretching frequency in Schiff's bases upon reaction with Lewis acids.

Methylimine, the simplest Schiff's base, and its protonated derivative provide a model system which can be used to study the electronic changes in the C=N bond when the nitrogen lone pair is encumbered by a proton. These species are difficult to deal with experimentally and only a few reports of their vibrational properties have appeared. Milligan<sup>116</sup>, in infrared spectroscopic studies of the photolysis of methyl azide, assigned the frequency of the C=N stretching mode of methylimine at 1628 cm<sup>-1</sup>. Confirmation of methylimine as a photolysis product was obtained by Moore et al.<sup>117</sup> in a study of diazomethane which showed that the C=N stretching vibration was observed

at  $1642\text{ cm}^{-1}$ . The difference in frequency between this result and that reported by Milligan's earlier work<sup>116</sup> may have been due to the presence of hydrogen cyanide which occurred as a second product in the matrix prepared by Moore et al.<sup>117</sup> Curiously, substitution of the hydrogens in methylimine by fluoride, i.e. perfluoromethanimine<sup>118</sup>, increases the C=N vibrational mode to  $1740\text{ cm}^{-1}$  despite the increase in mass of the substituents.

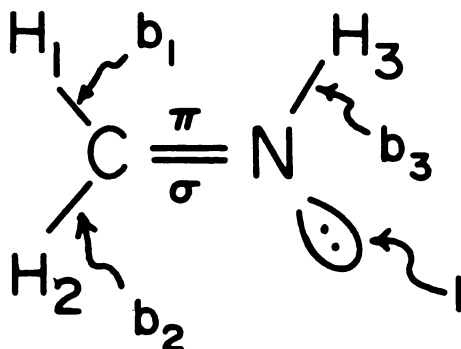
Theoretical work on the vibrational frequencies in the methylimine system has also been done. Beginning with the results of Moore et al<sup>117</sup>, Botschwina<sup>119</sup> used ab initio methods and a small basis set to calculate the force field of methylimine. For methylenimmonium ion (protonated methylimine), calculations of neither the C=N stretching force constant nor of the contribution of the s and p orbitals to the  $sp^2$  hybrid forming the C=N bond have appeared. However, Eades et al<sup>120</sup>, using SCF calculations and a PRDDO geometry, estimated that the C=N-H bond angle increases by approximately 10 degrees and that the C=N bond length increases by  $0.019\text{ \AA}$  upon protonation. In the same work the vibrational frequencies for methylimine and methylenimmonium ion were calculated, but for neither molecules were attempts made to assign the frequencies or estimate the force constants of the C=N stretching mode. Kollman and co-workers<sup>121</sup>, in SCF calculations of the electronic structure of  $\text{CH}_2\text{NH}_2$ , indicated that the nitrogen appears to be partially negatively charged.

With this previous work in mind we have carried out ab initio electronic structure calculations for methylimine and methylenimmonium ion, at the Generalized Valence Bond (GVB)<sup>77</sup> and Self Consistent Field

(SCF) levels.<sup>78</sup> The GVB results show an increase in the nitrogen s character contributing to the C=N sigma bond, an increase of 0.51 mdyn/Å in the C=N force constant, a slight decrease in the C=N bond length and a decrease in the carbon electronic charge when methylimine is protonated.

### B. Theoretical Details.

In the GVB calculations the 12 valence electrons of methylimine were represented by 6 electron pairs, each of which was represented by two natural orbitals. The assignment of the electron pairs to the molecular structure is given as:



where  $b_1$ ,  $b_2$ ,  $b_3$ , and  $l$  represent the CH's, the NH and the nitrogen lone pair, respectively and the  $\sigma$  and  $\pi$  correspond to the particular bonds between nitrogen and carbon. For the protonated methylimine an NH bond ( $b_4$ ) replaces the lone pair  $l$ .

The expansion basis was the Huzinaga<sup>122</sup> 9s5p set on both C and N and the Dunning<sup>123</sup> 4s set on each H. These were augmented with polarization functions (d's for C and N ( $\alpha=0.75$  and 0.80, respectively) and p's for each H ( $\alpha=1.0$ )), the resulting basis was (9s5p1d/4s1p) and was contracted

to [3s2p1s/2s1p] by using the general contraction of Raffanetti.<sup>124</sup> Total charge distribution as well as the per cent s and p character in the N contribution to the C=N bond were calculated from the natural orbitals of the GVB wave function by using the Mulliken Population Analysis.<sup>125</sup>

To calculate the C=N stretching force constant we use the following geometry optimization procedure. As a starting point, we fixed all geometric parameters for both methylimine and methylenimmonium ion at the Eades et al<sup>120</sup>, PRDDO optimized geometry values and varied the C=N distance by 0.025 au (0.01323 Å) symmetrically about the initial minimum energy geometry. This calculations gives the energy at a given C=N distance and the new equilibrium geometry. For both molecules the resulting potential energy curves were fit to a 4th order polynomial<sup>126</sup> in  $(R-R_{eq})$  where  $R_{eq}$  is the calculated C=N bond length, and the force constant for the C=N stretching mode was determined from the coefficient of the quadratic term in this expansion. All calculations were carried out by using the Argonne National Laboratory Collection of Electronic Structure Codes (QUEST-164). In particular, the integrals were by done using the program ARGOS written by Pitzer<sup>83</sup> and the GVB calculations were done by using the program GVB 164 written by R. Bair.<sup>84</sup> The calculations were done on an FPS 164 attached array processor.

### C. Results.

Calculated potential curves at the GVB and SCF level for the C=N and C=N<sup>+</sup> stretching modes are show in Figure 17 (see also Tables 7 and 8 respectively). Figure 18 show the calculated GVB equilibrium geometry

**Figure 17. Ab initio potential curves for the C=N stretching motion. (a) C=N<sub>SCF</sub> methylimine SCF . (b) C=N<sub>SCF</sub> methylenimmonium ion SCF. (c) C=N<sub>GVB</sub> methylimine GVB. (d) C=N<sub>GVB</sub> methylenimmonium ion GVB, calculations.**

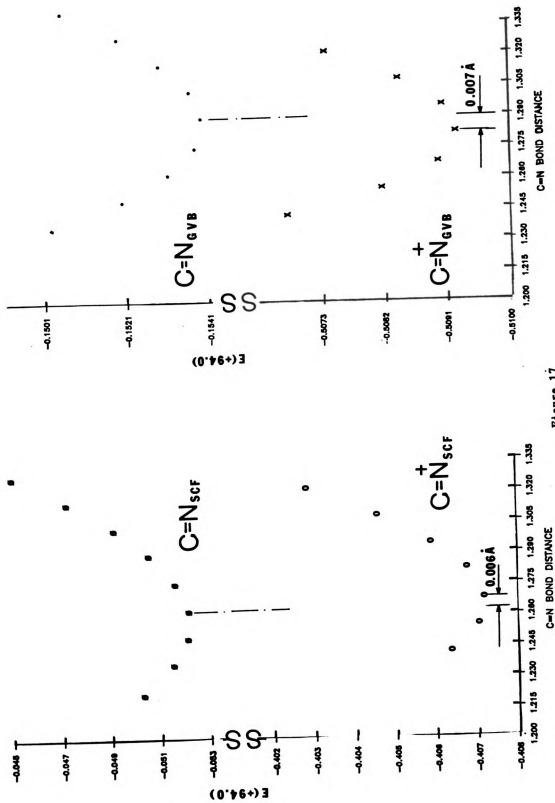


Figure 17

**Table 7** Methylimine Potential Curve<sup>(1,2)</sup>. Total Energy for the C=N Stretching Motion.

$R_{\text{C=N}}$	$E_{\text{SCF}}(+94.0 \text{ au})$	$E_{\text{GVB}}(+94.0 \text{ au})$
1.222	-0.05033	-0.14801
1.236	-0.05155	-0.15031
1.249	-0.05216	-0.15201
1.262	-0.05218 <sup>(3)</sup>	-0.15315
1.275	-0.05168	-0.15379
1.289	-0.05064	-0.15395 <sup>(3)</sup>
1.302	-0.04924	-0.15367
1.315	-0.04729	-0.15295
1.328	-0.04512	-0.15196
1.341	-0.04250	-0.15058

1. Energy in hartrees and bond length in Å.
2. Points closest to the equilibrium geometry used for a quadratic polynomial fit.
3. Computed point nearest the equilibrium geometry.

Table 8      Methyleneiminium ion Potential Curve<sup>(1)</sup>. Total Energy for the C=N Stretching Motion.

---

$R_{\text{C=N}}$	$E_{\text{SCF}}(+94.0 \text{ au})$	$E_{\text{GVB}}(+94.0 \text{ au})$
1.242	-0.406378	-0.506805
1.255	-0.407058	-0.508163
1.268	-0.407179 <sup>(1)</sup>	-0.508968
1.282	-0.406776	-0.509238 <sup>(2)</sup>
1.295	-0.405888	-0.509043
1.308	-0.404572	-0.508417
1.321	-0.402836	-0.507373

---

1. See footnotes in Table 7.

2. Computed point nearest the equilibrium geometry.

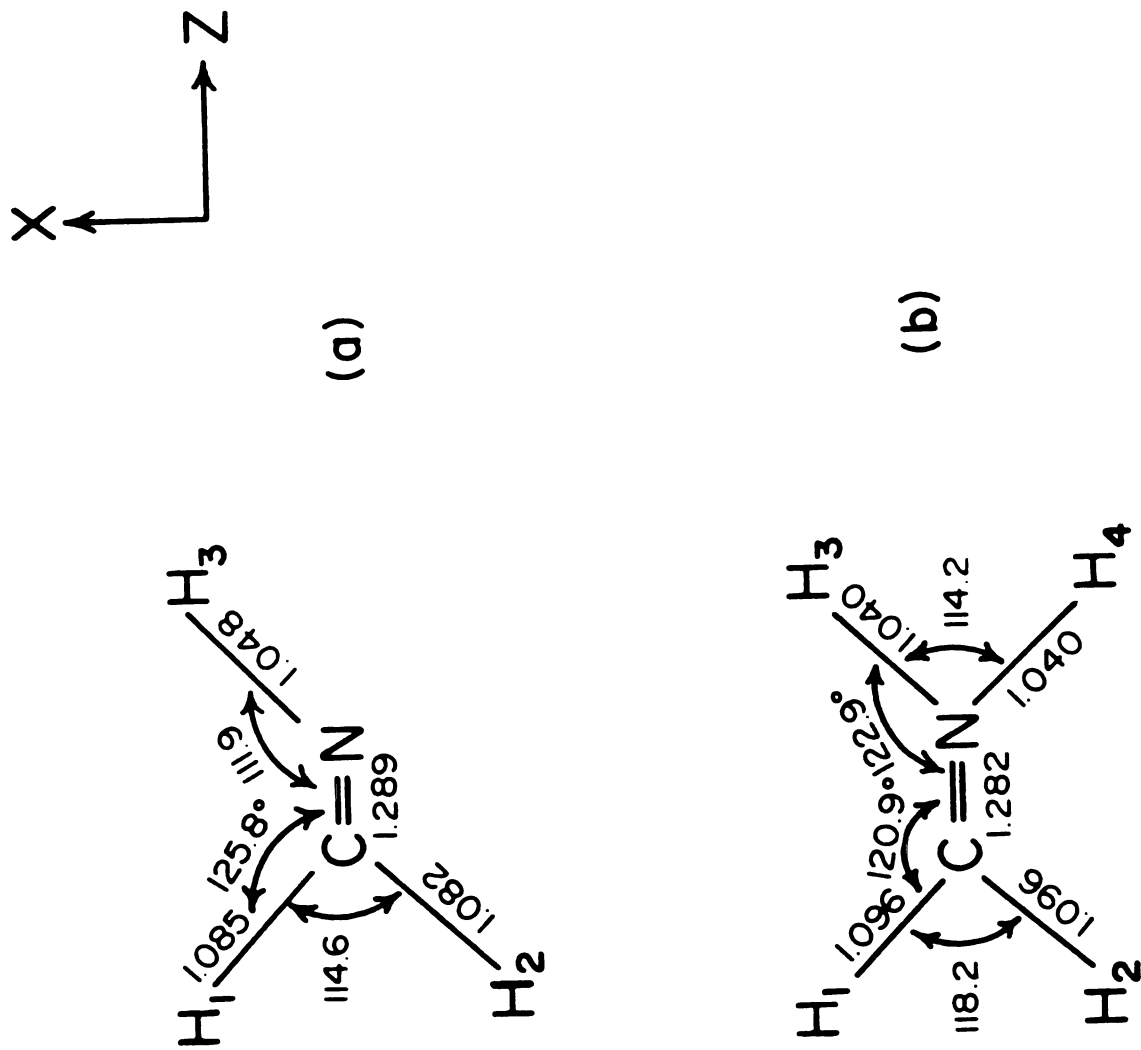


Figure 18. Geometry of methylimine (a) and protonated (methylenimmonium ion)

(b). Bond length in Å and bond angles in degrees

for methylimine and the protonated derivative. The protonated species shows a potential minimum at an energy lower than the unprotonated one. This is in agreement with previous calculations in which a small basis set and the SCF formalism<sup>120,121</sup> were used. The GVB calculation predicts that upon protonation of methylimine, the C=N bond will be slightly shorter than in the unprotonated one (1.282 Å and 1.289 Å, respectively). Opposite to this trend, the SCF calculation predicts, in agreement with the SCF calculation of Eades et al.<sup>120</sup>, that the bond distances of the protonated specie (1.268 Å) will be slightly longer than the neutral species (1.262 Å).

The fitted potential surfaces were used to determine the coefficients of the quadratic terms which in turn give the force constant for the C=N and C=N<sup>+</sup> stretching modes. These are shown in Table 9. We estimated the anharmonicity corrections and found them to be insignificant. The protonated species at the GVB level shows an increase in the C=N<sup>+</sup> stretching force constant, relative to the C=N stretching force constant, of 0.51 m dyn/Å, while the SCF level shows a decrease of 0.52 m dyn/Å; in addition, the values at the SCF level are higher than at the GVB level. It is generally recognized that SCF calculations overestimate force constants by between 10-30%.<sup>127-131</sup> Since the GVB wave function contains a more appropriate mixture of ionic and covalent terms and separates to the correct asymptotic products, the GVB force constants should be more reliable.

Table 9      Calculated<sup>(1)</sup> Force Constants<sup>(2)</sup> for the C=N<sup>(3)</sup>  
C=N<sup>+</sup><sup>(4)</sup> Stretching Motion.

---

Force constant	C=N	C=N <sup>+</sup>
$k_{\text{GVB}}$	11.14	11.65
$k_{\text{SCF}}$	13.77	13.25

---

1. From a polynomial fit of the GVB and SCF potential curves (see text for details).
2. Quadratic valence force constant in  $\text{mdyn}/\text{\AA}$ .
3. Methylimine.
4. Methylenimmonium ion.

One may think of the GVB wave function as being the SCF function plus various correction terms.

$$|GVB\rangle = |SCF\rangle + |Corr. Terms\rangle$$

The "correction terms" correct for the wrong distance dependent behavior of the SCF, i.e., when bond lengths are changed. We are not too concerned with the SCF predicted trend upon protonation since we realize it is a much less complete function than the GVB. When one has two approximate wave functions and one is considerably less approximate than the other it seems prudent to trust the predictions of the more complete functions over those of the less complete functions. Note also that the GVB is equivalent to an SCF with limited configuration interactions. The GVB contains electron correlation while the SCF does not.

Tables 10 and 11 present the Mulliken Population Analysis for both the protonated and unprotonated methylimine species calculated at the minimum energy geometry. Figures 19 and 20 show the corresponding contribution of the  $\sigma$  and  $\pi$  systems to the total electron distribution, while the sp electron distribution to various bonds in the  $\sigma$  system is shown in Table 12. Figure 21 indicates the change in the sp character of the nitrogen when methylimine is protonated. Under the same circumstances, Figure 21 also shows the electron distribution in the  $\pi$  systems in the C=N and C=N<sup>+</sup> bonds.

**Table 10 Methylimine: Electron Distribution.**

Atom	Orbitals						
	$s_{\sigma}$	$p_{\sigma}$	$d_{\sigma}$	$p_{\pi}$	$d_{\pi}$	$\sigma$	$\pi$
Carbon	3.19	1.98	0.05	0.89	0.01	5.22	0.90
Nitrogen	3.58	2.60	0.02	1.08	0.01	6.20	1.09
H <sub>1</sub>	0.89	0.01	—	0.00	—	0.90	0.00
H <sub>2</sub>	0.88	0.01	—	0.00	—	0.89	0.00
H <sub>3</sub>	0.78	0.02	—	0.00	—	0.80	0.00
<b>TOTAL</b>						<b>14.01</b>	<b>1.99</b>

**Table 11 Methylenimmonium ion: Electron Distribution.**

Atom	Orbitals						
	$s_{\sigma}$	$p_{\sigma}$	$d_{\sigma}$	$p_{\pi}$	$d_{\pi}$	$\sigma$	$\pi$
Carbon	3.23	2.03	0.04	0.61	0.02	5.30	0.63
Nitrogen	3.42	2.41	0.03	1.35	0.01	5.86	1.36
H <sub>1</sub>	0.77	0.01	—	0.00	—	0.78	0.00
H <sub>2</sub>	0.77	0.01	—	0.00	—	0.78	0.00
H <sub>3</sub>	0.61	0.02	—	0.00	—	0.63	0.00
H <sub>4</sub>	0.61	0.02	—	0.00	—	0.63	0.00
<b>TOTAL</b>						<b>13.98</b>	<b>1.99</b>





**Table 12 Electron Distribution of the Bond System<sup>a</sup>**

Bond <sup>(b)</sup>	Atom	Orbital <sup>(c)</sup> /Atom <sup>(d)</sup>	Methylimine	Methyleniminium Ion
	Carbon	s/C	0.32	0.33
		p/C	0.57	0.61
		s/H <sub>1</sub>	0.14	0.07
H <sub>1</sub> -C	Hydrogen(1)	s/H <sub>1</sub>	0.81	0.75
		s/C	0.09	0.12
		p/C	0.11	0.12
	Carbon	s/C	0.31	0.33
		p/C	0.58	0.61
		s/H <sub>2</sub>	0.13	0.07
H <sub>2</sub> -C	Hydrogen(2)	s/H <sub>2</sub>	0.80	0.75
		s/C	0.09	0.12
		p/C	0.12	0.12
	Carbon	s/C	0.33	0.29
		p/C	0.51	0.49
C-N	Nitrogen	s/N	0.31	0.42
		p/N	0.58	0.52

Cont. Table 12

	Nitrogen	s/N	0.20	0.33
		p/N	0.69	0.62
		s/H <sub>3</sub>	0.11	0.07
N-H <sub>3</sub>				
	Hydrogen(3)	s/H <sub>3</sub>	0.75	0.61
		s/N	0.04	0.13
		p/N	0.23	0.27
	Nitrogen	s/N	0.41	—
		p/N	0.51	—
N-(lone-pair)				
	Lone-Pair	s/N	0.57	—
		p/N	0.50	—
	Nitrogen	s/N	—	0.33
		p/N	—	0.62
		s/H <sub>4</sub>	—	0.07
N-H <sub>4</sub>				
	Hydrogen(4)	s/H <sub>4</sub>	—	0.61
		s/N	—	0.13
		p/N	—	0.27

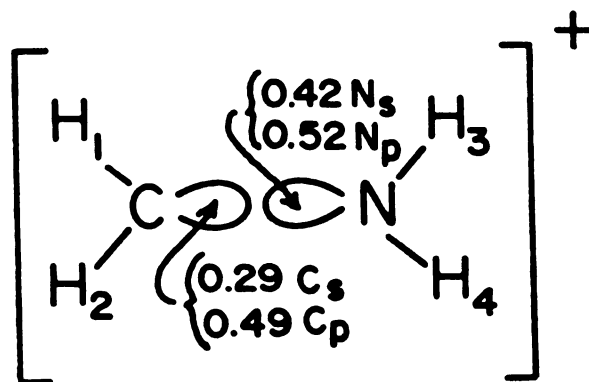
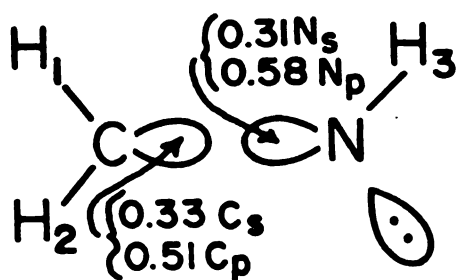
a. Calculated from Mulliken Population Analysis.

b. See Figure 18 for the particular geometry.

c. s and p stands for s and p orbitals, respectively.

d. C, N and H stands for the carbon, nitrogen and hydrogen atoms involved in the particular bond.

### $\sigma$ system



### $\pi$ system

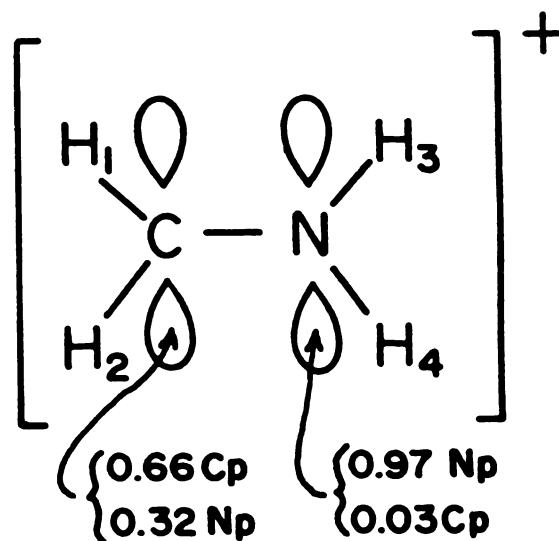
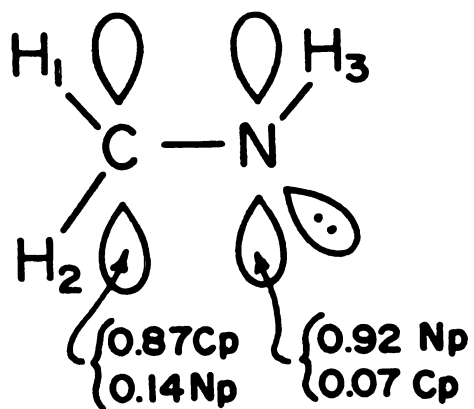


Figure 21.  $s$ - $p$  and  $p$  electron distribution of the  $\sigma$  and  $\pi$  systems in the C=N bond of methylimine and methylenimmonium ion.

#### D. Discussion.

Further insight into the mechanism responsible for the increase in the C=N stretching force constant upon protonation may be gleaned from the detailed electron distribution predicted by the GVB functions used in this work. If the nitrogen atom in methylimine did not use its 2s electrons in the bonding to the H or CH<sub>2</sub> group we would expect a CNH angle of 90° and no nitrogen 2s character in either the C-N or N-H sigma bonds. The calculated value of 111.9° for the CNH angle in CH<sub>2</sub>NH reflects the extent to which the nitrogen 2s electrons participate in the bonding and from Figure 21 we see that the GVB calculations allot 0.31 electrons from the nitrogen 2s to this C-N bond. When methylimine is protonated at the nitrogen lone pair, the CNH angle increases further to 122.9° and the calculated number of nitrogen 2s electrons in the C-N bond increases to 0.42. This enhanced nitrogen 2s character in the C-N bond is reflected in a smaller bond length in the positively charged ion relative to the neutral species and in the increase in the stretching force constant.

The calculations above indicate that it is possible to attribute the increase in the C=N stretching force constant in methylenimmonium species to a change in the electronic environment of the C=N bond upon protonation of methylimine. This increase in the C=N stretching force constant for the protonated species translates into an increase in the C=N stretching frequency of 30 cm<sup>-1</sup> (see next Chapter) and suggests that the same kind of mechanism may be responsible for the observable increase in the C=N stretching frequency in protonated or Lewis acid-complexed

Schiff's bases.

Several studies have suggested that when one protonates a polyene Schiff's base the C=N bond order decreases resulting in a corresponding decrease in the C=N force constant.<sup>4,5,8,11,13</sup> If the encumbered lone pair mechanism (rehybridization model) is to be dominant for such systems then the change in the bond order and component of the C=N force constant must be smaller than these earlier studies predict. Note, however, that numerical experiments within the normal coordinate analysis model, presented in the next Chapter, suggest that the increase in the C=N stretching frequency observed upon protonation in a variety of molecules can not be reproduced with a "sensible" set of interaction force constants when there is a decrease of  $0.3 \text{ mdyn/\AA}$  in the C=N force constant.

The electronic structure of the methylenimmonium ion shows (see Figure 20) that the nitrogen appears to be partially negatively charged and the carbon carries partial positive charge. Since the charge of the system is +1, the hydrogens bear the rest of the positive charge. Mulliken atomic populations tend to be basis set dependent, which may indicate that the above charge distribution in methylenimmonium ion is not necessary correct. However, a similar charge distribution was obtained by Kollman and co-workers<sup>121</sup> by using a STO-3G and double Zeta basis set. Moreover, Birge et al.<sup>64</sup> in their semi-empirical calculations on the cis-trans isomerization of rhodopsin, indicated that the INDO-CISD atomic charges of a 11-retinal Schiff's base show that the nitrogen retains a negative charge (despite the fact that the chromophore carries

a net positive charge) and that the Schiff's base carbon is more positively charged than the nitrogen atom. Thus, our results suggest, in agreement with Birge et al.<sup>64</sup> that the common approach of assigning nitrogen a +1 core charge will overestimate the  $\pi$  potential in semi-empirical calculation of retinal Schiff's bases or Schiff's bases in general.

## CHAPTER 5

### NORMAL COORDINATE ANALYSES

#### A. Introduction.

Resonance Raman and Fourier Transform infrared spectroscopy have been used to study the mechanism of excitation and photochemical properties of the retinal Schiff's base chromophore in rhodopsin, bacteriorhodopsin and related photopigments.<sup>1-17</sup> Comparison of the vibrational spectra of the retinal Schiff's base model with the pigment spectra has been used to examine the interaction between the retinal chromophore and the protein. For example, the C=N stretching mode in the 1620-1655  $\text{cm}^{-1}$  region has been used to identify the state of protonation of the retinal Schiff's bases. A vibrational frequency 25  $\text{cm}^{-1}$  lower upon deuteration has helped to determine that in rhodopsin the Schiff's base is protonated.<sup>2,35,132</sup> The finger print region of the retinal-based proteins, between 1100-1400  $\text{cm}^{-1}$ , often correlates with the isomeric form of the chromophore. Isotopic substitution in this case has helped to distinguish between the particular vibrations of the isomeric forms.<sup>2,11,3</sup> However, the environment of the protein can affect the vibrational frequencies of the retinal chromophore. Moreover, the C=N stretching frequency of the protonated Schiff's base species is higher than the non-protonated species. Thus, normal mode calculation have been used to predict the vibrational spectral changes of the chromophore upon interaction with the protein. In particular, the normal mode calculations have been used to emphasize that, upon protonation of the retinal Schiff's bases (or Schiff's bases in general), the C=N stretching

force constant decreases. The increase of the C=N stretching frequency, relative to the unprotonated Schiff's base, is attributed to the coupling between the C=N stretching and C=N-H bending motions.<sup>4,5,8,11,13</sup> For more details see section C in Chapter 1.

As discussed in Chapter 3, the stretch-bend model can not account for the experimental increase in the C=N stretching frequency when aromatic imines and retinal Schiff's bases are reacted with the general Lewis acid  $\text{BF}_3$ ,  $\text{BCl}_3$ ,  $\text{BBr}_3$  or when ketimines are protonated. In the preceding Chapter we have shown that upon protonation of methylimine there is a reorganization of the electronic environment around the C=N bond in such way that the C=N stretching force constant increases and we called this effect the rehybridization model.<sup>73-76</sup>

To analyze the implications of the rehybridization model on the Schiff's bases vibrational frequency,  $\nu_{\text{C=N}}$ , we have carried out normal coordinate analyses for methylimine and its protonated derivatives and for the model structures  $\text{CH}_3\text{CH=NCH}_3$  and its protonated and  $\text{BF}_3$  analogs. We have also carried out vibrational analyses for the  $\text{CH}_3\text{CH=NHCH}_3$  structure in which the C=N stretching force constant is allowed to decrease upon protonation. This latter calculation allows us to explore the predictions of the stretch/bend interaction model in light of a restricted set of force constants. For both types of force fields, we systematically varied the force constants of the modes which can influence the C=N stretching frequency, which allows an evaluation of the various contributions to the observed behavior of the C=N stretching mode.

The results of these analyses indicate, in agreement with the rehybridization model<sup>73-76</sup>, that the electron density redistribution which occurs upon protonation plays a mayor role in determining the C=N stretching frequency, the stretch bend interaction is prominent to a much lesser extent.

#### B. Numerical Calculations and Methylimine and Methylenimmonium Ion Force Fields.

In-plane vibrational frequencies and the corresponding potential energy distribution for methylimine and for a hypothetical methylenimmonium ion have been calculated. The ab initio geometry determined for methylimine and methylenimmonium ion<sup>120</sup> (with the exception of the C=N bond distance, see below), and the force field calculated for methylimine<sup>119</sup> were used. The methylenimmonium force field was constructed from the methylimine force field. The C-H cis force constants of the neutral species were used for the two C-H bonds of methylenimmonium owing to the greater lengths of these bonds in the protonated form and the  $C_{2v}$  symmetry of the ion. The C=N bond distance and the C=N stretching force constant for methylimine and protonated methylimine were substituted with our ab initio results. Figure 22 shows the geometries and Table 13 and 14 summarize the force fields. The Shimanouchi program<sup>85,86</sup> was used to calculate the frequencies and the potential energy distribution in terms of an internal basis set (see Figure 22). In order to check consistency of the C-H modes in the potential energy distribution, the in-plane  $5A_1$  and  $4B_2$  vibrational frequencies of the protonated methylimine have been calculated, first, by

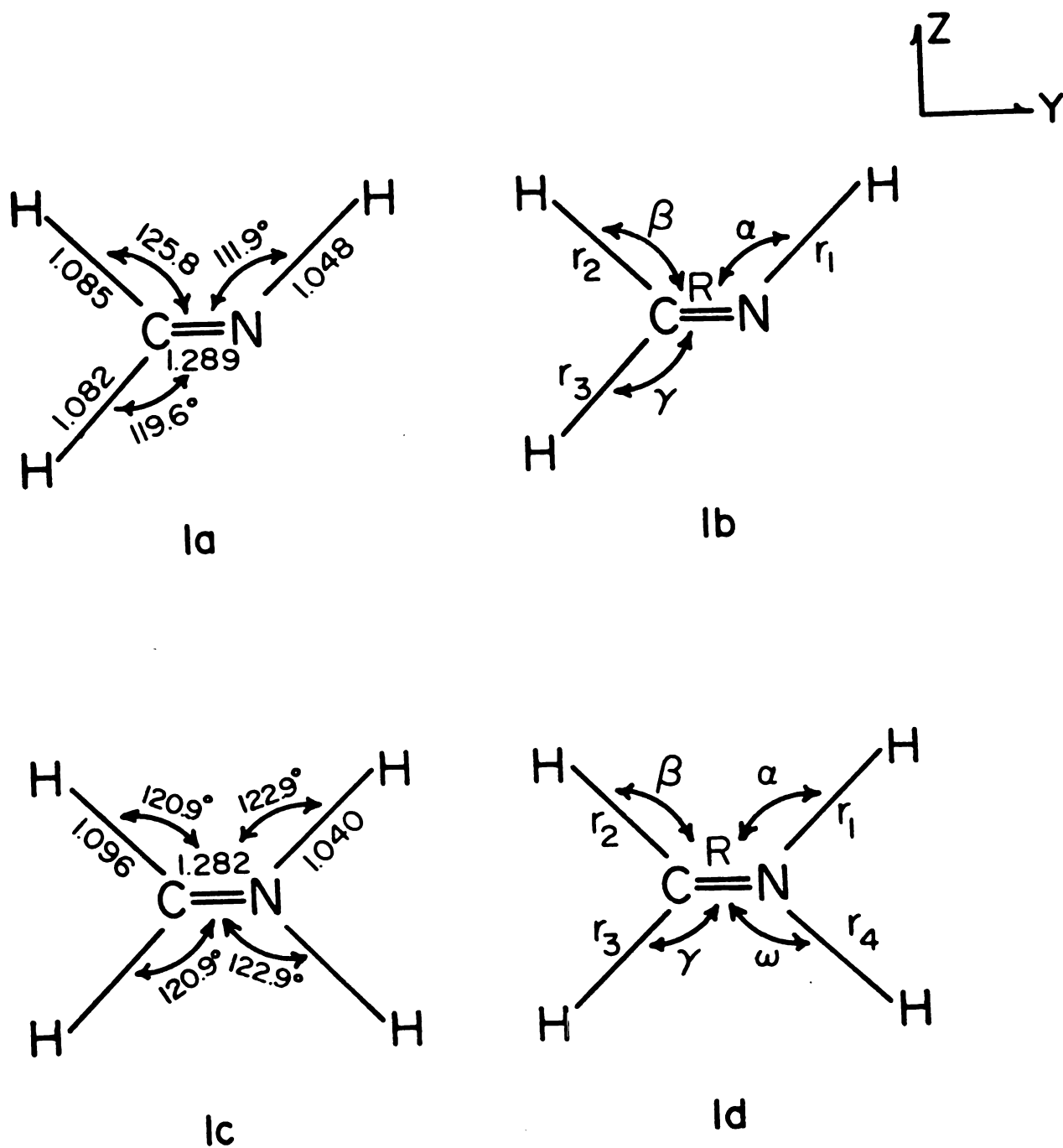


Figure 22. Geometry and internal coordinates employed for the normal coordinate analyses of methylimine and methylimmonium ion. The molecules were assumed to be planar. Bond lengths in Å. Bond angles in degrees.

**Table 13 F\* Matrix Elements for Methylimine\*\*.**

R	r <sub>1</sub>	r <sub>2</sub>	r <sub>3</sub>	α	β	γ
11.14 <sup>(a)</sup>	0.087	0.231	0.259	0.682	0.345	0.479
	5.736	0.040	-0.030	0.277	-0.075	0.086
		4.923	0.048	-0.067	-0.026	-0.181
			4.994	0.025	-0.169	0.003
				0.882	-0.021	0.078
					1.061	0.458
						1.046

\*Stretching force constants - m dyn/Å; bending force constants - m dyn Å/rad<sup>2</sup>;

stretching-bending interactions force constants - m dyn/rad.

\*\*Force constant from Reference 119.

From Reference 73.

**Table 14 F<sup>o</sup> Matrix Elements for Methyleniminium Ion**

R	$r_1$	$r_2$	$r_3$	$r_4$	$\alpha$	$\beta$	$\gamma$	$\omega$
11.65 (a)	0.087	0.231	0.231	0.087	0.682	0.345	0.345	0.682
	5.736	0.040	-0.030	0.048	0.277	-0.075	0.086	-0.181
	4.923	0.048	0.048	-0.030	-0.067	-0.026	-0.181	0.086
		4.923	0.040	0.040	0.025	-0.181	-0.026	-0.067
			5.736	-0.181	0.086	-0.075	0.277	
				0.882	-0.021	0.078	0.458	
					1.046	0.458	0.078	
						1.046	-0.021	
								0.882

\* See text and definitions in Table 13.

means of a symmetrical coordinate basis set (see Table 15) and second, by using an internal basis set (see Figure 22). The potential energy distribution of the C-H bonds were the same in both coordinate systems.

### C. Force Fields for the Model $\text{CH}_3\text{CH}=\text{NCH}_3$ and Its Derivatives.

Vibrational analyses also have been carried out for the Schiff's bases,  $\text{CH}_3\text{CH}=\text{NCH}_3$ , and for its protonated, deuterated and  $\text{BF}_3$ -complexed derivatives. The geometry and force field for 2-propaneimine<sup>133</sup>, allylimine<sup>134</sup>, ethylideneimine<sup>135</sup>, propargylimine<sup>136</sup>, methylimine and methylenimmonium ion<sup>114,121</sup> were employed to construct the geometry and force field for the normal mode calculation, see Figure 23. The C=N bond lengths were taken from the ab initio calculations reported in the previous Chapter. The molecules were assumed to be planar and the  $\text{CH}_3$  and the  $\text{BF}_3$  groups were employed, as in other studies<sup>4,8</sup>, as point masses.

Table 16 presents the main diagonal and off-diagonal force constants for a series of imines.<sup>133-136</sup> A combination of these force fields with the force constants associated with the N-C motions in N-methylacetamide<sup>137</sup> was used to construct an initial force field for the  $\text{CH}_3\text{CH}=\text{NCH}_3$  Schiff's base and its protonated species. Semi-refined force fields for the unprotonated and protonated models were obtained (see Table 17) from a fit of the initial force field to the frequencies of the C=N stretch, C=N-H bend and ring Schiff's base ( $\text{CHC}=\text{NR}$ ) motion in N-benzylidene-n-butylamine and its protonated and deuterated derivatives ( see Figures 7-8 and Table 1 in Chapter 3). For the C=N/C=N-H

**Table 15 Symmetry Coordinates for In-Plane Vibrations of Methylenimmonium Ion**


---

	$A_1$	$B_2$
$S = R$		
$S_{14}^+$	$= \frac{1}{\sqrt{2}} (r_1 + r_4)$	$S_{14}^- = \frac{1}{\sqrt{2}} (r_1 - r_4)$
$S_{23}^+$	$= \frac{1}{\sqrt{2}} (r_2 + r_3)$	$S_{23}^- = \frac{1}{\sqrt{2}} (r_2 - r_3)$
$S_{\alpha\omega}^+$	$= \frac{1}{\sqrt{2}} (\alpha + \omega)$	$S_{\alpha\omega}^- = \frac{1}{\sqrt{2}} (\alpha - \omega)$
$S_{\beta\gamma}^+$	$= \frac{1}{\sqrt{2}} (\beta + \gamma)$	$S_{\beta\gamma}^- = \frac{1}{\sqrt{2}} (\beta - \gamma)$

---

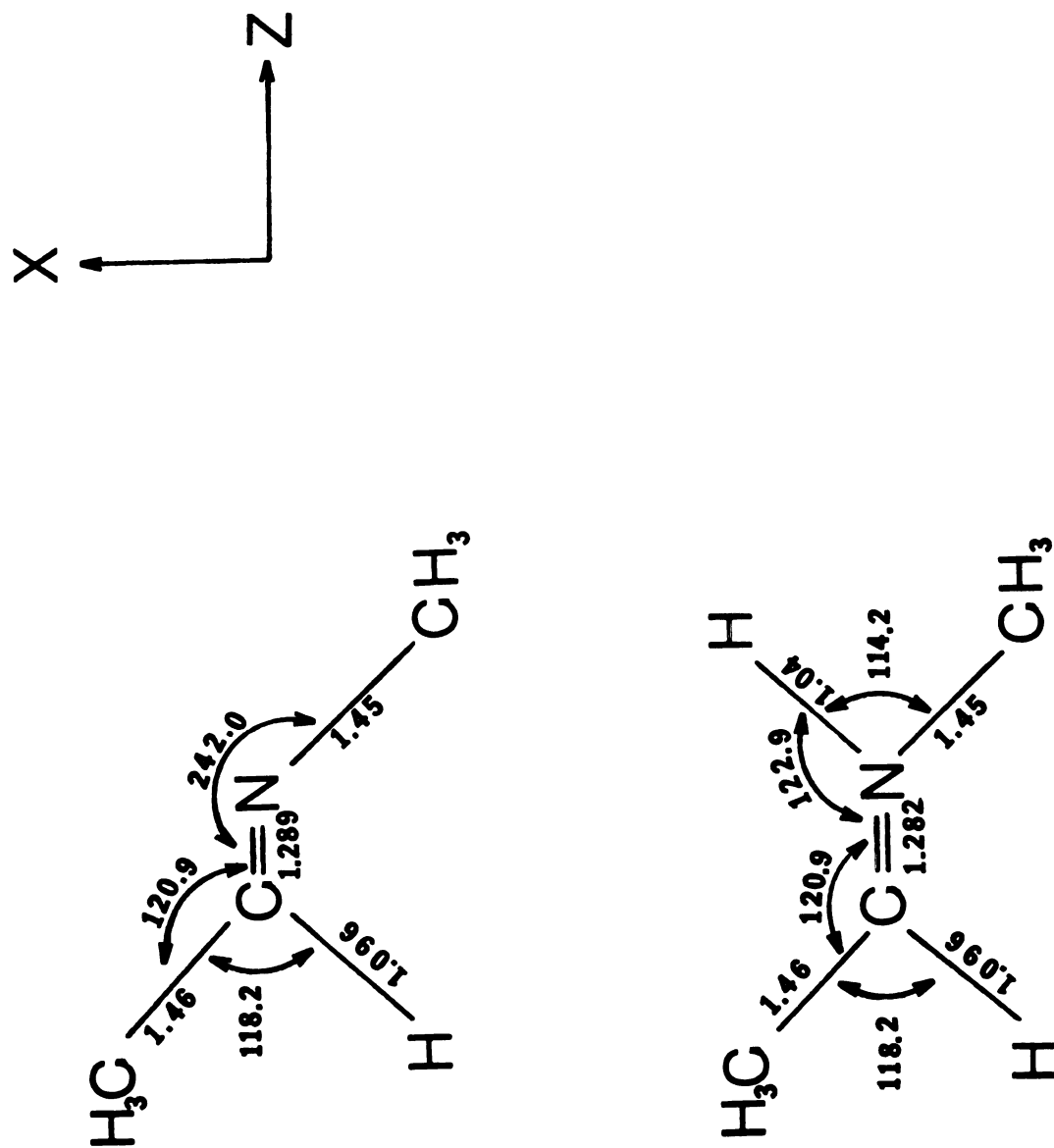


Figure 23. Geometry and internal coordinates employed for the normal coordinate analyses of the model  $\text{CH}_3\text{CH}=\text{NCH}_3$  and its protonated and  $\text{BF}_3$  derivatives. The molecules were assumed to be planar. Bond lengths in Å. Bond angles in degrees.

Table 16 Diagonal and Off-Diagonal Force Constants<sup>a</sup> of Some Imines.

Compounds <sup>b</sup>	CN <sub>s</sub>	CH <sub>s</sub>	CC <sub>s</sub>	NH <sub>s</sub>	HCN <sub>b</sub>	CNH <sub>b</sub>	CCN <sub>b</sub>	CN <sub>s</sub> /CH <sub>s</sub>	CN <sub>s</sub> /NH <sub>s</sub>	CN <sub>s</sub> /CC <sub>s</sub>	CN <sub>s</sub> /HCN <sub>b</sub>	CN <sub>s</sub> /CNH <sub>b</sub>	CN <sub>s</sub> /CCN <sub>b</sub>
Allylimine	10.89	4.50	3.96	7.60	0.50	0.86	0.80	0.29	-0.05	0.56	0.31	0.58	0.25
Methylimine <sup>c</sup>	11.14	4.92	--	5.73	1.05	0.88	--	0.26	0.09	--	0.48	0.68	--
Ethylidene- imine	13.65	5.75	5.08	7.50	0.72	1.03	1.04	0.37	-0.09	0.34	0.35	0.59	0.15
Propargyl- imine	13.60	6.01	6.17	7.60	0.70	1.01	1.00	0.28	0.02	0.68	-0.36	0.56	0.29
2-Propane- imine	13.40	--	5.10	7.40	--	1.06	0.70	--	--	0.60	--	0.59	--
Isocyanic acid	15.10	--	--	--	--	0.35	--	--	--	--	--	1.128	--

a. Units are m dyn/Å for the stretching (s) and stretching-stretching (s/s); m dyn/rad for the stretch-bending (s/b); m dyn Å/rad<sup>2</sup> for the bending (b) and bending-bending (b/b) force constants.

b. See references 133 to 139 for detail of force fields.

c. See reference 119.

Table 17 F Matrix Elements<sup>a</sup> for the Model Structures<sup>b</sup>.

C=N(s)	N-H(s)	C-C(s)	C-H(s)	N-C(s)	CNH(s)	CCN(b)	HCN(b)	CNC(b)
(11.10)10.60	(0.04)	0.58	0.15	0.58	(0.53)	0.42	0.28	0.42
	(5.40)	(0.16)	(-0.06)	(0.25)	(0.15)	(-0.05)	(0.14)	(-0.04)
		4.30	0.23	-0.09	(0.09)	0.18	0.29	-0.08
			5.15	0.08	(0.09)	0.09	0.09	-0.15
				4.50	(0.09)	-0.05	-0.09	-0.06
					(0.85)	(0.15)	(0.20)	(0.11)
						0.70	0.09	-0.09
							0.62	-0.05
								0.70

a. Force constants same units as Table 16.

b. Table 17 contains the force field for two Schiff's base models; the unprotonated model is represented by the matrix elements without parentheses and the protonated force field is represented by both, the matrix elements with and without parentheses.

(stretch/bend) interaction term a value of 0.53 mdyn/rad, which is similar to the interaction force constants reported in Table 16 and also to that calculated by Botschwina<sup>119</sup> for methylimine, was used. Starting with these force fields for the various Schiff's base derivatives, we then determined the C=N stretching frequency as a function of the force constants of the principal modes which are likely to interact to produce the observed frequency in the neutral and complexed Schiff's bases. These calculations were carried out by fixing the force constants according to their values in Table 16 and allowing the force constant of interest to vary. We carried out these calculations for two different scenarios for the effect of complex formation on the C=N stretching force constant: case A, for an increase of 0.5 mdyn/Å upon complexation and rehybridization as we calculate in the last Chapter and Case B, for a decrease of 0.3 mdyn/Å upon complexation. This approach makes possible a comparison of these differing views of the effect of complex formation.

To our knowledge, there is no force field available for an imine-BF<sub>3</sub> complex. Therefore, we employed the geometry of Figure 23 and the force field used for this species was the same as that used for the protonated derivative with the modifications that the N-B stretch and the C=N-B bend were fixed at 3.85 mdyn/Å and 0.5 mdyn/Å rad, respectively. These force constant values are similar to those reported in the literature for the trimethylamine-BF<sub>3</sub> complex<sup>139,140</sup>, in which the N-B stretching frequency is at 690 cm<sup>-1</sup>, and for the acetonitrile-BF<sub>3</sub> complex<sup>65</sup>, in which the above mode appears at 661 cm<sup>-1</sup> and the C=N-B bending motion occurs at 100 cm<sup>-1</sup>. The C=N/N-B (stretch/stretch) and the C=N/C=N-B (stretch/bend) interaction force constants were optimized to fit the C=N stretching

frequency in the N-benzylidene-n-butylamine-BF<sub>3</sub> complex. The final matrix elements were: 0.53 mdyn/Å for the C=N/N-B (stretch/stretch) and 0.39 mdyn/rad for the C=N/C=N-B (stretch/bend) interaction force constants.

#### D. Results of the Vibrational Analyses.

##### 1. Methylimine and Methylenimmonium Ion Vibrational Frequencies.

Table 18 shows the calculated in-plane vibrational frequencies and the potential energy distribution for methylimine. The C=N stretching frequency occurs at 1675 cm<sup>-1</sup>. For this particular mode, there is a 83% contribution of the C=N stretch and the remaining contributions involve primarily the C-H stretching and bending modes. Methylenimmonium ion (Table 19) shows similar behavior: the C=N stretching mode makes an 81% contribution to the C=N stretching frequency at 1703 cm<sup>-1</sup>. Table 20 compares the C=N normal mode frequencies calculated for neutral, protonated, deuterated and N substituted methylimine. Also given in the table are the C=N force constants calculated in the preceding Chapter.

##### 2. Vibrational Frequencies of CH<sub>3</sub>CH=NCH<sub>3</sub> and Its Derivatives.

Table 21 shows the C=N stretching frequency and the potential energy distribution (PED) calculated for the model structures according to the force fields in Table 17. The C=N vibration of the unprotonated species occurs at 1645 cm<sup>-1</sup>. For this mode, the C=N stretching force constant contributes 92% to the PED; the remaining contributions involve mainly the N-C and C-C stretches and the C-C-H bending modes. The normal mode composition of the C=N stretching frequency in Tables 18, 19, 21 is very

**Table 18 Methylimine Calculated Frequencies ( $\text{cm}^{-1}$ ) of In-Plane Vibrations.**

Calculated	PED*	Assignments
3217	$r_1$ (98)	N-H stretch
3028	$r_3$ (69) $r_2$ (30)	Asym. $\text{CH}_2$ stretch
2966	$r_2$ (69) $r_3$ (30)	Sym. $\text{CH}_2$ stretch
1675	R(83) $\beta$ (12) $\gamma$ (6) $\beta\gamma$ (8) $R\alpha$ (1.4)	C=N stretch
1483	$\beta$ (23) $\gamma$ (29) $\beta\gamma$ (23)R(15)	Sym. $\text{CH}_2$ deformation + C=N stretch
1326	$\alpha$ (75) $\beta$ (21)R(20)	CNH bend + $\text{CH}_2$ (in-plane) rocking + C=N stretch
993	$\beta$ (68) $\gamma$ (68) $\alpha$ (32)	$\text{CH}_2$ (in-plane) rocking + CNH bending

\* Potential energy distribution, major internal coordinate contribution (in percent). The overall percent distribution in the calculation was 100%.

\*\* See definition Figure 22 and Table 15.

**Table 19 Methyleneimmonium Ion Calculated Frequencies of In-Plane Vibrations.**

Calculated	PED <sup>*</sup>	PED <sup>**</sup>	Assignment
3228	$r_1(48)r_4(48)$	$S_{14}^-(97)$	Asym. N-H stretch
3198	$r_4(48)r_1(48)$	$S_{14}^+(98)$	Sym. N-H stretch
3012	$r_3(50)r_2(48)$	$S_{23}^-(98)$	Asym. C-H stretch
2952	$r_2(50)r_3(48)$	$S_{23}^+(100)$	Sym. C-H stretch
1703	R(81) $\beta$ (9) $\gamma$ (9) $\beta\gamma(8)R\alpha(0.7)RW(0.7)$	$S_{12}(81)$ $S_{\beta\gamma}^+(27)$	C=N stretch
1472	$\alpha(26)W(26)\alpha W(27)$	$S_{\alpha W}^+(75)$ $S_{\beta\gamma}^+(22)$	Sym. NH <sub>2</sub> deformation + Sym. CH <sub>2</sub> deformation
1442	R(24) $\alpha(10)\beta(18)\gamma(18)$ W(10)	$S_{12}(24)$ $S_{\beta\gamma}^+(52)$ $S_{\alpha W}^+(30)$	C=N stretch + Sym. CH <sub>2</sub> deformation + Sym. NH <sub>2</sub> deformation
1203	$\beta(54)\gamma(54)\alpha(29)W(29)$	$S_{\beta\gamma}^-(61)$ $S_{\alpha W}^-(28)$	Asym. CH <sub>2</sub> deformation + NH <sub>2</sub> deformation
762	$\alpha(89)W(89)\beta(38)\gamma(38)$	$S_{\alpha W}^-(85)$ $S_{\beta\gamma}^-(43)$	Asym. NH <sub>2</sub> deformation + Asym. CH <sub>2</sub> deformation

\* Potential energy distribution, major internal coordinate contribution (in percent). The overall percent distribution in the calculation was 100%.

\*\* See definition Figure 22 and Table 15.

**Table 20** Calculated C=N Stretching Frequency of Methylimine Derivatives.

	CH <sub>2</sub> NH	CH <sub>2</sub> NH <sub>2</sub> <sup>+</sup>	CH <sub>2</sub> NHD <sup>+</sup>	CHDNH <sub>2</sub> <sup>+</sup>	CH <sub>2</sub> <sup>15</sup> NH <sub>2</sub> <sup>+</sup>
k <sub>C=N</sub> <sup>a</sup>	11.14	11.65	11.65	11.65	11.65
ν <sub>C=N</sub> <sup>b</sup>	1675	1703	1685	1695	1688

a. Quadratic valence force constant in mdyn/Å (reference 73)  
 b. Frequency in cm<sup>-1</sup>

Table 21 C-N Stretching Frequency of Model Structures<sup>a</sup>.

Structure <sup>b</sup>	C-N(cm <sup>-1</sup> )	PED <sup>c</sup>	$\Delta^d$ (cm <sup>-1</sup> )
RHC=NR	1645	92(C=N), 9(C-C), 4(C-H), 4(HCN),	
RHC= <sup>15</sup> NR	1625	91(C=N) 11(C-C), 5(C-H) 4(HCN)	20 <sup>(e)</sup>
[RHC-NHR] <sup>+</sup>	1680	89(C=N), 10(C-C), 6(HCN), 5(N-C), 5(CNH)	35 <sup>(e)</sup>
[RHC-NDR] <sup>+</sup>	1659	84(C=N), 6(C-C), 6(HCN), 6(N-C), 4(CND)	21 <sup>(f)</sup>
[RDC-NHR] <sup>+</sup>	1664	85(C=N), 10(C-C), 4.5(DLN), 5(N-c), 6.8(CNH)	16 <sup>(f)</sup>
[RHC= <sup>15</sup> NHR] <sup>+</sup>	1660	84(C=N), 10(C-C), 7(HCN), 4(N-C), 6(CNH)	20 <sup>(f)</sup>
RHC=N(BF <sub>3</sub> )R	1691	94(C=N), 8(C-C), 4.5(HCN), 4(N-C)	46 <sup>(e)</sup>

a. Calculations based on force field Table 17.

b. R=CH<sub>3</sub>.

c. PED, Potential energy distribution, major internal coordinate contribution in the calculation was 100%.

d.  $\Delta$ , difference in the C-N stretching frequency relative to the unprotonated (e) and protonated species (f), respectively.

similar to that reported recently for a series of simple imines.<sup>133-138</sup>

In the protonated species the C=N stretching frequency occurs at  $1680\text{ cm}^{-1}$  with an 89% contribution from the C=N stretching force constant. Other contributions involve the same modes present in the nonprotonated species plus a 5% contribution from the C=N-H bending motion. The contribution from the bending motion was expected since the force field for the protonated model was optimized to reproduce a C=N-H bending frequency between  $1425$  and  $1420\text{ cm}^{-1}$  as observed experimentally for N-benzylidene-n-butylamine and 2-naphthylidene-n-butylamine (see Figures 7 and 9). Other molecules, such as allylimine ( $\text{CH}_2=\text{CH}-\text{CH}=\text{NH}$ ) in which the C=N-H bending motion occurs at  $1368\text{ cm}^{-1}$ , show no involvement of the bending mode in the C=N stretching frequency.<sup>133-136</sup>

Because the normal coordinate analyses for the neutral and protonated Schiff's bases are reasonably well-constrained by the force constant values in Table 17, we have carried out further calculations to investigate the behavior of the C=N linkage. Figure 24 shows the difference between the C=N stretching frequency in the protonated and neutral Schiff's base,  $\text{CH}_3\text{CH}=\text{NCH}_3$ , as a function of the force constants of the principal modes which contribute to the PED. As noted in the Methods section, the calculations were carried out for both rehydrization model and stretch/bend interaction model scenarios. For the former we used our calculated increase of  $0.5\text{ mdyn/\AA}$  in the C=N force constant upon protonation (Case A), denoted as  $[\text{H}^+(\downarrow)]$ ; for the latter we allowed the C=N force constant to decrease by  $0.3\text{ mdyn/\AA}$  upon protonation (Case B, denoted as  $[\text{H}^+(\downarrow)]$ ). Also shown are calculations for the deuterated

**Figure 24. Difference between the C=N stretching frequency in the protonated and neutral Schiff's base  $\text{CH}_3\text{CH}=\text{NCH}_3$ , as a function of the force constant of the principal modes which contributed to the potential energy distribution.**

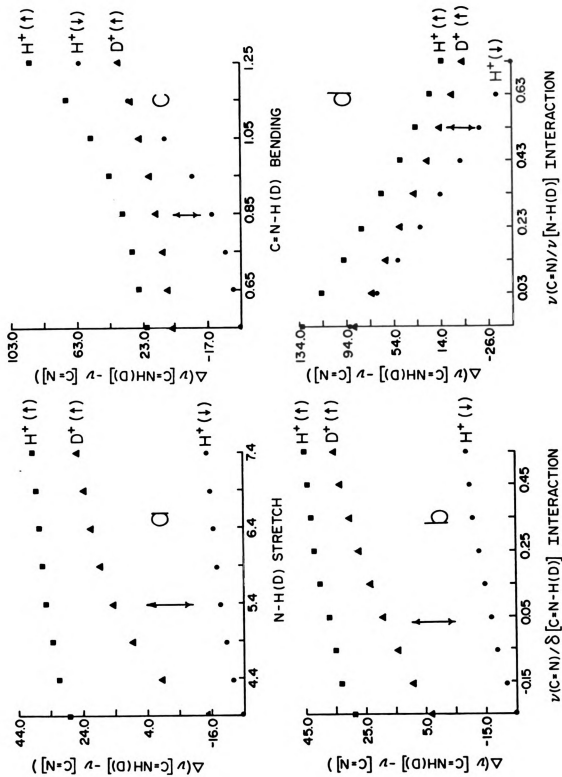


Figure 24

Schiff's base for the rehybridization model, case A,  $[D^+(\downarrow)]$ . Indicated in each panel is the value used for the particular force constant from our constrained normal coordinate analysis (Tables 16-17). From the slopes of the curves near these values, these plots provide an indication as to how the  $\nu_{C=N}$  frequency is influenced by the force constants of the various relevant modes. For both cases A and B, Figures 24a and 24b show that the N-H stretch and C=N/N-H stretch/stretch interaction force constants are unlikely to lead to the observed increase in  $\nu_{C=N}$  upon protonation. Figures 24c and 24d show that the dependence of  $\nu_{C=N}$  on the C=N-H bending and C=N/C=N-H stretch/bend interaction force constants is more pronounced. For case B,  $[H^+(\downarrow)]$ , for example, Figure 24d shows that  $\nu_{C=N}$  increases by  $68 \text{ cm}^{-1}$  when a force constant of  $0.03 \text{ m dyn/rad}$  is used for the C=N/C=N-H stretch/bend interaction term. Figure 24c shows for Case B that a bending force constant of  $1.15 \text{ m dyn } \dot{\text{A}}/\text{rad}$  leads to an increase of  $31 \text{ cm}^{-1}$  in the C=N stretching frequency. These observations suggest that a small stretch/bend interaction term in conjunction with a relatively high bending force constant could account for the  $35 \text{ cm}^{-1}$  increase in the C=N stretching frequency in the case where the stretching force constant is assumed to decrease upon protonation. However, in allylimine,  $(\text{CH}_2=\text{CH}-\text{CH}=\text{NH})$ , the simplest form of an alkene-imine conjugated  $\pi$  system, the bending force constant is  $0.86 \text{ m dyn } \dot{\text{A}}/\text{rad}$  and the stretch/bend interaction force constant is reported to be  $0.58 \text{ m dyn/rad}$ .<sup>64b</sup> These values appear to be typical for this class of compounds (see Table 16). Figure 24 shows that a stretch/bend interaction force constant in this range is unable to account for the increase in  $\nu_{C=N}$  in the Case B  $[H^+(\downarrow)]$  situation. If the force constant increases upon protonation, as our calculations indicate, then a

stretch/bend interaction of this magnitude reproduces the observed C=N frequency (Figure 24d) under conditions when the other force constants are within constraints imposed by Table 17. This suggests that the increased C=N force constant we calculated for the protonated Schiff's base plays a more important role in increasing  $\nu_{\text{C=N}}$  than does the stretch/bend interaction force constant. Similar conclusions regarding the bending force constant are indicated by Figure 24c.

For Case A, Figure 24 also shows that the deuterium isotope shift for the protonated Schiff's base is not linear with a change in force constants of the C=N-H fragment. This is apparent for all four of the force constants in Figure 21, but the difference in slopes for the  $[\text{H}^+(\uparrow)]$  and  $[\text{D}^+(\uparrow)]$  plots at their calculated, Table 17 values, is most pronounced for the N-H(D) stretch (Figure 24a) and the C=N/N-H(D) stretch/stretch (Figure 24b) interaction force constant.

Analogous calculations for the  $\text{BF}_3$  derivative shown in Figure 25, indicate that the dependencies of  $\nu_{\text{C=N}}$  on C=N- $\text{BF}_3$  vibrational parameters are generally attenuated relative to those of the C=N-H(D) group in Figure 24. The C=N/N- $\text{BF}_3$  stretch/stretch interaction, which is somewhat similar to the C-C/C-CH stretch/stretch interaction that increases the C-C frequency in methylated linear polyenes,<sup>6,35</sup> did produce a comparable shift in  $\nu_{\text{C=N}}$  ( $7 \text{ cm}^{-1}$  when varied from 0.73 to 0.03 mdyne/Å) but this appears to be too modest to account for both a decrease in C=N force constant and a 50-80  $\text{cm}^{-1}$  increase in  $\nu_{\text{C=N}}$ . The attenuated dependence on C=N- $\text{BF}_3$  parameters contrasts with the more pronounced  $\nu_{\text{C=N}}$  increase upon  $\text{BF}_3$  complex formation (e.g. for benzaldehyde protonation increases C=N

**Figure 25. Difference between the C=N stretching frequency in the  $\text{BF}_3$  and neutral Schiff's base  $\text{CH}_3\text{CH}=\text{NCH}_3$ , as a function of the force constant of the principal modes which contributed to the potential energy distribution.**

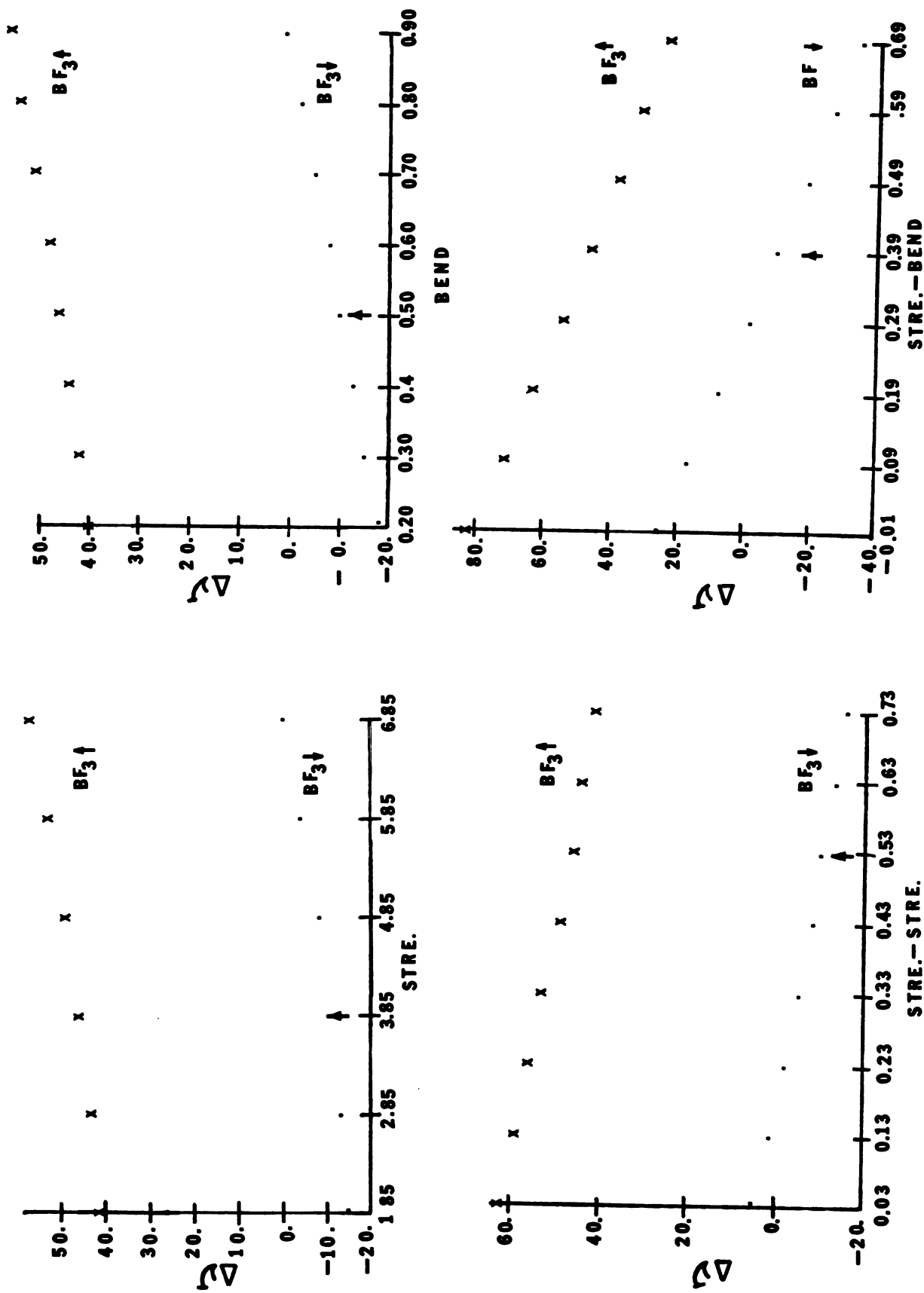


Figure 25

by  $35 \text{ cm}^{-1}$ , whereas  $\text{BF}_3$  complex formation leads to an increase of  $45 \text{ cm}^{-1}$ ). Thus, even though there is uncertainty in the  $\text{BF}_3$  force field, as noted in the Methods section, a reasonable set of force constants that includes an increase in the C=N stretching force constant provides agreement with the experimental data. We conclude, therefore, that the Case A scenario most likely applies to these adducts as well.

#### D. Discussion.

For methylimine and methylenimmonium ion the results show that an increase in the C=N stretching force constant from  $11.14 \text{ mdyn/\AA}$  to  $11.64 \text{ mdyn/\AA}$  increases the C=N stretching frequency upon protonation by  $28 \text{ cm}^{-1}$  and upon deuteration by  $10 \text{ cm}^{-1}$  (see Table 20). For the model structure,  $\text{CH}_3\text{CH}=\text{NCH}_3$ , and its derivatives, the same increase of the C=N stretching force constant increases the C=N mode by  $35 \text{ cm}^{-1}$  and shifts the deuterium substituted species by  $21 \text{ cm}^{-1}$ . These values are typical of those observed experimentally (Table 6). Moreover, the calculated frequencies in Table 21 for various isotopically substituted imines follow the same trend as those measured experimentally by Mathies and co-workers<sup>11</sup> and Bagley et al.<sup>16</sup> in their extensive study of protonated retinal Schiff's bases. Their results<sup>11</sup> show that deuteration of the Schiff's base nitrogen produces a  $23 \text{ cm}^{-1}$  shift in the C=N stretching frequency and we calculated a  $21 \text{ cm}^{-1}$ , decrease in close agreement with our experimental results. Deuteration at the carbon of the protonated retinal is observed<sup>11,16</sup> to decrease the C=N stretching frequency between  $12\text{--}15 \text{ cm}^{-1}$ , and Table 21 shows that the calculated decrease for this substitution is  $16 \text{ cm}^{-1}$ . Substitution by  $^{15}\text{N}$  produces a  $14 \text{ cm}^{-1}$  decrease

in the C=N stretching frequency in trans-retinylidene-n-butylamine.<sup>11</sup> In their calculations, Mathies and co-workers<sup>11</sup> obtained an  $18 \text{ cm}^{-1}$  shift for the  $^{15}\text{N}$  substituted protonated species; we calculated a  $20 \text{ cm}^{-1}$  shift for both the unprotonated and protonated derivatives. The shift observed upon deuteration of the Schiff's base nitrogen has been used as an argument in support of the stretch/bend interaction model.<sup>4,5,8,11,13</sup> But, as Figure 24 indicates, this shift is also dependent upon the N-H (stretch), C=N/N-H (stretch/stretch) and C=N-H (bend) force constant and suggests that their inclusion in the force field representing a protonated Schiff's base, in as constrained a manner as possible, is necessary.

The calculations summarized in Figure 24 and the recent results collected in Table 21 also provide some insight into previous force fields which were used and the normal coordinate analysis which resulted for Schiff's base species. For example, Aton et al.<sup>4</sup> used a relatively low value for the C=N stretching force constant ( $8.1 \text{ m dyn}/\text{\AA}$ ) and a negative stretch/bend interaction force constant ( $-0.2 \text{ m dyn}/\text{rad}$ ) to produce a protonated retinal Schiff's base C=N stretching frequency of  $1659 \text{ cm}^{-1}$ . It is apparent from Figure 24d that the negative interaction force constant will compensate for the low stretching force constant and push the stretching frequency up. Similarly, Kakitani et al.<sup>8</sup> calculated C=N stretching frequencies of  $1659 \text{ cm}^{-1}$  and  $1657 \text{ cm}^{-1}$  for the protonated retinal Schiff's base and for rhodopsin, respectively. For the protonated retinal model they used a C=N stretching force constant of  $9.7 \text{ m dyn}/\text{\AA}$  and a stretch/bend interaction constant of  $0.2 \text{ m dyn}/\text{rad}$ . The C=N-H bending force constant was used as a parameter to fit the C=N

stretching frequency and they obtained a value of  $0.6 \text{ m dyn } \dot{\text{A}}/\text{rad}$ . For rhodopsin, they used a smaller C=N stretching force constant ( $9.3 \text{ m dyn}/\dot{\text{A}}$ ) and a negative stretch/bend interaction force constant ( $-0.1 \text{ m dyn}/\text{rad}$ ); The bending force constant ( $0.5 \text{ m dyn } \dot{\text{A}}/\text{rad}^2$ ) was again optimized to reproduce the  $1657 \text{ cm}^{-1}$  rhodopsin C=N stretching frequency. Figure 24c indicates that the difference in bending force constants in these two calculations,  $0.1 \text{ m dyn } \dot{\text{A}}/\text{rad}$ , will not strongly influence the results. Our calculations suggest, however, that the  $0.4 \text{ m dyn}/\dot{\text{A}}$  decrease in the stretching force constant used by Kakitani et al.<sup>8</sup> for rhodopsin relative to the protonated model Schiff's base is compensated by the decrease (by  $0.3 \text{ m dyn}/\text{rad}$ ) they assumed in the stretch/bend interaction force constant and that this leads to the similarity in calculated values of  $\nu_{\text{C=N}}^j$  in the two compounds.

In our normal coordinate analysis of the methyl-substituted Schiff's base we used a C=N/C=N-H stretch bend interaction force constant of  $0.53 \text{ m dyn}/\text{rad}$ , a value that is similar to the interaction terms compiled in Table 16. To provide some physical insight into this positive value, it is useful to note that the values in Table 16 are for neutral Schiff's bases. Upon protonation we expect a change in C=N-H bond angle and N-H bond length. Mills<sup>141</sup> notes that changes of interbond angle will produce changes in hybridization for the central atom owing to orbital following of the bending coordinate. For situations in which bond angle increases lead to greater s content in the bond and hence to shorter bondlengths, a positive value for the stretch/bend interaction force constant is expected. This appears to be the case for the Schiff's base linkage as Eades et al.<sup>120</sup> have calculated that the C=N-H bond angle increases by

$11^\circ$  and the N-H bond length decreases by  $0.008 \text{ \AA}$  upon protonation of methylimine. In our own calculations we find an increase in nitrogen s character in the N-H bond in methylimine upon protonation.<sup>73</sup> These arguments suggest that the C=N/C=N-H interaction force constant will be positive and relatively large in the protonated species, in agreement with the value we have used. These arguments also indicate that hydrogen bonding to the protonated Schiff's base, to the extent that it alters the hybridization at the nitrogen, the C=N-H bond angle and the C=N and N-H bond lengths, will have strong effects on the C=N stretching frequency. A recent example of such a situation may be the work on pyridoxal Schiff's bases<sup>21,22</sup> which shows a C=N stretching frequency at  $1646 \text{ cm}^{-1}$  and a vibration at  $1465 \text{ cm}^{-1}$  with contributions from the C=N-H bending mode. In this particular case, the imine proton is intramolecularly hydrogen bonded to a nearby oxygen which constrains the system and likely perturbs the force constants associated with the C=N-H group.

In conclusion, the results of our analysis above indicate that the behavior of the nitrogen lone pair is involved in determining the properties of the C=N vibrational mode; changes in the electronic environment of this lone pair, upon protonation or reaction with a Lewis acid, affect the electron density distribution in the C=N linkage.

## CHAPTER 6

### SUMMARY AND FUTURE RESEARCH

#### A. Introduction.

A main effort in research on visual and related systems is directed toward understanding the conditions that the retinal Schiff's base chromophore experience in the protein to regulate the optical absorption properties of the photopigments. The lack of any detailed X-ray crystallographic information about rhodopsin and bacteriorhodopsin has prevented the identification of the charged amino acid near the retinal Schiff's base chromophore. In this regard, the original point charge model suggested by Nakanishi et al.<sup>61,103</sup> has been undermined by new data presented by Mathies et al.<sup>94</sup> on the "opsin shift" of retinal Schiff's base models in bacteriorhodopsin. Their results show that much of the "opsin shift" in bacteriorhodopsin (contrary to the original indications) is due to chromophore-protein interactions near the Schiff's base end of the chromophore. In addition, no crystallographic information is available for Schiff's bases and protonated analogs that indicate if the C=N bond is longer or shorter for the Schiff's base complexed species than for the uncomplexed derivative. In other words, no bond length data is available at present for retinal Schiff's base models that can show the state of the C=N bond order in the protonated photopigments, relative to the unprotonated species.

It is important to know the state of the C=N bond upon protonation, because a protonated retinal Schiff's base is the fundamental

photopigment in both rhodopsin and bacteriorhodopsin. Furthermore, a protonated retinal Schiff's base is the chromophore present in almost all the intermediates of the rhodopsin and bacteriorhodopsin photocycles. Thus, to understand the primary changes of the electronic structure upon protonation of the C=N moiety is a key step for the understanding of the wavelength regulation processes in vivo. Analogously, a protonated aromatic Schiff's base has been found to be the key intermediate in the reaction mechanisms of a series of metabolic coenzymes (i.e. pyridoxal phosphate) which play an important role in the interconversion of amino acids. In these cases, as well, changes in the electronic structure upon protonation of the C=N moiety are key to the catalytic action of such coenzymes as discussed in more detail in Chapter 1.

If crystallographic information were available for Schiff's bases and Lewis acid derivatives, it should be possible to determine if the increase in the C=N stretching frequency upon complexation of the nitrogen electron lone pair is attributable to the stretch-bend coupling model<sup>4,5,8,11,13</sup> (i.e. longer bond length and a weaker C=N stretching force constant upon Schiff's base protonation) or to the rehybridization model suggested in this thesis<sup>73-76</sup> (i.e. shorter bond length, stronger C=N stretching force constant).

Spectroscopic studies on models Schiff's bases offer a good method for understanding the C=N bond, and the insight obtained may easily be extended to rationalizing the properties of the covalent linkage between the retinal and the protein. As a direct consequence, determination of the properties of the C=N bond can lead to a further understanding of the

mechanism of wavelength regulation by the naturally-occurring photopigments. In the preceding Chapters, the application of optical, Raman and resonance Raman spectroscopies, normal coordinate analysis and ab initio calculations had proved to be very useful in providing detailed information about optical, vibrational, structural and electronic changes that are experienced by the C=N chromophore upon its complexation with general Lewis acid, for example,  $H^+$ ,  $BF_3$ ,  $BCl_3$  and  $BBr_3$  .

#### B. Summary.

1. Spectroscopic Studies. The spectroscopic studies, see Chapter 3, have shown that the basic operating mechanism which produces changes in the electronic structure of the protonated retinal Schiff's base and of retinal Schiff's base-Lewis acid complexes are very similar. This conclusion is based on the experimental results which show that, relative to the free species, protonation or complexation of retinal Schiff's bases with the Lewis acid  $BF_3$ ,  $BCl_3$  and  $BBr_3$  lead to similar chromophore responses as follows. a) Similar red shifts in the absorption maximum of the chromophore are observed. b) The C=N stretching frequency increases by approximately the same order of magnitude. c) The C=C stretching frequency is inversionally proportional to the absorption maximum for both kinds of complexes. (d) Similar conclusion apply for the protonated and general Lewis acid complexed aromatic Schiff's bases.

2. Ab initio Studies. The ab initio calculations at the GVB level (see Chapter 4), have indicated that upon protonation of methylimine the following occur. a) There is reorganization in the electronic structure

of the C=N bond such that the nitrogen s orbital contributing to the  $sp^2$  hybrid C=N bond increases. b) The electron charge distribution calculation show, though the chromophore carries a +1 charge, that the nitrogen appear to be partially negatively charged while the carbon and hydrogen carry the rest of the positive charge. c) These electronic changes in the protonated methylimine, relative to the unprotonated species, lead to a decrease in the C=N bond length and to an increase in the C=N stretching force constant of the protonated derivative relative to the uncomplexed analog.

3. Normal Coordinate Analyses Studies. Normal coordinate analyses indicated (see Chapter 5) the following. a) The calculated increase in the C=N stretching force constant upon protonation leads to a  $30\text{ cm}^{-1}$  in the C=N stretching frequency. This indicates that the C=N stretching frequency increase observed upon protonation or reaction of Lewis acid with the Schiff's bases is primarily due to the increase in the C=N stretching force constant. b) The calculations summarized in Figure 24 provide some insight into previous force fields used to calculate the C=N stretching frequency for protonated retinal Schiff's bases. The results show that the vibrational calculations which support the stretch-bend coupling model used low or negative C=N/C=N-H (stretch-bend) interaction force constants which can compensate for the decrease in the C=N stretching force constant (assumed upon protonation) and push the C=N stretching frequency up. However, recent studies (see Chapter 5) indicate, in agreement with our rehybridization model, that the C=N/C=N-H interaction force constant is positive and possibly relatively large. c) Numerical calculation within the normal mode analysis show that the

deuterium shift associated with the decrease in the C=N stretching frequency upon substitution of the Schiff's base hydrogen by deuterium is dependent to some extent on the N-H(D) stretch, C=N-H(D) bend, C=N/N-H(D) (stretch-stretch) and C=N-H(D) (stretch-bend) interaction force constants. These force constants therefore need to be taken into consideration for any well restricted normal coordinate analysis of Schiff's bases. Furthermore, the nonlinearity of this shift (see Figure 24) indicates that the deuterium shift attributed by the stretch-bend model to the decrease in coupling between the C=N stretch and C=N-D bend can be explained, within the rehybridization formalism, by the increase in mass of the C=N-D center relative to the C=N-H moiety.

### C. Conclusions.

The results presented here show that adduct formation between Schiff's bases and Lewis acids (i.e.  $H^+$ ,  $BF_3$ ,  $BCl_3$ ,  $BBr_3$ ) leads to C=N stretching frequency increases because the C=N bond rehybridizes such that the C=N stretching force constant increases. As a result of the rehybridization, the nitrogen and carbon in the C=N group carry partial negative and positive charges, respectively. How the increase in the C=N bond order and charge separation in the C=N bond in the protonated retinal Schiff's bases are used by the photopigments (rhodopsin and bacteriorhodopsin) in conjunction with local environmental effects to regulate the changes in the absorption maximum of the retinal chromophore are not clear yet. The interplay between these factors constitute a very good field of research and form the basis for the future work described below.

#### D. Future Work.

1. Introduction. Our long-term objective is to determine how the charge distribution of the protonated Schiff's base, in particular, the charge separation in the C=N bond, is altered and transmitted to the rest of the retinal moiety. The presence of a positive or negative charge near the C=N group or by the orientation and strength of possible hydrogen bonds between the imine hydrogen and a nearby counter ion are reasonable candidates for this process. An understanding of the contribution of a particular charge distribution within the C=N bond to the absorption maximum of the protonated retinal Schiff's base chromophore and how variation in the former can lead to variation in the latter is a major goal. Insight into the magnitude of this contribution to the "opsin shift" in rhodopsin and bacteriorhodopsin due to the interaction of the protein with the Schiff's base end of the chromophore will be gained.

These goals can be addressed by using X-ray crystallographic studies on all-trans-retinylidene-n-butylamine and 2-naphylidene-n-butylamine and their protonated and  $\text{BF}_3$  derivatives to determine the change in the C=N bond distance upon complexation of the free Schiff's base with Lewis acid. In addition, ab initio calculations and vibrational studies can be used to obtain the geometry, electronic charge density distribution, force constants and frequency changes that occur upon protonation or  $\text{BF}_3$  reaction of the allylimine,  $(\text{CH}_2=\text{CH}-\text{CH}=\text{NH})$  and its methylated analog  $(\text{CH}_2=\text{CH}-\text{CH}=\text{NCH}_3)$ . Resonance Raman scattering and  $^{13}\text{C}$  and  $^{15}\text{N}$  nuclear magnetic studies can be used to determine the vibrational frequencies and

charge density distribution upon complexation of the retinal Schiff's bases with Lewis acids of the general kind  $\text{BF}_3$  and  $\text{BF}_2\text{X}$ . Vibrational analysis at the general valence force field<sup>86</sup> level (GVFF) can be used in conjunction with the allylimine results to estimate the force constants and vibrational frequencies of the retinal Schiff's base. Comparison of these vibrational frequencies with those from the retinal Schiff's base in models and photopigments<sup>1-17</sup> can give insight into the net effect of the protein on the retinal Schiff's base chromophores.

## 2. Specific Aims and Methods.

The specific aims are the following:

i. To obtain X rays crystallographic data for the C=N bond in all-trans retinylidene-n-butylamine, 2-naphtylidene-n-butylamine and their protonated and  $\text{BF}_3$  derivatives.

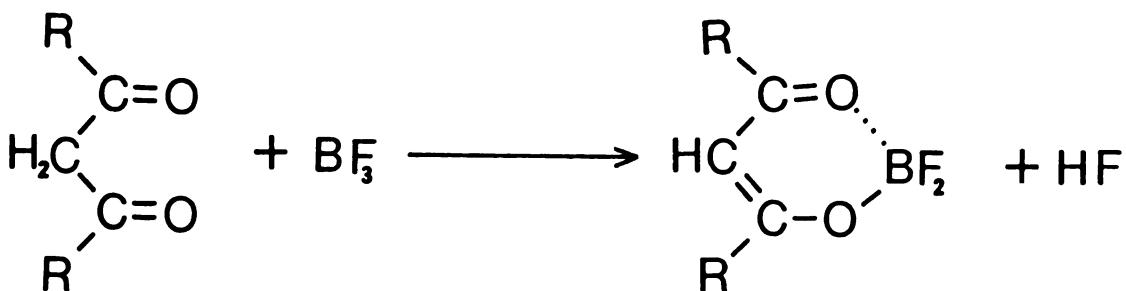
ii. Ab initio electron density, force constant and frequency calculations for the imine  $\text{CH}_2=\text{CH}-\text{CH}=\text{N}-\text{R}$  (where  $\text{R}=\text{H}$ ,  $\text{CH}_3$ ) and its protonated and  $\text{BF}_3$  analogs. Isotopic derivative can also be used to assign the particular vibrations. Comparison of the electron density, force constant and frequency of the complexed and uncomplexed species will allow us to determine the effect of nitrogen lone pair occupancy on the electronic environment and normal modes of the imine  $\text{CH}_2=\text{CH}-\text{CH}=\text{NR}$ . For the protonated allylimine derivative, calculation of the absorption maximum of the chromophore as a function of the change in distance and orientation between the imine proton (C=N-H) hydrogen bonded to a counter

ion (negatively charged) can be useful in predicting the influence of the strength of hydrogen bonded counter ion to the absorption maximum of the retinal chromophore. Furthermore, the above calculations will be the starting point for calculating changes in the absorption maximum of the allylimine model as a function of the distance between the protonated Schiff's base nitrogen and a positive or negative point charge.

iii. A synthetic method can be developed to prepare the complexes  $[\text{CH}_2=\text{CH}-\text{CH}=\text{NH}]$  and  $[\text{CH}_2=\text{CH}-\text{CH}=\text{NRBF}_3]$ , which will allow us to study the C=C, C-C and C=N vibrational modes in a more localized environment than in retinal Schiff's bases. To achieve this goal a matrix isolation technique<sup>142-144</sup> can be developed to study the experimental vibrational frequencies of the free imine and its complexes. Comparison of both systems will give insight into the effect of lone pair occupancy and electron density on the vibrational frequencies of the imine normal modes.

iv. The study of the retinal Schiff's base- $\text{BF}_3$  complexes can be extended to determine the behavior of the absorption maxima and associated vibrational frequencies for a variety of solvents different than those presented in Table 4.  $^{13}\text{C}$  and  $^{15}\text{N}$  magnetic resonance information can be obtained for the Schiff's base and  $\text{BF}_3$  complex. A comparison of these results with those present in the literature<sup>94,145-148</sup> for protonated retinal Schiff's base should allow us to establish the role of the counter-ion in determining the absorption maximum of the protonated Schiff's bases.

v. A synthetic method to prepare retinal Schiff's base- $\text{BF}_2\text{X}$  complex that can incorporate perturbation to the nitrogen lone pair Schiff's base of the C=N bond can be developed. In principle, the synthetic method will consist in the preparation and isolation of the condensation product formed upon reaction of  $\text{BF}_3$  with  $\beta$ -diketones,<sup>149,150</sup> i.e.



The isolation of the  $\text{BF}_2\text{X}$  complex from the HF product must be the first step in the sequence, since any trace of HF will not allow a clean reaction between  $\text{BF}_2\text{X}$  and the retinal Schiff's base. If the isolation of the  $\text{BF}_2\text{X}$  product is satisfactory, the next step will be to determine whether the spectroscopic characteristics of this new retinal Schiff's base- $\text{BF}_2\text{X}$  complex resemble those of the protonated retinal Schiff's base. If this is the case, the R group that initially will be a  $\text{CH}_3$  group, will be substituted by electron donating, electron withdrawing, positively and negatively charged groups. The effects of these substituents on the absorption maximum and vibrational properties of the complex will be used to understand the "opsin shift" in the photopigments rhodopsin and bacteriorhodopsin.

vi.  $^{13}\text{C}$  and  $^{15}\text{N}$  nuclear magnetic resonance studies of the above retinal Schiff's base-Lewis acid complexes will provide information about the electron density distribution in C=N bond in the retinal system under different conditions of nitrogen lone pair occupancy.

vii. Absorption and resonance Raman spectroscopy will provide information about the relation between a particular change in the electronic structure of the chromophore and the C=N, C=C and C-C vibrational frequencies.

viii. A vibrational analysis with the GVFF method will be used in combination with the information obtained from the  $\text{CH}_2=\text{CH}=\text{CH}=\text{N}-\text{R}$  system and the data present in the literature<sup>1-17</sup> to deduce the effect of protonation and  $\text{BF}_3$  reaction on the retinal Schiff's base system and to construct an accurate force field for the Schiff's base end of the retinal chromophore. This force field then will be used to provide information on the protein-induced changes in the vibrational frequency and force constants of the retinal chromophore due to protein interactions at the Schiff's base.

ix. With the above information on the structure of the unprotonated, protonated and  $\text{BF}_3$  complex retinal Schiff's base models for the chromophore-protein interaction for rhodopsin and bacteriorhodopsin will be proposed and evaluated.

x. Finally, it can be proposed to study the experimental behavior observed upon hydrogen bond formation or protonation of a chromophore

containing the groups, C=O, C=N and C=N. For example, chromophores containing the carbonyl (C=O) group usually show a decrease in the C=O stretching frequency and a red shift in the absorption maximum on hydrogen bond formation. This behavior is contrary to the trend of the imines and nitriles which show an increase in the C=N and C=N stretching frequency respectively, and a red shift in the absorption maximum. Note, however, that the experimental behavior of the absorption maxima is in all the cases the same. Ab initio calculations can be used to study the effect that electron lone pair occupancy can have in the electronic characteristics and properties of the C=O, C=N and C=N bonds in ketones (RR'C=O) nitriles (RC≡N), and imines (C=N) respectively. A comparative ab initio study of formaldehyde and cyanide with methylimine and allylimine will help to distinguish between the effect of having one lone pair (nitrogen) or two lone pair (oxygen) on the C=X force constant and C=X stretching frequency. This comparative study will indicate if the rehybridization model, suggested to explain the observed increase in frequency for protonated Schiff's bases, can be extended to explain the experimental trends in the vibrational frequencies for the carbonyl and nitrile containing chromophores.

**LIST OF REFERENCES**

## LIST OF REFERENCES

1. Ottolenghi, M. Adv. Photochem. 1980, 12, 97-200.
2. Mathies, R. A. in "Spectroscopy of Biological Molecules" Sandorfy, C.; Theophanides, T. Ed. D. Reidel Publishing Company. Dordrech/Boston/Lancaster, 1983; pp. 303-328.
3. Argade, P. V.; Rothschild, K. J. Biochem. 1983, 22, 3460-3466.
4. Aton, B.; Doukas, A. G.; Narva, D.; Callender, R. H.; Dinur, U.; Honig, B. Biophys. J. 1980, 29, 79-94.
5. Smith, S. O.; Pardoen, J. A.; Mulder, P. P. J.; Curry, B.; Lugtenburg, J.; Mathies, R. Biochem. 1983, 22, 6141-6148.
6. Smith, S. O.; Myers, A. B.; Pardoen, J. A.; Winkel, C.; Mulder, P. P. J.; Lugtenburg, J.; Mathies, R. Proc. Natl. Acad. Sci. USA 1984, 81, 2055-2059.
7. Schiffmiller, R.; Callender, R. H.; Waddell, W. H.; Govindje E, R.; Ebrey, T. G.; Kakitani, H.; Nakanishi, K. Photochem. Photobiol. 1985, 41, 653-567.
8. Kakitani, H.; Kakitani, T.; Rodman, H.; Honig, B.; Callender, R. J. Phys. Chem. 1983, 87, 3620-3628.
9. Massig, G.; Stockburg, M.; Gartner, W.; Oesterhelt, D.; Towner, P. J. Raman Spect. 1982, 12, 287-294.
10. Deng, H.; Pande, C.; Callender, R. H.; Ebrey, T.G. Photochem. Photobiol. 1985, 41, 467-470.
11. Smith, S. O.; Myers, A. B.; Mathies, R. A.; Pardoen, J. A.; Winkel, C.; van den Berg, E. M. M.; Lugtenburg, J. Biophys. J. 1985, 47, 653-664.
12. Heyde, M. E.; Gill, D.; Kilponen, R. G.; Rimai, L. J. Am. Chem. Soc. 1971, 93, 6776-6780.
13. Marcus, M. A.; Lemley, A. T.; Lewis, A. J. Raman Spect. 1979, 8, 22-25.
14. Aton, B.; Doukas, A. G.; Callender, R. H.; Becher, B.; Ebrey, T. G. Biochem. 1977, 16, 2995-2998.
15. Cookingham, R. E.; Lewis, A.; Lemley, A. T. Ibid. 1978, 17, 4699-4711.

16. Bagley, K. A.; Balogh-Nair, V.; Croteau, A. A.; Dollinger, G.; Ebrey, T. G.; Eisenstein, L.; Hong, M. K.; Nakanishi, K.; Vittitow, J. Ibid. 1985, 24, 6055-6071.
17. Gerwert, K.; Siebert, F. EMBO J. 1986, 5, 805-811.
18. Witkop, B.; Beiler, T.W. J. Am. Chem. Soc. 1954, 76, 5589-5597.
19. Karube, Y.; Ono, Y.; Matsushima, Y.; Ueda, Y. Chem. Pharm. Bull. 1978, 26, 2642-2648.
20. Ledbetter, J. W. J. Phys. Chem. 1982, 86, 2449-2451.
21. Benecky, M. J.; Coopeland, R. A.; Hays, T. R.; Lobenstine, E. W.; Rava, R. P.; Pascal, Jr., R. A.; Spiro, T. G. J. Biol. Chem. 1985, 260, 11663-11670.
22. Benecky, M. J.; Copeland, R. A.; Rava, R. P.; Feldhaus, R.; Scott, R. D.; Mezler, C. M.; Metzler, D. E.; Spiro, G. T. Ibid. 1985, 260, 11671-11678.
23. Ward, B.; Callahan, P. M.; Young, R.; Babcock, G. T.; Chang, C. K. J. Am. Chem. Soc. 1983, 105, 634-636.
24. Hanson, L. K.; Chang, C. K.; Ward, B.; Callahan, P. M.; Babcock, G. T.; Head, J. D. Ibid. 1984, 106, 3950-3958.
25. Ward, B.; Chang, C. K.; Young, R. Ibid. 1984, 106, 3943-3950.
26. Maggiora, L. L.; Maggiora, G. M. Photochem. Photobiol. 1984, 39, 847-849.
27. Petke, J. D.; Maggiora, G. M. J. Am. Chem. Soc. 106, 3129-3133.
28. Hargrave, P. A.; McDowell, J. H.; Curtis, D. R.; Wong, J. K.; Jozczak, E.; Fong, S. L.; Mohanc Roo, J. K.; Argus, P. Biop. Struc. Mech. 1983, 9, 235-241.
29. Dratz, E. A.; Hargrave, P. A. Trends in Biochem. Sci. 1983, 8, 128-134.
30. Ovchinnikov et al. Biorg. Khim. 1982, 8, 1011-1017.
31. Oseroff, A. R.; Callender, A. R. Biochem. 1974, 13, 4243-4248.
32. Mathies, R.; Freedman, T. B.; Stryer, L. J. Mol. Biol. 1977, 109, 367-373
33. Wald, G. Nature (London), 1968, 219, 800-807.
34. Yoshizawa, T.; Wald, G. Ibid. 1963, 197, 1279-1286.
35. Mathies R. A.; Smith, S. O.; Palings, I. To be published in "Biological Applications of Raman Spectroscopy."

36. Stoeckenius, W.; Lozier, R. H.; Bogomolni, R. A. Biochim. Biophys. Acta 1979, 505, 215-278.
37. Ovchinnikov, Yu. A.; Abdulaev, N. G.; Fligina, M. Yu.; Kiselev, A. V.; Lobanev, N. A. FEBS Lett. 1979, 100, 219-224.
38. Khorana, H. G.; Gerber, G. E.; Herlihy, W. C.; Gray, C. P.; Anderegg, R. J.; Nihei, K.; Briemann, K. Proc. Natl. Acad. Sci. USA 1979, 76, 5040-5050.
39. Callahan, P. M.; Babcock, G. T. Biochem. 1983, 22, 452-461.
40. Babcock, G. T.; Callahan, P. M. Ibid. 1983, 22, 2314-2319.
41. Wikstrom, M.; Krab, K.; Saraste, M. in "Cytochrome Oxidase A Synthesis." Academic Press, London, 1981.
42. Wikstrom, M. K. F. Nature (London), 1977, 266, 271-273.
43. Callahan, P. M. PhD Thesis, Michigan State University, 1983.
44. Ondrias, M. R.; Babcock, G. T. Biochem. Biophys. Res. Commun. 1980, 93, 29-35.
45. Babcock, G. T.; Callahan, P. M.; Ondrias, M. R.; Salmeen, I. Biochem. 1981, 20, 959-966.
46. Katz, J. J.; Norris, J. R.; Shipman, L. L.; Thurnauer, M. C.; Wasielewski, M. R. Annu. Rev. Biophys. Bioengineer. 1978, 7, 393-434.
47. Maggiora, G. M. Int. J. Quantum Chem. 1979, 16, 331-352.
48. Sauer, K. Annu. Rev. Phys. Chem. 1979, 30, 155-178.
49. Karpeisky, M. Ya.; Ivanov, V. I. Nature 1966, 40, 493-496.
50. Christen, P.; Metzler, D. E. in "Transaminases". John Wiley and Sons, Inc. New York, 1985.
51. Fersht, A. in "Enzyme Structure and Mechanism." Freeman and Company, New York, 1985; pp. 69-75.
52. Zerner, B.; Coutts, S. M.; Lederer, F.; Waters, H. H.; Westheimer, F. H. Biochem. 1966, 5, 813-816.
53. Warren, S.; Zerner, B.; Westheimer, F. H. Ibid. 1966, 5, 817-823.
54. Grazi, E.; Cheng, T.; Horecker, B. L. Biochem. Biophys. Res. Commun. 1962, 7, 250-256.
55. Speck, J. C.; Rowley, Jr. P. T.; Horecker, B. L. J. Am. Chem. Soc 1963, 85, 1012-1013.

56. Horecker, B. L.; Tsolas, O.; Lai, C. Y. The Enzymes. 1972, 7, 213-219.
57. Tsolas, O.; Horecker, B. L. The Enzymes. 1972, 7, 259-264.
58. Fabian, M. J.; Legrand, M.; Poirier, P. Bull. Soc. Chim. Fr. 1956, 1499-1509.
59. Fabian, M. J.; Legrand, M. Ibid. 1956, 1641-1643.
60. Blatz, P. E.; Mohler, J. H. Biochem. 1975, 14, 2304-2309.
61. Sheves, M.; Nakanishi, K. J. Am. Chem. Soc. 1983, 105, 4033-4039.
62. Baasov, T.; Sheves, M. Ibid. 1985, 107, 7524-7533.
63. Kakitani, H.; Kakitani, T.; Rodman, H.; Honig, B. Photochem. Photobiol. 1985, 41, 471-479.
64. Birge, R. R.; Hubbard, L. M. J. Am. Chem. Soc. 1980, 102, 2195-2205.
65. Freedman, K. A.; Becker, R. S. Ibid. 1986, 108, 1245-1251.
66. Nakanishi, K.; Balogh-Nair, V.; Arnaboldi, M.; Tsujimoto, K.; Honig, B. Ibid. 1980, 102, 7945-7947.
67. Samuel, B.; Snaith, R.; Summerford, C.; Wade, K. J. Chem. Soc. (A) 1970, 2019-2022.
68. Coerver, H. J.; Curran, C. J. Am. Chem. Soc. 1958, 80, 3522-3523.
69. Figeys, H. P.; Geerlings, P.; Berckmans, D.; Alsenoy, C. V. J. Chem. Soc. Faraday Trans. (2) 1981, 77, 721-740.
70. Horac, M.; Vitek, A. "Interpretation and Processing of Vibrational Spectra" 1978, John Wiley, New York, pp. 302-303.
71. Swanson, B.; Shriver, D. F.; Ibers, J. A. Inorg. Chem. 1969, 8, 2182-2189.
72. Gerrard, W.; Lappert, M. F.; Pyszora, H.; Wallis, J. W. J. Chem. Soc. 1960, 2182-2186.
73. López-Garriga, J. J.; Hanton, S.; Babcock, G. T.; Harrison, J. F. J. Am. Chem. Soc. 1986 Accepted for publication.
74. López-Garriga, J. J.; Babcock, G. T.; Harrison, J. F. Biophys. J. 1985, 47, 96a.
75. Lopez-Garriga, J. J.; Babcock, G. T.; Harrison, J. F. J. Am. Chem. Soc. Accepted for publication.
76. Lopez-Garriga, J. J.; Babcock, G. T.; "Tenth International Conference on Raman Spectroscopy", Eugene, OR, 1986.

77. Goddard, III, W. A.; Dunning, Jr., T. H.; Hunt, w. J.; Hay, P.J. Acc. Chem. Res. 1973, 6, 368-376.
78. Hehre, W. J.; Radom, L.; Schleyer, P. vR.; Pople, J. A. "Ab Initio Molecular Orbital Theory" John Wiley and Sons, Inc. New York, 1986.
79. Santerre, G. M.; Hansrote, Jr., C. J.; Crowell, T. I. J. Am. Chem. Soc. 1958, 80, 1254-1257.
80. Layer, R. W. Chem. Rev. 1963, 63, 489-510.
81. Pickard, P. L. Tolbert, T. L. J. Org. Chem. 1961, 26, 4886-4888.
82. Lane, C. F.; Kramer, G. W. Aldrichimica Acta. 1977, 10, 11-18.
83. The ARGOS integral program was developed by R. M. Pitzer (Ohio State University).
84. The GVB-164 program was written by R. Blair (Argonne National Laboratory)
85. Shimanouchi, T. Computer Programs for Normal Coordinate Treatment of Polyatomic Molecules, Tokyo University, Tokyo, Japan, 1969.
86. Nam, H. H.; Leroi, G. E. Spectrochim. Acta, 1985, 41A, 67-73.
87. Hart, D. L.; Kanai, K. J. Am. Chem. Soc. 1983, 105, 1255-1263.
88. Yoon, U. C.; Quillen, S. L.; Mariano, P. S.; Swanson, R.; Stavinoha, J. L.; Bay, E. Ibid. 1985, 105, 1204-1218.
89. Patai, S. "The Chemistry of the Carbon Nitrogen Double Bonds" 1970 Interscience Pub. New York. Cap 1.
90. Lewis, A. Phil. Trans. R. Soc. Lond. A. 1979, 293, 315-327.
91. Susz, B. P.; Cooke, I. Helv. Chim. Acta 1954, 37, 1273.
92. Susz, B. P.; Chalandon, P. Ibid., 1958, 41, 1332.
93. Lappert, M. F. J. Chem. Soc. 1962, 542.
94. Lugtenburg, J.; Muradin-Szweykowska, M.; Heeremans, C.; Pardoen, J. A.; Harbison, G. S.; Herzfeld, J.; Griffin, R. C.; Smith, S.O. J. Am. Chem. Soc. Accepted for publication.
95. Kropf, A.; Hubbard, R. Ann. N. Y. Acad. Sci. 1958, 74, 266.
96. Irving, C. S.; Byers, G. W.; Leermakers, P. A. Biochemistry 1970, 9, 858-862.
97. Blatz, P. E.; Mohler, J. H. Ibid. 1972, 11, 3240-3242.

98. Ebrey, T. C.; Honig, B. Q. Rev. Biophys. 1975, 8, 129-159.
99. Waddel, W. H.; Schaffer, A. M.; Becker, R. S. J. Am. Chem. Soc. 1977, 99, 8456-8460.
100. Warshel, A. Proc. Natl. Acad. Sci. USA 1978, 75, 2558-2563.
101. Ishikawa, K.; Yoshihara, T.; Suzuki, H. J. Phys. Soc. Jpn. 1980, 49, 1505-1511.
102. Blatz, P. E.; Mohler, J. A.; Navangul, H. V. Biochem. 1972, 11, 848-855.
103. Honig, B.; Dinur, U.; Nakanishi, K.; Balogh-Nair, V.; Gawinowicz, M. A.; Arnaboldi, M.; Motto, M.G. J. Am. Chem. Soc. 1979, 101, 7084-7086.
104. Zwarich, R.; Smolarek, J.; Goodman, L. J. Molecular Spec. 1971, 38, 336-357.
105. Perry, K. A. W.; Robinson, P. J.; Sainsburry, P. J.; Waller, M.J. J. Chem. Soc. (B), 1970, 700-703.
106. Patai, S. "The Chemistry of Carbon Nitrogen Double Bond." 1970, Interscience Publishers, New York, Chapters 1 and 4.
107. Grodcsik, A.; Kubinyi, M.; Fogarasi, G. J. Mol. Struct. 1982, 89, 63-70.
108. Sharma, O. P.; Singh, S. N.; Singh, R. D. Indian J. Phys. 1974, 48, 494-503.
109. Sharma, G. M.; Roels, O. A. J. Org. Chem. 1973, 38, 3648-3651.
110. Datin, A. P.; Lebas, J. M. Spectrochim. Acta. 1969, 25A, 169-185.
111. Yanovskaya, L.A.; Kryshtal, G. V.; Yakovlev, I. P.; Kucherov, V.F.; Simkin, B. Y.; Bren, V. A.; Minkin, V. I.; Osipov, O.; Tumakaova, I. A. Tetrahedron 1973, 29, 2053-2064.
112. Favrot, J.; Vocelle, D.; Sandorfy, C. Photochem. Photobiol. 1979, 30, 417-421.
113. Besnainou, S.; Thomas, E.; Bratov, S. J. Mol. Spect. 1966, 21, 113-124.
114. Alshuth, T.; Stockburger, M.; Hegemann, P.; Oosterhelt, D. FEBS Lett. 1985, 179, 55-59.
115. Brown, R. D.; Penfold, A. Trans. Faraday Soc. 1957, 53, 397-402.
116. Milligan, D. E. J. Chem. Phys. 1961, 35, 1491-1497.
117. Moore, C. B.; Pimentel, G. C. Ibid. 1965, 43, 63-70.

118. Christen, D.; Oberhammer, H.; Hammaker, R. M.; Chang, S. C.; DesMarteau, D. D. J. Am. Chem. Soc. 1982, 104, 6186-6190.
119. Botschwina, P. Chem. Phys. Letters 1974, 29, 580-584.
120. Eades, R. A.; Weil, D. A.; Elenberger, M. R.; Farneth, W. F.; Dixon, D. A.; Douglas, Jr. C. H. J. Am. Chem. Soc. 1981, 103, 5372-5377.
121. Kollman, P. A.; Trager, W. F.; Rothenberg, S.; Williams, J. E. J. Am. Chem. Soc. 1973, 95, 458-463.
122. Huzinaga, S. J. Chem. Phys. 1965, 42, 1293-1320.
123. Dunning, Jr., T. H. H. Ibid. 1970, 53, 2823-2833.
124. Raffenetti, R. C. Ibid. 1973, 58, 4452-4458.
125. Mulliken, R. S. ibid. 1955, 23, 1833-1840.
126. Alvarado, A.; Harrison, J. Curfit Program, Michigan State University, East Lansing, MI.
127. Fogarasi, G.; Pulay, P. Acta Chim. Acad. Sci. Hung. 1981, 108, 55-73.
128. Dunning, Jr., T. H.; Pitzer, R. M.; Aung, S. J. Chem. Phys. 1972, 57, 5044-5051.
129. Wahlgren, U.; Pacansky, J.; Bagus, P. S. Ibid. 1975, 63, 2874-2881.
130. Binkley, J. S.; Frisch, M. J.; Schaeffer III, H. F. Chem. Phys. Lett. 1986, 126, 1-6.
131. Yamaguchi, Y.; Schaefer III, H. F. J. Chem. Phys. 1980, 73, 2310-2318.
132. Oseroff, A. R.; Callender, R. H. Biochemistry 1974, 13, 4243.
133. Inamori, T.; Hamada, Y.; Tsuboi, M.; koga, Y.; Kondo, S. J. Mol. Spect. 1985, 109, 256-268.
134. Hamada, Y.; Tsuboi, M.; Matsuzawa, T.; Yamanouchi, K.; Kuchitsu, K. Ibid. 1984, 105, 453-464.
135. Hashiguchi, K.; Hamada, Y.; Tsuboi, M.; Koga, Y.; Kondo, S.; Ibid. 1984, 105, 81-92.
136. Hamada, Y.; Tsuboi, M.; Takeo, H.; Matsumura, C. Ibid. 1984, 106, 175-185.
137. Sugawara, Y.; Hirakawa, A. Y.; Tsuboi, M. Ibid. 1984, 108, 206-214.

138. Botschwina, P.; Nachbaur, E.; Rode, B. M. Chem. Phys. Letters 1976, 41, 486-489.
139. Laswick, P. H.; Taylor, R. C. J. Mol. Struct. 1976, 34, 197-218.
140. Cyvin, B. N.; Cyvin, S. J.; Hargittai, M.; Hargittai, I. Z. Anorg. Allg. Chem. 1978, 440, 111-118.
141. Mills, I. M. Spectrochimica Acta, 1963, 19, 1585-1594.
142. Swanson, I.; Jones L. H. "Vibrational Spectra and Structure" Elsevire Science Pub. 1983, vol. 12, pp. 1-63.
143. Redington R.L. Ibid. pp. 323-391.
144. Jodl, H.J. Ibid. 1984, vol 13, pp. 285-416.
145. Allen, M.; Roberts, J. D. Can. J. Chem. 1981, 59, 451-458.
146. Allen, M.; Roberts, J. D. J. Org. Chem. 1979, 45,130-135.
147. Harbison, G. S.; Herzfeld, J.; Griffin, R. G. Biochemistry, 1983, 22, 5-12.
148. Mateescu, G. D.; Abrahamson, E. W.; Shriver, J. W.; Copan, W.; Muccio, D.; Igbal, M.; Waterhous, V. in "Spectroscopy of Biological Molecules" Sandorfy, C.; Theophanides, T. Ed. D. Reidel Publ. Com. Dordrech/Boston/Lancarter, 1983; pp 257-290.
149. Niedenzu, K.; Dawson, J. in "Boron-Nitrogen Compounds" Academic Press. Inc. Springer-Verlag Ed. Berlin/Heidelberg/New York 1965.
150. Gerrard, W. in "The Organic Chemistry of Boron" Academic Press. London, New York, 1961.